ULTRASENSITIVE DETECTION OF PROTEINS AND PEPTIDES BY CAPILLARY ELECTROPHORESIS AFFINITY ASSAYS

By

IGOR GERMAN

A DISSERTATION PRESENTED TO THE GRADUATE SCHOOL
OF THE UNIVERSITY OF FLORIDA IN PARTIAL FULFILLMENT
OF THE REQUIREMENTS FOR THE DEGREE OF
DOCTOR OF PHILOSOPHY

UNIVERSITY OF FLORIDA

2001

To my wife Julia for her never-ending love.

ACKNOWLEDGMENTS

I would like to thank Dr. Robert T. Kennedy for his guidance, support, and encouragement during my study at the University of Florida. Members of the Kennedy research group provided invaluable support and encouragement, as well as created a positive working environment.

I am grateful to members of the departmental machine and electronic shops for their support and patience during my stay at the Department of Chemistry. Special recognition goes to Dr. Samuel Colgate and to Todd Prox for their help in the Student Machine Shop.

I am thankful to Waters Corporation for sponsoring the Desty Memorial Lecture and for selecting me a winner of the lecture in 1998. I am grateful to the American Chemical Society Division of Analytical Chemistry Graduate Fellowship sponsored by the Society of Analytical Chemists of Pittsburgh and to Dr. Roger G. Bates and Mrs. Bates for their generous establishment of the Roger G. and Jo Bates Fellowship.

I would like to express my deepest appreciation to my parents for their guidance, support, and sacrifice. This work would not be possible without the love and support of my wife, Julia, and without the joy brought to me by my son, Richard Amadey.

TABLE OF CONTENTS

Page

ACKNOWLEDGMENTS iii

ABSTRACT vii

CHAPTERS

1 INTRODUCTION 1

Affinity Probes 1
Antibodies 1
Combinatorially Derived Antibodies and Peptides 2
Combinatorially Derived Oligonucleotides (Aptamers) 3
Affinity Assays 4
Capillary Electrophoresis 5
Detection Methods in CE 7
Laser-Induced Fluorescence (LIF)Detection 8
Amperometric Detection 8
Absorbance Detection 9
Sample Injection in CE 9
Capillary Electrophoresis Affinity Assays 12
Non-competitive Assays 14
Competitive Assays 19
Binding Constant Determination by CE-Affinity Assays 22

2 APTAMERS AS LIGANDS IN AFFINITY PROBE CAPILLARY ELECTROPHORESIS 27

Introduction 27
Experimental 29
Chemicals 29
Capillary Electrophoresis 30
Aptamer-Based APCE 31
Serum Sample Preparation 32
Dissociation Constant Estimation 32
Results and Discussion 33
Separation Conditions for Aptamer Assay for IgE 33
Quantification 35
Selectivity 36
Effect of Label on Binding 37

Complex Samples 37
Aptamer based APCE for thrombin 38
Conclusion 39

3 RAPID SIMULTANEOUS DETERMINATION OF GLUCAGON AND INSULIN BY COMPETITIVE CAPILLARY ELECTROPHORESIS IMMUNOASSAYS ... 47

Introduction 47
Experimental 50
Chemicals 50
Preparation of fluorescein-labeled glucagon (Glu*) 50
Capillary Electrophoresis 51
Data Acquisition and Analysis 51
Flow-Injection Immunoassay for Glucagon 52
Simultaneous Immunoassay of Insulin and Glucagon 52
Islet Content Analysis 53
Results and Discussion 53
CE-LIF Based Immunoassay for Glucagon 53
Ultrafast Determination of Glucagon 57
Simultaneous CE-LIF Immunoassay for Glucagon and Insulin 57
Measurement of Glucagon Content of Islets 59
Conclusion 60

4 REVERSED-PHASE CAPILLARY LIQUID CHROMATOGRAPHY COUPLED ON-LINE TO CAPILLARY ELECTROPHORESIS IMMUNOASSAYS 68

Introduction 68
Experimental 71
Chemicals 71
Preparation of fluorescein-labeled glucagon (Glu*) 72
Capillary Electrophoresis 72
Capillary RPLC 73
On-Line RPLC-CEIA 75
Data Acquisition and Analysis 76
Sample Analysis and Calibration 76
Analysis of Islet Secretion 77
Results and Discussion 77
On-Line CE Immunoassay 77
RPLC Separation and Preconcentration 81
CE-Immunoassay with RPLC Preconcentration 83
Glucagon Secretion from Single Islets 86
RPLC Separation With CE-Immunoassay detection 86
Comparison to other techniques 87
Conclusion 88

5 HPLC PRECONCENTRATION AND SEPARATION OF PEPTIDES WITH ON-LINE CAPILLARY ELECTROPHORESIS IMMUNOASSAY DETECTION 101

Introduction 101
Experimental 104
Chemicals 104
Preparation of fluorescein-labeled glucagon (Glu*) neuropeptide Y (NPY*) 104
Capillary Electrophoresis 105
On-Line Competitive CEIA for NPY 106
Capillary HPLC-CEIA 107
Meaurements of the Anti-NPY—NPY* Affinity Constant 108
Data Acquisition and Analysis 109
Sample Analysis and Calibration. 109
Measurements of Biological Samples 110
Results and discussion 110
On-Line CE-LIF Immunoassay for NPY 110
Detecton of NPY with Capillary HPLC-CEIA 113
Analysis of Brain Samples 114
High Efficiency Separations with CEIA Detection 115
Conclusion 119

6 SUMMARY AND FUTURE DIRECTIONS 131

APPENDICIES

A FLUORESCENT LABELING AND PURIFICATION OF PEPTIDES 134

B BRIEF MANUAL FOR USE WITH SPF AUTOMATIC PEAK FINDER 137

Introduction 137
System requirements 137
Peak definition 138
Main Menu 139
Using the program to analyze individual data files 139
Automatic Peak determination 141
Processing the sequence of files automatically 142

C FREQUENTLY USED RELATIONSHIPS IN CHROMATOGRAPHY 144

Chromatographic Resolution 144
Column Parameters 145
LSS Gradient Elution 147

REFERENCES 150

BIOGRAPHICAL SKETCH 156

Abstract of Dissertation Presented to the Graduate School
Of the University of Florida in Partial Fulfillment of the
Requirements for the Degree of Doctor of Philosophy

ULTRASENSITIVE DETECTION OF PROTEINS AND PEPTIDES BY
CAPILLARY ELECTROPHORESIS AFFINITY ASSAYS

By

Igor German

May 2001

Chairman: Robert T. Kennedy
Major Department: Chemistry

This work focused on development of novel methods for detection of ultra dilute solutions of proteins and peptides in biological matrices by affinity assay and capillary electrophoresis with laser induced fluorescence detection. Both competitive and non-competitive formats of affinity assays were investigated.

A combinatorially selected DNA ligand (aptamer) against IgE was labeled with fluorophore and used as a selective fluorescent tag for determining IgE by non-competitive format. Separations of samples containing aptamer and IgE were complete in less than 60 s and revealed two zones, corresponding to free and bound to IgE aptamer. Concentration of IgE could be determined with the detection limit of 46 pM and a linear dynamic range of 10^5. Similar separation conditions and application of thrombin aptamer allowed detection of thrombin.

A rapid capillary electrophoresis competitive immunoassay has been developed for the determination of glucagon. In the assay, fluorescein-conjugated glucagon is mixed with the sample followed by addition of anti-glucagon. Free and antibody-bound, tagged glucagon could be separated in 3 s using CE to obtain quantitative determination of glucagon with a concentration detection limit of 760 pM. The method was used to determine glucagon content of islets of Langerhans.

Capillary reversed-phase liquid chromatography was coupled on-line to competitive capillary electrophoresis immunoassay to improve concentration sensitivity of the assay and to provide a means for detecting multiple species that cross-react with antibody. After injection, samples were desorbed by gradient elution, mixed on-line with immunoassay reagents, incubated in a continuous-flow reaction capillary, and analyzed by capillary electrophoresis with flow-gated injections. Electrophoretic analysis of the reactor stream was performed every 1.5 s allowing nearly continuous monitoring of the RPLC separation. Preconcentration achieved by RPLC allowed improvement in the detection limit from 760 pM to 20 pM for glucagon and from 850 nM to 38 nM for neuropeptide Y. The technique was used to measure glucagon secretion from single islets of Langerhans and extracellular concentration of neuropeptide Y in rat brain

CHAPTER 1
INTRODUCTION

Technologies that allow detection and quantification of macromolecules of biological origin have become an important aspect of research and clinical diagnosis. As a result, these technologies must constantly evolve to improve their performance and to widen the range of applications. Affinity probes—molecules that recognize and bind to biological analytes with high affinity and specificity—have found wide utilization in many analytical techniques. Although antibodies are the most common example of the affinity probes, other molecules including receptors, proteins, and combinatorially selected peptides and oligonucleotides can be used. In this work, effort has been put forth to enhance current analytical methodology by a combined use of affinity probes and separation science.

Affinity Probes

Antibodies

Antibodies are proteins know as immunoglobulins produced by the immune system in response to invasion by antigens. As an example, a single mouse is capable of generating millions of different immunoglobulin species, each highly specific to a certain target. The most common type of antibodies is IgG, with molecular weight around 160,000 Daltons, containing two identical binding regions called paratopes. Each paratope is able to bind specifically to a certain area of the complementary antigen known

as epitope. Applications of antibodies became widespread in 1970s when polyclonal antisera from the immunized animals became widely available. Later, Kohler and Milstein (Koh75) discovered technology that allowed production of monoclonal antibodies in cultured cells in large quantities to make them inexpensive tools for the variety of research.

Combinatorially Derived Antibodies and Peptides

Recombinant DNA technology provides an alternative way to derive an enormous number of antibodies and antibody fragments. This can be accomplished by inserting a combinatorially derived portion of DNA into the gene coding for the antibody (Hus89, Chr92). In addition, a new bacteriophage-based screening system has been developed (Chr92, Smi97). Phage display is an artificial chemical evolution system that uses standard recombinant DNA techniques to develop libraries of peptides and small proteins. Phages are viruses that infect bacterial cells and insert segments of foreign DNA into the host cell, which then replicates and multiplies phages using its own resources. Phage display differs from conventional expression systems such that the expressed protein or peptide from the inserted DNA is displayed on the outer surface of the newly produced phages. A phage display library is a heterogeneous mixture of such phage clones, each carrying a different peptide or protein on its surface.

Since displayed peptide is accessible to the outside solution, common screening techniques can be applied to find the group that possesses necessary binding properties toward the target. Once the binder is identified, phages can be amplified by infecting them into the fresh cells.

Combinatorially Derived Oligonucleotides (Aptamers)

Combinatorially derived oligonucleotide ligands are obtained in a way similar to the peptides; however, the derivation is done *in vitro* (Jay99). The technique by which aptamers are obtained is called systematic evolution of ligands by exponential enrichment (SELEX) (Tue90, Ell90, Osb97). SELEX process is a procedure for screening very large combinatorial libraries of oligonucleotides by an iterative course of *in vitro* selection and amplification. The SELEX process begins with a random sequence library obtained by a special type of chemical synthesis of DNA (in cases where an RNA aptamer is needed, an additional step of transcription is required). Each member in a library is a linear oligonucleotide of a unique sequence. Although a library containing 40 bases long randomized region would be expected to contain 2^{40} individual molecules, practical libraries are limited to $10^{14} - 10^{15}$ sequences. Nevertheless, this immense number of molecules is assumed to have at least one that will possess the necessary characteristics to bind to the target.

In the screening step, the pool of random sequences is incubated with the target; stringency of selection is varied using changes in buffer and temperature. A small number of oligonucleotide molecules interact with the target, and the complex is separated from the bulk solution by means of common separation techniques. Alternatively, the library could be passed through an affinity column on which the target molecules have been immobilized. Recovered oligonucleotides are amplified by polymerase chain reaction (PCR) and used in the subsequent rounds of selection (if RNA aptamer is used, a reverse transcription is performed before the amplification). The enrichment efficiency of SELEX is governed by the stringency of selection at each round. Binding assays are carried out between rounds to determine the affinity of the enriched

pool of molecules. Once desired affinity has been achieved, oligonucleotides are sequenced and further analyzed to obtain the best binder.

Affinity Assays

Affinity assays are among the most sensitive and specific methods available for the quantitative determination of proteins and peptides. Affinity assays can be classified as competitive and non-competitive. In a non-competitive assay format, an excess of the labeled affinity probe is added to the sample to determine the target. A competitive format of affinity assays utilizes competition between labeled and analyte targets for binding to the limited amount of probe. All types of affinity assays rely on labeled molecules for detection. Most common types of labels are radioisotopes, enzymes, and fluorophores (But84).

Radioimmunoassay (RIA) is an example of the affinity assay that utilizes radiochemical labeling for detection. Although highly sensitive, uses of radioactive species in RIAs create environmental hazards, which generates interest in development of alternative labeling procedures. Enzyme labels, which has virtually no environmental problems, have been widely used in the enzyme linked immunosorbent assay (ELISA). In this assay, an affinity probe is coated on the surface of the wall of the microtiter plate where it binds to the corresponding target. The complex is quantitated by the addition of the other antibody labeled with the enzyme that converts its substrate (added in a separated step) to the easily detectible form. One of the major advantages of ELISA is its ability to perform chemical signal amplification by accumulating product of the enzymatic reaction.

A major disadvantage of the current formats of the affinity assays is that they are slow and often manually intensive. Typically, incubation steps of several hours are required as well as numerous washing steps. Significant levels of automation and parallel analysis brought to the field by advances in robotics and computers decreased human involvement and shortened time required for the assay; however, applications that do not allow parallel analysis such as chemical monitoring, clinical assays, and process control are still difficult or impossible to perform in a reasonable amount of time.

Capillary Electrophoresis

Capillary electrophoresis is a highly efficient separation technique based on the differences in migration of analytes in a high electric field applied across a narrow-bore capillary (5 – 100 μm i.d.). The small cross section of the capillary results in less sample consumption and, more importantly, higher electrical resistance and heat dissipation compared to the conventional electrophoresis. An added advantage to the technique is the plug flow profile that results in a significantly less band broadening than parabolic flow profile in liquid chromatography. Combination of the above properties results in highly efficient separation that requires a small amount of sample. Many different modes of capillary electrophoresis have been described including capillary zone electrophoresis (CE or CZE), capillary gel electrophoresis (CGE), micellar electrokinetic capillary chromatography (MEKC or MECC), capillary electrochromatography (CEC), capillary isoelectric focusing (CIEF), and capillary isotachophoresis (CITP). Although all of the modes of capillary electrophoresis have been used, the free zone mode is the most

popular. In addition, zone CE has been the only mode used in development of the described work.

Most common CE instrumentation consists of a fused silica capillary with inside diameter (i.d.) ranging between 5 and 100 μm. Each end of the capillary is immersed in a vial containing separation buffer and electrodes which connect the capillary to the high voltage power supply. Voltages up to 30 kV are used routinely; however, much higher voltages have been reported (Hut00). This applied voltage causes sample to move inside the capillary by two mechanisms: electrophoretic mobility and electroosmotic flow. The electrophoretic mobility of a charged sphere is approximated by Debye-Huckel-Henry equation:

$$\mu = q / 6\pi\eta r \tag{1.1}$$

where q is the charge of the particle, η is the viscosity of the buffer, and r is the Stokes radius of the particle. The mass of the particle, M, can be related to the Stokes' radius by $M=(4/3)\pi r^3 V$, where V is the partial specific volume of the solute. With the additional derivation and empirical observations, it is possible to determine that electrophoretic mobility of a molecule is directly proportional to the charge and inversely proportional to the mass to the 2/3 power (Chu92):

$$\mu \propto q / M^{2/3} \tag{1.2}$$

For bare fused silica capillaries, electroosmotic flow (EOF) originates from the negative charges on the inner wall of the capillary under appropriate conditions. These negative charges cause the formation of the double layer adjacent to the stagnant Helmlotz layer. Positively charged molecules on the solution side of the double layer

migrate toward the negative electrode under electric filed dragging the solvent with them. Linear velocity, ν, of the EOF is given by

$$\nu = \varepsilon\xi E / 4\pi\eta, \tag{1.3}$$

where ε is the dielectric constant of the solution, ξ is zeta potential which is related to the separation buffer, pH, and condition of the capillary wall, E is the applied electric filed, and η is the viscosity of the solution. Since the double layer is typically very thin, compared to the size of the capillary, the EOF is considered to originate at the walls of the capillary and, therefore, gives rise to the plug flow profile. This increases efficiency of separation by reducing broadening caused by the parabolic flow profile commonly observed in pressure driven systems such as HPLC (Ste83).

Detection Methods in CE

Commonly used detection systems for capillary electrophoresis are fluorescence detection, absorbance detection, amperometric detection, conductivity detection, refractive index gradient detection, and mass-spectroscopic (MS) detection. Although all of these types of detectors have important advantages, such techniques as conductivity detection, and refractive index gradient detection do not possess sufficient sensitivity to be used for high sensitivity CE affinity assays. Extremely sensitive and selective MS detection could be used for the assays; however, the fact that the identity of analyte is known prior to the experiment together with the price tag of the MS system makes it an unlikely choice as a detector.

Laser-Induced Fluorescence (LIF) Detection

LIF is the one of the most sensitive detection techniques developed for CE. Since LIF is concentration sensitive, high sensitivity can be achieved even in the smallest capillaries. Detection limits on the level of yoctomoles (10^{-24} moles) have been demonstrated as has counting individual molecules during rapid separations (Che94a, Fis98). A limitation of LIF detection is that most analytes are not fluorescent and, therefore, require derivatization. An ideal derivatization reagent should possess the following characteristics: 1) fast and favorable reaction kinetics with the analyte; 2) high fluorescent yield of the reaction product; 3) good stability before and after derivatization. A majority of the derivatization methods and reagents for CE have recently been reviewed in literature (Bar97). Some of the more common derivatization reagents used to label primary amines include dansyl (DNS), *o*-phthalaldehyde (OPA, fluorogenic reagent), naphthalene-dialdehyde (NDA), fluorescein isothiocyanate (FITC), Fluorescein succinmidyl ester, flouorescamine, phenylthiohydantoin derivatives (PHT), and 3-(2-furoyl) quinoline-2-carbaldehyde (FQ) (Hau96).

Amperometric Detection

Electrochemical detection has the appropriate sensitivity to be used with capillary columns used in CE (Ewi94). Since CE requires high electric fields that might interfere with electrochemical detection, special designs have to be used to isolate electrochemical current measurements from the CE circuitry. On-column and end-column designs have both been successfully used (Hua87, Hua91, Wal88) for amperometric detection. Excessive band broadening associated with the electrode size, adjoining capillary (off-column detection), or column-electrode spacing (end-column detection) is possible

especially in the case where separation capillary is short. Utilization of chip-based systems with integrated electrochemical detection may allow the control needed for rapid separation. As an example of this direction, Woolley *et al.* (Woo98) separated 3 electroactive small molecules in less than 100 s on a chip with an integrated Pt working electrode. Another potential limitation of using amperometry for fast separations is that fast separations will have the maximum current flow and this electrophoresis current is a dominant source of noise in electrochemical detection.

Absorbance Detection

UV-Visible absorbance detection is one of the most frequently utilized detection techniques for CE. The main reason for the popularity of the absorbance detection is its universal nature and widespread availability. However, Beer's law indicates that small i.d. capillaries with short path length will produce small absorbance values. The short path length limitation can be counteracted by Z-shaped flow cells (Che90), multi-reflection cells (Wan91), rectangular capillaries (Tsu90), bubble cell capillaries (Xue94), and signal averaging by use of a photodiode array (Cul98). Most of these techniques, however, require changes to capillary profile, which may decrease the separation efficiency of the system.

Sample Injection in CE

In most separation systems, sample volume injected onto the separation column should not exceed 1-5% of the total column volume. This results in the need for reproducible injections of sub-microliter volumes in cases of standard CE and sub-nanoliter volumes in cases where short narrow-bore capillaries are used. Hydrodynamic

and electrokinetic modes are the most widely used procedures for the sample loading. During hydrodynamic loading, sample is forced onto the capillary by means of pressure, vacuum, or siphoning achieved by the elevating injection end of the capillary. In electrokinetic sample loading, the injection end of the capillary is immersed into the vial that contains the sample and high voltage connection. The other end of the capillary is kept in the separation buffer. Upon application of a voltage for a short period of time, sample plug will be drawn into the capillary by electric filed and EOF. After injection, the inlet of the capillary is returned to the buffer vial and separation voltage is applied. An important property of the electrokinetic sample loading is the fact that the quantity of the sample loaded depends on the electrophoretic mobility of sample components. This means that sample components with higher electrophoretic mobility will be injected in larger quantities compared to samples with low mobility. Thus, results obtained with electrokinetic loading frequently do not correspond to the actual sample concentration.

Despite the wide universality of these techniques, injection of even smaller volumes without significant band broadening is challenging. Additionally, in cases where separation length is shorter than a few centimeters, utilization of the above methods is technologically difficult. In these cases, sample loading has been performed using gating techniques. One type of the gating injection is flow gating (Lem93). In flow gating (see Figure 1-1), sample stream is directed towards a flow gate by any means. At the interface, a high volumetric flow of separation buffer (typical volumetric flow rates for the gating flow are between 0.3 and 1.0 mL/min) washes sample stream to waist. To perform an injection, a pneumatically actuated valve stops the gating flow for a brief period of time (usually between 50 and 250 ms), and small volumes of sample can then

be drawn onto the separation capillary by electrokinetic effects. Refinements to this system have since been described (Hoo97) including altering the voltage during the injection to achieve an additional level of control over the injection volume and using conically shaped capillary tips to improve the fluid dynamics around the column inlet. Photographs of the injection process showing the flow are illustrated in Figure 1-2. Using this improved interface, separations with over 480,000 plates in just 35 s have been achieved for several FITC labeled amino acids (Lem93). Equally important, the precision of such injections results in relative standard deviations below 4% for all analytes. Finally, the method is well suited for ultra-micro scale analysis as flow rates through the sample capillary can be used from 79 nL/min up over 1 μL/min (Lad96, Lad97, Lad98).

Optical gating is another way to inject samples onto CE column in cases where LIF detection is used (Moo93). This injection technique takes advantage of the fact that fluorescent molecules can be photodegraded by high power laser beam. The system for optical gating consists of two laser beams focused onto the separation capillary. One of the beams focused at the injection end of the capillary has the power required to photobleach fluorescent components of the solution. The other beam focused at the detection end of the capillary is used to perform LIF detection. Separation length is defined by distance between two beams. To perform the separation, the injection end of the capillary is immersed in the sample that allows sample to be electrokinetially pumped towards detection. Once the sample reaches the photobleaching beam, the majority of fluorescent molecules are bleached which renders them undetected. When injection is needed, a shutter is used to close the photobleaching beam for a short time, thus allowing

a small plug of fluorescent sample to pass through. This plug is then separated by the usual means and detected at the detection beam.

Capillary Electrophoresis Affinity Assays

Capillary electrophoresis (CE) affinity assays are a collection of analytical techniques in which an affinity probe (AP) is allowed to bind to the target analyte (T) and the resulting complexes separated from free reagent by CE. As with the standard types of the affinity assay, competitive and non-competitive formats of the CE-affinity assays are possible. In a competitive assay, a labeled target (T*) competes with T for binding to a limited amount of AP. CE (equipped with the necessary detection system to detect the label) produces two distinct peaks corresponding to T* and T*-AP complex, the intensities of which can be related to the original concentration of T. In a non-competitive assay, an excess of labeled affinity probe (AP*) is added to the solution containing T. A CE separation of AP* and T-AP* allows for determination of concentration of T.

The main principle that allows separation of assay components by the CE is change in the electrophoretic mobility of the analyte upon binding of affinity probe. As indicated earlier, electrophoretic mobility, μ, of the sample is proportional to $q/M^{2/3}$, thus, a change in mass and in charge that occurs upon binding will result in a change in net electrophoretic mobility of complex as depicted in Table 1-1 (Chu92). From this table, it is easy to see that success of the CE affinity assay depends heavily on the differences in the charges and masses of interactive molecules.

Table 1-1. Theoretical basis for the CE affinity assays

	T	+	AP	=	AP:T
Mass	m		M		M + m
Net Charge	q		Q		Q + q
Mobility	$q / m^{2/3}$		$Q / M^{2/3}$		$(Q + q) / (M + m)^{2/3}$

Since complex formation and stability are key factors in successful affinity assays, time scale of separation is important. Non-covalent AP-T complexes have a limited half-life ($t_{1/2}$), which can be expressed by the following equation:

$$t_{1/2} = \ln 2 / k_{-1}. \tag{1.4}$$

In order to detect complex quantitatively, the separation must be considerably faster than the $t_{1/2}$ of the complex; therefore, speed of separation becomes important, especially in cases where the dissociation rate is fast. If separation is significantly fast, the size of both free and complex peaks should represent equilibrium concentration of the respective species, thus allowing determination of dissociation constants. As will be seen in some of the examples given below, the speed of separation is also important since immunoassays are an important component of clinical assays and drug monitoring where high throughput or rapid feedback are necessary.

Compared to conventional affinity probe assays, such as ELISA or RIA, CE-based methods offer a number of advantages including 1) higher mass sensitivity, 2) faster analysis for single assays, 3) potential for real-time monitoring, and 4) compatibility with multi-analyte determination. CE-based assays are usually no better, and are often worse, than other types of affinity probe assays in terms of concentration detection limits. The use of preconcentration techniques in combination with CE affinity

assays, as discussed later in this work, may generate assays with comparable or superior concentration detection limits. With appropriate automation or parallel operation, the throughput possible with a CE-based assay is at least as high as conventional ELISA's; however, this has yet to be demonstrated.

To date, a majority of CE affinity assays have been immunoassays since antibody is the most popular type of the AP. However, other ligands mentioned above may be used as APs including phage display peptides (Smi97), aptamers (Tue90, Osb97), combinatorially selected ligands (Lam97), or naturally occurring ligands such as receptors (Oft88) or transcription factors (Xue97, Ste96).

Non-competitive Assays

In a non-competitive CE affinity assay, also called an affinity probe capillary electrophoresis (APCE) (Shi94), an excess of labeled AP (AP*) is added to sample solution and is used to determine the target. Such format of the affinity assay can be described by the following equilibrium:

$$AP^* + T \rightleftarrows AP^*{:}T. \tag{1.5}$$

Once the equilibrium is established, a CE separation of the mixture would produce two detectable bands corresponding to the remaining excess of AP* and to AP*:T complex. Barring kinetic dissociation of the complex on the time scale of CE separation and a favorable affinity constant of the AP*, the AP*:T peak is a direct measure of the T present in the solution. An important property of the direct affinity assay is ability to detect a possible cross-reactive species. If the sample contains a cross-reactive analyte T' (a frequent possibility in cases where specificity of antibody is inadequate), such analyte

will also form a complex with the AP* that can be effectively detected provided it can be separated from the other analytes by the CE.

Quantitatively, the following equation relates concentration of the complex to concentrations of original constituents (denoted by subscript 0):

$$[AP^*:T] = [T]_0 \{ [AP^*]_0 / (K_d + [AP^*]_0) \}, \qquad (1.6)$$

where K_d is the equilibrium dissociation constant. This equation assumes that $[AP^*]_0 >> [T]_0$, and demonstrates two important properties of the assay: (1) expected linearity of the assay, and (2) the assay's diminished dependency on the value of K_d as any significant increase in it can be counteracted by the increase in the experimentally controlled $[AP^*]_0$. In cases where the above assumption cannot be fulfilled, a theoretical calibration curve for the non-competitive assay can be generated using the following equation:

$$[AP^*:T]^2 - [AP^*:T] \{ [AP^*]_0 + [T]_0 + K_d \} + [AP^*]_0[T]_0 = 0 \qquad (1.7)$$

A series of the theoretical calibration curves with different K_ds are shown on Figure 1-3. To generate this series of curves, the [AP*] was set at 5 nM and kept constant, and K_d values were 0.01, 3, and 50 nM. As evident from the figure, even when the [AP*] is kept constant and at the moderate levels, the calibration curve still has a large linear region and K_d has small effect on the slope of the linear region of the calibration curve.

Non-competitive assays are the preferred mode of assay since, compared to competitive assays, they have 1) larger linear dynamic range, 2) better detection limits, and 3) easier detection of cross-reactivity. Despite these advantages, non-competitive assays have not been as fully developed because of two problems that make them harder to implement. The first problem is if the affinity probe is a large complex molecule, e.g., an antibody or antibody fragment, it can be difficult to label such that a homogenous

product is formed. Inhomogeneous products lead to broad or multiple peaks that can be difficult to separate from the complex. The second problem is the separation may also be difficult if the AP is a large molecule and the target is relatively small since the electrophoretic mobility of the complex may not be significantly different from the AP. Despite these difficulties, a number of non-competitive assays have been successfully demonstrated.

The most popular application of non-competitive assays has been for determination of antibodies. In an early example, FITC-insulin was used as an affinity probe to determine anti-insulin with a 60 s separation in a simple demonstration of the concept (Sch95). Reif *et al.* developed a method for detecting human IgG using FITC-labeled protein G (Rei94). Protein G has a natural affinity to bind to the Fc region of antibody and can be used in the CE-AP assay to detect IgG. To perform the assay, the authors mixed previously labeled protein G with the human IgG and incubated for a certain amount of time. The mixture was then hydrodynamically injected on to a 27 cm long (20 cm effective) 50 μm id capillary. Separation of the analytes was performed in less than 3 min using 15 kV applied across the capillary filled with 0.05 M borate buffer (pH 10.5). The authors indicated that if the separation took longer than 3 min, the majority of the complex would dissociate. Thus, separation time had to be minimized. Length of incubation had little effect on the complex suggesting rapid formation of complexes; however, increase in the temperature of incubation significantly decreased the size of the complex peak. Using the above separation conditions and incubation at 20 ^{o}C, the authors were successful in measuring concentrations of IgG in serum. Furthermore, the authors developed a sandwich assay in which a mixture of protein G

and anti-human IgG_1 has been added to the serum. After incubation, the mixture was separated and revealed two bands corresponding to protein G-anti-human IgG_1 and to protein G-anti-human IgG_1-IgG_1. One of the disadvantages of this method was formation of excessively wide peaks due to inhomogeneity of FITC-protein G. This group was also able to use Protein A as an affinity probe for IgG (Lau95). In this case, they were able to obtain a separation between the affinity complex and FITC-protein A in under 3 min.

Rapid CE-AP assays have been used to screen antibodies and evaluate their binding and crossreactivity for the antigen. Evangelista *et al.* used Cy5-labelled morphine to determine the best commercially available antibody against morphine and to analyze its crossreactivity with morphine analogs (Eva94). In this work, a 25 cm long 20 μm id capillary was used to obtain a complete separation of the complex in under 2 min. The authors used 0.01 M phosphate buffer at pH 7.0 as background electrolyte and applied 20 kV. Due to vast variation between commercially available antibodies, it is important to be able to screen for the best antibody for a given application. The authors have determined that for their desired application, the Biodesign (Biodesign International, Kennebunkport, ME) produced antibody performed the best. The authors also tested this antibody for cross-reactivity with nine morphine analogues and determined that the antibody has poor affinity for them. According to the authors this antibody can be used for the practical drug screening and forensic analysis.

One of the problems often encountered during non-competitive assays is little or no difference in migration between the complex and a free affinity probe. Chen utilized charge modification to change the electrophoretic mobility of FITC-anti-IgA used to determine IgA (Che94a). He used succinic anhydride to gain extra negative charge on

the surface of the FITC-anti-IgA. Using a 27 cm long 20 μm id capillary filled with borate buffer (pH 10.2), he was able to obtain a separation between free and bound IgA in under 120 s (applied potential 20 kV). Again, the width of the peaks appears excessive due to inhomogeneity of FITC-anti-IgA. The reported detection limit for IgA was 66 nM.

While determination of antibodies is certainly an important application, the ability to expand this technique to other targets would be important for widespread acceptance and application. An elegant solution to the problems of antibody labeling, effective separation, and preconcentration has been demonstrated by Shimura *et al.* (Shi94). In this report, a Fab' fragment was labeled with iodoacetamidorhodamine at a free thiol formed at the hinge region away from the binding site allowing formation of a singly labeled protein that formed a narrow band in separation. The separation performed by isoelectric focusing which gave good resolution of bound and free AP (the target was human growth hormone). Furthermore, the IEF allowed a significant preconcentration for a detection limit in the low picomolar range. The only drawback of the method was the low yield in production of the labeled Fab' and the slow speed of the IEF separation (several minutes).

Non-competitive assays have also been used to study protein-DNA interactions involved in transcription. Such binding experiments have typically been performed as described above for non-competitive CE affinity assays except the separation was done by gel electrophoresis and the technique called gel-mobility shift assay. When done by conventional gel electrophoresis, a dense gel must be used to allow "caging," an effect in which dissociated components of a complex are held in the pores of a gel and allowed to

reform complex before separating. Using CE, the separation is fast enough that caging does not need to be used for detection of complexes (Can98).

Competitive Assays

Competitive assays make use of a tracer molecule (T*), which commonly is a labeled target molecule although a separate cross-reactive to the AP target can be used. To perform the assay, a limited amount of antibody is added to the sample already containing T and T*. The resulting equilibria is given by the subsequent set of equations:

$$\begin{aligned} T^* + AP &\rightleftarrows T^*{:}AP \\ T + AP &\rightleftarrows T{:}AP \end{aligned} \tag{1.8}$$

During the equilibration, the tracer is competing with the analyte for binding to the limited number of binding sites, and the amount of the AP-T* complex depends primarily on the amount of analyte present. An ensuing CE separation reveals two bands, one corresponding to the T* and the other to the T*:AP. Since at no time is the analyte or its complex detected, the assay is an indirect measurement in which analyte is determined by measuring either of the peaks or, more frequently, by a ratio of both peaks. Contrary to the direct assays, indirect assays do not provide the means for detection of any cross-reactive analytes that might be present in the sample.

Although non-competitive assays have analytical advantages discussed above, competitive assays have been much more popular due to their ease of implementation, especially for small analytes. In this case, the small analyte can be simply labeled and the separation required (T* from T*:AP) is much simpler.

In our laboratory, significant amount of work has been put forward to develop a competitive immunoassay for insulin. In early versions, the assay was performed in a 4 cm separation distance (25 μm i.d.) at 3000 V/cm. Using these conditions complete

separation of bound and free FITC-insulin was achieved in about 7 s. Since our final goal was to develop a system for monitoring release of insulin by the single islet of Langerhans with high temporal resolution, the above assay was further improve to allow on-line reaction of insulin and the antibody. Additionally, the separation capillary was shortened to an injection to detector length of only 8 mm and the i.d. of the separation capillary was decreased to 5 μm to allow E = 4000 V/cm. The automated assay system incorporated a flow-gated interface with injection times of 200 ms. Such modifications resulted in complete separation between bound and free FITC-insulin in about 1 s. (Tao98). This system allowed continuous monitoring of insulin in sample streams for several hours generating thousands of assays. This device was demonstrated for flow injection analysis and for continuous monitoring of the release of insulin from single islets of Langerhans (Tao96). These assays have a concentration detection limit of 270 pM and a mass detection limit of 432 zmol.

Schmalzing *et al.* have developed a competitive immunoassay for determination of cortisol in serum (Sch95a, Sch95b). In the assay, the authors used fluorescein labeled cortisol molecules as tracer which competed with analyte cortisol for binding the antibody. A 50 μm id 20 cm long (27 cm total length) coated capillary filled with 20 mM TAPS/AMPD buffer (pH 8.8) was used to perform the analysis. The authors investigated possible use of polyclonal or monoclonal antibodies and antibody fragments for the analysis. Although use of antibody fragments produced the best complex peak shapes in a 2 min. long separation as depicted on Figure 1-4, the authors indicate that polyclonal antibodies can be successfully used for the assay when determination is made using free cortisol peak only. The same group was able to perform similar assays on a microchip

suggesting the possibility of a highly automated immunoassay (Lou96). In these experiments, a 2.2 cm long channel with cross-sectional area that is equivalent to that of a 44 μm id capillary and E = 800 V/cm, the authors were able to perform separations in less than 30 s. This work demonstrated repetitive injections of the same sample mixed on-line in a chip. Several other groups have investigated applications of microchips to the immunoassays (Bru95, Chi97).

Ye *et al.* have used competitive CE immunoassay to rapidly determine cyclosporine A (CsA) (Ye98). To improve detection limits, the authors used a sheath flow cuvette with a fluorescence polarization detector. The assay performed using 10 mM phosphate buffer in a 40 cm long 20 μm id capillary was completed in less than 3 min and had a limit of detection for CsA of 0.9 nM (applied electric field was 500 V/cm). This method was successfully used to analyze whole blood samples from patients who were administrated the drug. This work presents another example of the clinical assay that has the speed and detection limits better than that of any currently utilized method. The authors indicate that one possible problem that could be encountered during development of similar or more complex immunoassays is cross reactivity of antibodies. One possible solution could be initial separation of the sample by other method such as HPLC followed by either on-line or off-line immunochemical reaction. Additionally, the analytes could be preconcentrated during the first separation step to improve limits of detection.

High separation power of CE allows for simultaneous multianalyte analysis by competitive immunoassay. Chen *et al.* have developed an assay for the analysis of urine for two drugs of abuse (Che94a). Morphine was derivatized with fluorescent label Cy5

and phenycilidine (PCP) was tagged with Cy5.5 for the analysis. In about 5 min, the authors were able to fully resolve all 4 peaks. The experimental conditions were 200 mM borate buffer (pH 10.2), untreated 27 cm long 20 μm id capillary. The authors indicated that they were able to perform the analysis routinely and reproducibly with detection limits of 4 nM for PCP and 40 nM for morphine.

Binding Constant Determination by CE-Affinity Assays

High speed and low limits of detection possible with CE-AP-LIF assays provide opportunity for simple and rapid measurement of binding constant between AP and T. Flouds and Etzkorn have measured a binding constant between yeast transcription activator GCNK58 and DNA sequence for which it is specific using CE (Fou98). In the experiment, fluorescein-labeled DNA molecule was mixed with the transcription activator and allowed to equilibrate. The mixture was than injected on to a 20 cm long (effective, 27 cm total) 75 μm id capillary and separated in less than 2 min. Separation was performed in 10 mM MOPS/TEA pH7.5 and applied voltage of 25 kV. By injecting a mixture containing several different concentrations of transcription activator and measuring the ratio between bond and free DNA, the authors were able to determine the binding constant of 35 nM.

In our laboratory, CE-AP-LIF system was used to determine binding constant between insulin and anti-insulin (Tao96). Additionally, inter-species binding constants were determined by allowing monoclonal anti-insulin to react with insulin from several species. By measuring the ratios of bound and free FITC-labeled insulin peaks, the binding constants for ovine, equine, porcine, bovine, and human species of insulins were measured.

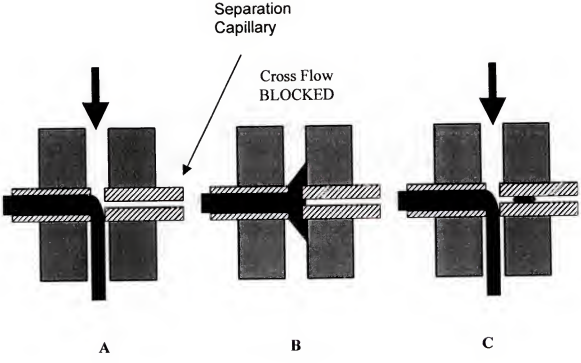

Figure 1-1. Operation of a flow-gated interface. (A) Normal operation. Sample is pumped towards a separation capillary where it is washed away by the cross-flow. (B) When cross-flow is blocked by a high-speed switching valve, a small pool of sample is formed in the junction between capillaries. Some of that sample is injected electrokinetically onto the separation capillary. (C) Cross flow is restored. Remaining sample is washed away.

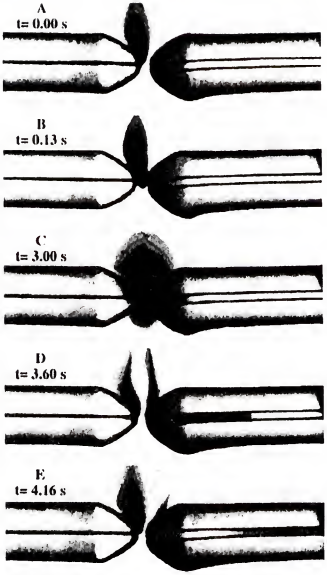

Figure 1-2. Frame-grabbed video images of the injection process using the flow gated interface. On the left, a solution of methylene blue dye is flowing out of a coned 17 μm i.d., 360 μm o.d. capillary into a $^{1}/_{16}$ in. channel in the interface through which the transverse buffer flows. On the right is a coned 50 μm i.d., 360 μm o.d. capillary into which electrophoretic injections of the dye are performed. In (A), the run voltage has been dropped to zero while the transverse flow remains on. In (B), the transverse flow has been shut off allowing sample to flow across from the infusion capillary to the CZE capillary. The electrokinetic injection is underway in (C), and a plug of sample can be seen filling the inlet of the capillary. The transverse flow has resumed and sample is washed out of the gap between the capillaries in (D). In (E), the gap between the capillaries is completely filled with buffer and the plug of dye has begun to migrate down the capillary due to the applied electric field. (Reprinted from Hoo97)

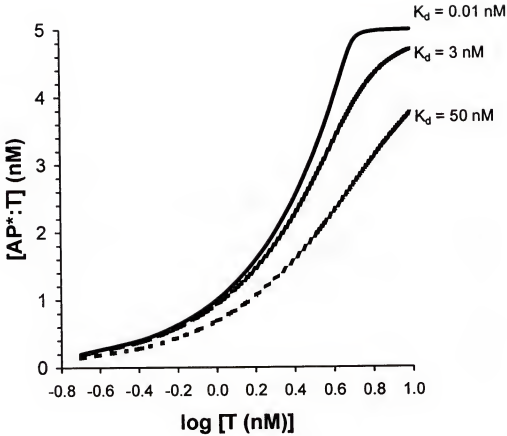

Figure 1-3. Series of calibration curve for a non-competitive affinity probe assays with different equillibrium dissociation constants.

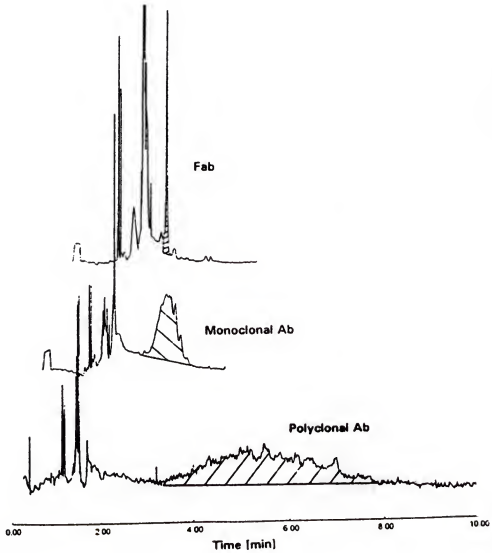

Figure 1-4. Comparison of the complex signal produced with three different antibody preparations for a cortisol CE competitive immunoassay. Conditions: 8 s pressure injection, coated capillary, 27 cm effective, 30 cm total length, 50 μm id. 20 mM TAPS/AMPD, pH 8.8, 30 kV. (Reprinted from Sch95a)

CHAPTER 2
APTAMERS AS LIGANDS IN AFFINITY PROBE CAPILLARY ELECTROPHORESIS

Introduction

Affinity probe capillary electrophoresis (APCE) refers to a collection of techniques in which high affinity binding is used in conjunction with CE separation to determine analytes. Combined with laser-induced fluorescence (LIF) detection, this technique has demonstrated potential for rapid determination of trace levels of analytes in complex mixtures (Sch93, Bao97, Ken97). Although APCE could involve many types of binding, the most commonly used form is immunoassay involving antigen (Ag)-antibody (Ab) binding. Both competitive (Sch93, Kou96) and non-competitive immunoassays (Shi94) have been described. In a competitive assay, a fluorescently labeled antigen (Ag*) competes with Ag for binding to a limiting amount of Ab. CE separation of the mixture produces two distinct fluorescent peaks corresponding to Ag* and Ag*-Ab complex, the intensities of which can be related to the original concentration of Ag (Tao96). In a non-competitive assay, excess of fluorescently labeled antibody (Ab*) is added to the solution containing Ag. A CE separation of Ab* and Ag-Ab* allows for determination of concentration of Ag.

In principle, non-competitive assays possess several advantages over competitive assays including larger linear dynamic range, detection limits that are less dependent

upon the binding constant between Ag and Ab, and ability to distinguish among cross-reactive species (Shi94). Despite these advantages, several practical problems have limited the development of non-competitive assays. The antibody itself can be difficult to fluorescently label such that a single, homogenous product is formed. Furthermore, Ab* may be difficult to separate from the Ab*-Ag complex, especially if the analyte is small and does not affect the electrophoretic mobility of Ab* significantly. Finally, antibodies have widely varying properties making their electrophoresis difficult to predict. Thus, despite the advantages of non-competitive assays, the majority of assays developed to date have utilized the competitive format (Sch93, Bao97, Eva94, Ste95).

A possible way to circumvent many of the disadvantages of the non-competitive assay is to utilize alternative ligands, which possess the desirable binding characteristics of an antibody but without the same limitations. In this work, we explore the possibility of using aptamers as such affinity probes. Aptamers are generally single-stranded DNA or RNA oligonucleotides that can specifically bind to target molecules with high affinity. Aptamers are developed using a combinatorial process known as systematic evolution of ligands by exponential enrichment (SELEX) (Joc89, Ell90, Tue90). In SELEX, a pool containing 10^{15} or more oligonucleotide molecules of the same length with randomized sequences is tested for binding to a target molecule by filter binding assays or similar methods. Binding molecules are collected, amplified by PCR (after reverse transcription if RNA is being used), and the resulting pool re-tested for binding. Several rounds of selection cause the pool to evolve towards a small collection of the tightest binding sequences. The best binding sequences can then be identified and synthesized by automated methods. SELEX relies on the assumption that the diversity of a large initial

pool will ensure that molecules possessing tertiary structures capable of tight binding to the target molecule will be found (Klu94). Aptamers for a variety of targets including proteins (Tue92, Par96), peptides (Nie95, Wil97), dyes (Ell92), amino acids (Fam92, Fam94), nucleotides (Sas93), and drugs (Jen94) have been identified using this method. While aptamers have generally been of interest for their potential as drugs, several groups have explored their use as analytical reagents in various applications including flow cytometry (Dav96), biosensors (Kle98, Hie98), and ELISA-type assays (Dro96).

Aptamers possess several properties that should make them especially valuable in APCE applications for non-competitive assays. In particular, aptamers are simple to fluorescently label to form a single product, inexpensive to synthesize in an automated format, and are highly stable (especially DNA aptamers). Their small size (most have molecular weights of a few thousand) and negative charge should make separation of free and target-bound aptamers straightforward. In this paper, we investigate application of aptamers to non-competitive APCE. As model systems, we have developed assays for human IgE and human thrombin using fluorescently labeled DNA-based aptamers. Neither of these targets have shown natural affinity to DNA, and the aptamers for them had been previously selected and characterized (Wie96, Boc92). The presented data demonstrates the potential of aptamers as affinity probes for highly sensitive and selective APCE assays.

Experimental

Chemicals

Unless stated otherwise, all chemicals, including serum samples, used in the experiments were purchased from Sigma Chemical Co. (St. Louis, MO). 4(5)-

carboxyfluorescein was purchased from Aldrich Chemical Co. (Milwaukee, WI). Human myeloma IgE was purchased from Athens Research and Technology, Inc. (Athens, GA). Oligonucleotides were synthesized and fluorescently labeled by Integrated DNA Technologies, Inc. (Coralville, IA). The fluorescein isothiocyanate (FITC) label was directly attached to the 5' end of the thrombin binding aptamer (5'-GGTTGGTGTGGTTGG-3'). IgE binding aptamer (5'-GGGGCACGTT TATCCGTCCC TCCTAGTGGCGTGCCCC-3') was labeled with FITC during synthesis at the 5' end using ethylene glycol linker (Figure 2-1) to reduce possible fluorescence quenching (Dav96). All solutions were made with deionized water purified by a Milli-Q Plus System (Millipore Corp., Marlborough, MA).

Capillary Electrophoresis

The CE apparatus used in this work consisted of two buffer reservoirs, a 30 cm long by 50 μm inner diameter and 360 μm outer diameter fused silica capillary column (Polymicro Technologies, Phoenix, AZ), and high voltage power supply (CZE 1000R Spellman High Voltage Electronics, Plainview, NY). The inner wall of the fused silica capillary was coated with polyacrylamide using a procedure described elsewhere (Sri97). The injection to detection length was 7 cm unless indicated otherwise. Electrophoresis buffer consisted of 5 mM Na_2HPO_4, 5 mM KH_2PO_4, 2 mM $MgCl_2$ (pH 8.2 unless stated otherwise) and was prepared daily. At the beginning of each day the column was rinsed with dilute acetic acid (pH 3) and electrophoresis buffer for 5 min each. For some separations, a vacuum pump (Air Dimensions Inc., Deerfield Beach, FL) was used to apply vacuum to the anode buffer reservoir to mobilize slow moving species. Detection was accomplished using a LIF detector described elsewhere (Tao97). Briefly, the LIF

detector used the 488 nm line of a 15 mW Ar ion laser (Spectra Physics, Mountain View, CA) as an excitation source. Fluorescence was collected through a 40x microscope objective (Melles Griot, Irvine, CA). Before detection by the photomultiplier tube (Model E717-21, Hamamatsu Photonics, Bridgewater, NJ), fluorescence was filtered both spectrally, using a 520 ±10 nm bandpass filter (Corion, Holliston, MA), and spatially, through two pinholes (5 mm x 7 mm and 1.5 x 4 mm). Signal from the PMT was amplified by a Keithley 428 current amplifier and collected using 486DX2-66Mz personal computer equipped with data acquisition board (AT-MIO-16, National Instruments, Austin, TX) controlled by the locally written software.

Aptamer-Based APCE

Before analysis, aptamer stock solutions (5 μM in electrophoresis buffer) were heated to 70 °C for 15 min and allowed to cool slowly to room temperature to place the aptamer in its favorable thermodynamic conformation. The desired volumes of 5 μM aptamer dissolved in separation buffer (the pH was always adjusted to 7.4 for sample mixing and incubation) and 1 mg/mL target (thrombin or IgE) dissolved in phosphate buffered saline were added to a volume of electrophoresis buffer so that the final volume was 30 μL. The resulting sample was mixed and incubated for at least 3 min at room temperature, and then injected into the separation capillary hydrodynamically ($\Delta h = 8$ cm) for 2 s. An electric field of 620 V/cm was used to drive the separation. For high flow experiments, a vacuum was applied to the anode buffer reservoir beginning 1 to 2 s after the free labeled-aptamer (A*) peak migrated past the detector. After each separation, the capillary was rinsed with dilute acetic acid (pH 3) and separation buffer for 3 min each.

Serum Sample Preparation

Lyophilized human serum was reconstituted according to the supplier's direction and used without any further treatment. 15 μL of serum was mixed with 5 μL of previously heated and cooled 3 μM solution of A* in electrophoresis buffer. Appropriate volumes of 5 μM IgE dissolved in phosphate buffered saline were spiked into the serum sample to produce the desired concentration. Separation buffer at pH 7.4 was used to bring the solution volume to a final volume of 30 μL. Samples were incubated and injected the same as the standards as indicated above.

Dissociation Constant Estimation

The dissociation constant (K_d) of A* with target (T) was estimated from calibration curves for the target as follows. Initial concentrations of A* and T and an arbitrary value of K_d were substituted into the expression for K_d ($K_d = [A^*][T]/[A^*\text{-}T]$) to predict the equilibrium concentrations of A* and A*-T. Predicted peak areas for A* and A*-T were determined by multiplying their equilibrium concentrations by previously determined response factors. Predicted peak areas were determined for all of the initial concentrations of A* and T used in the calibration curves, and results were compared to experimental values using least square analysis. K_d was varied until the best fit (minimum least squares) was obtained. Although it should be possible to use both A* and A*-T peaks to determine K_d, concern over the effects of possible loss of complex due to adsorption or dissociation led to use of the A* peak for K_d determinations.

Results and Discussion

Separation Conditions for Aptamer Assay for IgE

Figure 2-2A compares electropherograms obtained for 500 nM of A* at pH 7.4 with and without 500 nM IgE in the sample. Fluorescein was used as an internal standard for these two analyses. The electropherogram with IgE shows a significant decrease in the free A* peak which can be attributed to the binding of the aptamer to the IgE; however, no complex peak is observed in the electropherogram. We expected the complex to migrate after A* since IgE is nearly neutral at this pH (Joh67) so that the resulting complex should have the charge of A* and the frictional drag of the IgE-A* complex; however, even if the electropherogram is recorded for 600 s, a complex peak is not detected (not shown). We suspect that the absence of a complex peak under these conditions can be attributed to slow migration of the complex. During long migration times the complex may dissociate, releasing free A* over a long period preventing detection of a well-defined zone. Furthermore, slow migration may be exacerbated, or even caused by, adsorption of IgE to the capillary. Supporting this hypothesis, we observed that if the capillary was not rinsed between electropherograms, the baseline would drift up or ghost peaks would appear suggestive of migration of adsorbed material through the column.

In an attempt to prevent these effects, we increased the migration buffer pH to 8.2 (higher pH buffers have been shown to decrease adsorption of many proteins) and created hydrodynamic flow of 0.02 cm/s by raising the inlet of the capillary in order to increase the migration rate of the complex through capillary. With this combination of modifications, electropherograms were obtained which had a broad complex peak in addition to peaks for free A* and the internal standard (Figure 2-2B). Use of higher pH

alone did not result in detection of a complex peak. Use of hydrodynamic flow alone only produced complex peaks on exceptionally well-coated columns. Thus, minimization of adsorption and decreasing time on column were both necessary to achieve reliable detection of complex.

Further decreases in analysis time could be obtained by decreasing the separation distance to 7 cm and using a protocol of: 1) applying electric field for a long enough time to separate A* from complex and migrate it past the detector, and 2) subsequently applying vacuum to the outlet to rapidly pull the complex peak through the column for detection (voltage remained on). To prevent possible interference from the internal standard under these conditions, fluorescein was replaced with 4(5)-carboxyfluoresein which at pH 8.2 possesses charge of -2 and migrates faster than DNA. Figure 2-2C shows a set of electropherograms obtained under the above conditions and demonstrates detection of both free A* and complex peaks in under 60 s. In this case, samples contained 300 nM A* and the samples contained 300 nM IgE or 1 nM IgE. The tailing of the free A* peak seen in the 1 nM sample is due to several unresolved peaks from impurities in the DNA.

The use of hydrodynamic flow is generally not desirable since it provides a new source of band broadening. In this case however, it is not a significant problem since IgE migrates as such a broad zone under conventional electrophoretic conditions that the additional band broadening is insignificant. In the long term, a better alternative would be to identify electrophoresis conditions that prevent adsorption and obviate the need for hydrodynamic flow.

Quantification

The rapid separation conditions described above were used to construct calibration curves based on the complex peak and free A* peak as a function of IgE concentration (Figure 2-3). The curves are linear up to about 300 nM IgE above which a decreasing slope is observed indicative of saturation of binding as expected for this type of assay. The linear dynamic range can be extended at the high end by using higher concentrations of A*. The assay had good reproducibility as repeated separations of the sample containing 200 mM IgE and 300 nM A* had relative standard deviation of 3.3% (n = 5) when normalized to the internal standard. The calibration curves show that quantification can be obtained based on either the decrease in the A* peak or the increase in the complex peak. For low concentrations, detection of the complex peak is preferred since the measurement is made against instrumental noise whereas if measurement is based on A*, a small decrease in the large A* signal must be measured. Figure 2-2C (expanded portion) shows detection of 1 nM IgE complex peak using these conditions. Based on this data, the detection limit, calculated as the concentration yielding a signal 2 times the peak to peak noise, is 46 pM. The estimated injection volume is 0.8 nL giving a mass detection limit of 37 zmol.

As the IgE concentration is increased above the A* concentration, it is expected that eventually the A* peak would be reduced to undetectable levels and the complex peak would appear as large as the A* peak in the blank. As illustrated in the calibration curve, however, it was not possible to completely use up the A* and the complex peak was generally smaller than or equal to the free A* peak (both in height and area). This result is not due to fluorescence quenching upon binding as fluorescent measurements did not reveal quenching upon addition of IgE to A*. Rather, we believe that this is due to

two factors. First, loss of complex due to adsorption or dissociation would cause the complex peak to be smaller than expected. Second, if not all of the DNA is in the correct conformation for binding, then we may expect that it will not be possible to use up all of the A* in binding. Optimization of denaturation/renaturation conditions for the aptamer may help minimize the amount of oligonucleotide in the non-binding conformation. Both of these effects hurt the detection limit and it may be expected that better conditions would allow larger complex peaks and better detection limits.

Selectivity

To determine selectivity of the labeled affinity probe under these conditions, a series of control experiments was performed. In one experiment, IgG at concentrations from 100 to 1000 nM was incubated with 300 nM A* and the mixture separated as for an assay. Even though IgG is structurally similar to IgE, the added IgG had no effect on the A* peak and did not produce a complex peak illustrating the selectivity of A* for IgE. A second control experiment was performed to ensure that IgE did not bind to other sequences of DNA. Addition of 300 nM IgE to thrombin aptamer in the concentration range of 100 to 1000 nM had no effect on the aptamer peak and did not produce a complex. In a third experiment, we observed that omission of Mg^{2+} from the sample resulted in no binding to IgE. Since Mg^{2+} is necessary for forming the tertiary structure of this aptamer (Wie96), this result demonstrates the specificity of binding to only the correct conformation of A*. Finally, we further evaluated the selectivity of binding by performing a competition experiment in which different concentrations of unlabeled aptamer were mixed with 200 nM A* and 200 nM IgE. As illustrated in Figure 2-4, increasing concentration of unlabeled aptamer caused the expected decrease in A*-IgE

complex and increase in free A*. These results indicate that A* binds to the same site on IgE as unlabeled aptamer further indicating the specificity of binding.

Effect of Label on Binding

The above results illustrate that A* has high selectivity for binding to IgE as does unlabeled aptamer. The effect of addition of the label on binding can be further evaluated by estimation of the K_d. From the IgE calibration curve (Figure 2-3) data we estimated the K_d of A* to IgE to be 64 nM. Using a previously described model for competitive binding (Joh67, Tao96) we estimated the K_d of unlabeled aptamer-IgE to be 8 nM from the competitive calibration data. This calculated value agrees well with the published value of 10 nM (Wie96). Based on these numbers, it is apparent that addition of fluorescent label caused a significant decrease in binding affinity of aptamer for IgE. This is not unexpected as the tertiary structure of the oligonucleotide may be dependent upon the access to both the 5' and 3' ends for interaction. Other labels, linkers, or label positions could be used to optimize labeling and minimize the effect on binding.

Complex Samples

The possibility of performing APCE analysis in complex mixtures containing high concentrations of potential interferences was assessed by carrying out the assay in human serum. In this experiment, samples of human serum spiked with various concentrations of IgE were mixed with A* to a final concentration of 300 nM and analyzed. Figure 2-5 shows a series of electropherograms from different concentrations of IgE for this experiment. The results show that the complex sample had little effect on separation, dynamic range, or detection limit for the assay. The only observable effect was an increase in tailing of the A* peak in the presence of serum (see expanded portion

of Figure 2-5). This effect may be due to weak binding of A* with some substances in the sample or an injection artifact caused by the serum sample. This experiment demonstrates the ability of aptamers to selectively bind to their target in the presence of the large amount of interferences and the possibility of performing clinically relevant assays on biological fluid samples.

Aptamer based APCE for thrombin

The principle of aptamer-based APCE was further tested using a thrombin aptamer to detect thrombin. Thrombin aptamer is a significantly weaker binder than IgE aptamer with a K_d of ~200 nM (Boc92). Figure 2-6A shows a pair of electropherograms obtained under conditions of no flow in the capillary. The electropherogram on the right shows that in the presence of thrombin the A* peak decreases and a large tail to the right of the A* appears. The tail has a fairly abrupt end at about 50 s indicative of a complex peak that is rapidly dissociating during the separation causing bridging between the zones for free and bound A*. Raising the pH to 8.2 and application of vacuum induced flow as done for the IgE assay yields a reasonable complex peak as shown in Figure 2-6B. Even with these conditions however, the baseline separation of the complex from the free aptamer was not possible due to the bridging effect.

A calibration curve for thrombin based on peak heights had similar characteristics to that for IgE. The detection limit based on detection of the complex peak was calculated to be 40 nM. The higher detection limit relative to that obtained for IgE was presumably due to more significant loss of the complex by dissociation resulting from the poor binding constant. A competition experiment between labeled and unlabeled thrombin aptamer revealed specific binding by the A*. Based on the curves obtained

from that experiment and the calibration, we measured dissociation constants for both A* and unlabeled aptamer to thrombin to be about 450 nM which is about 55% higher than the published value of 200 nM (Boc92). This discrepancy may be due to use of different incubation conditions than was used for selection or perhaps rapid dissociation during the separation may have caused the dissociation constant to appear higher. Interestingly, both A* and unlabeled aptamer had similar dissociation constants suggesting no effect of the label on binding for this aptamer.

Conclusion

The data presented here demonstrate the feasibility of using aptamers as affinity probes in non-competitive APCE assays. Using conditions that promote rapid separation and migration allows observation of both free and bound aptamer even for dissociation constants of hundreds of nanomolar. Detection limits, linearity, selectivity, and assay speed are suggestive of assays that could have broad utility including clinical applications. Use of SELEX-derived aptamers instead of antibodies is advantageous because the affinity probe is easily and inexpensively prepared and the electrophoresis properties are easily predicted. At the same time, the binding and selectivity of aptamers are comparable to antibodies. Fluorescent labeling had some effect on binding in one case, but it was not severe as non-competitive assays are less dependent on binding constant compared to competitive assays. The main problem encountered was adsorption and dissociation of the complex. This effect is likely to be dependent on the analyte and will not necessarily be a problem in all cases. Better separation conditions should reduce this effect and result in better detection limits and higher resolution separations. The

development of higher resolution separation conditions will also allow multiple analyte determinations and detection of cross-reactive components.

Future development of this approach will depend largely upon improvement of aptamer technology. For example, the use of non-standard bases (Pic90) and modified backbone structures (Tha96) that are compatible with the SELEX process should allow for development of affinity probes for more diverse molecules, better binding and improved stability. Given continued development of aptamers, it seems that aptamer-based APCE has the potential for becoming a fast and inexpensive alternative to conventional immunoaffinity assays in some applications.

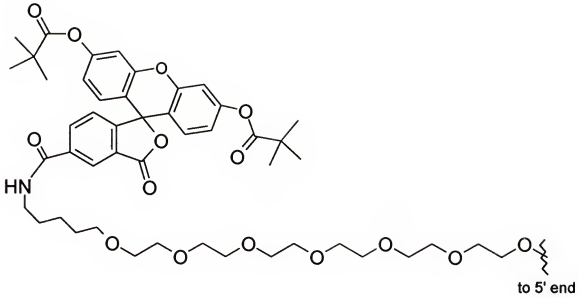

Figure 2-1. Structure of the fluorescein with ethylene glycol linker used to label IgE aptamer.

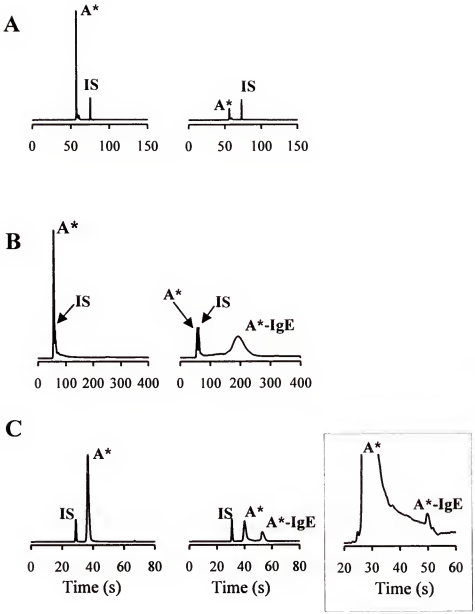

Figure 2-2. Determination of IgE using aptamer-based APCE. (A) Electropherograms obtained for 500 nM of A* with 0 (left) and 500 nM (right) IgE. (B) Separation of same solutions in 10 mM phosphate at pH 8.2 and gravity induced flow of 0.02 cm/s. (C) Solutions of 300 nM of A* with no IgE (left), 300 nM IgE (middle), and 1 nM IgE (right) were separated with injector to detector length of 7 cm. After 48 s of separation, a vacuum was applied to the outlet to rapidly pull the complex to the detector. Fluorescent signal scale for the 1 nM IgE sample is expanded by 10-fold relative to the other electropherograms.

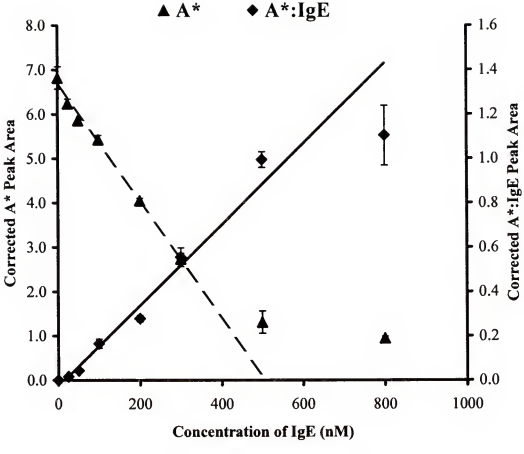

Figure 2-3. Calibration curve constructed using samples containing 300 nM A* with various concentrations of IgE. Peak areas were corrected for variations in injection volume by dividing by the area of the internal standard peak. Line is the best fit from linear regression for concentrations from 0 to 300 nM IgE. Lines are extended beyond this concentration to demonstrate the non-linearity at higher concentrations. Peak heights are corrected by dividing by the internal standard peak height. Error bars are ±1 S.D. from 5 runs.

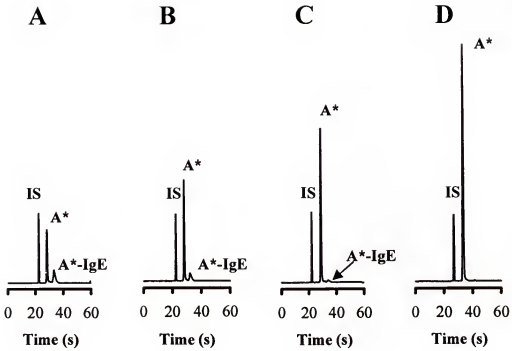

Figure 2-4. Competition experiment. All samples contained 200 nM A* and 5 nM 4(5)-carboxyfluorescein was used as internal standard (IS). Samples A through C contained 200 nM IgE and 0, 200, and 400 nM respectively of unlabeled aptamer. Sample D is a blank containing just 200 nM A* shown for comparison. Increase of the A* peak with the increase in the concentration of A demonstrates that both A and A* are binding to the same site on the IgE.

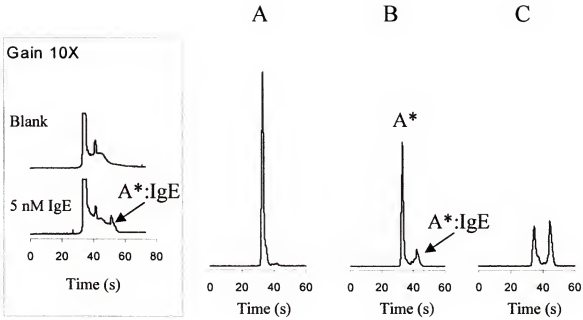

Figure 2-5. Determination of IgE in serum. Electropherograms obtained for samples prepared in reconstituted human serum. Each sample contained a final concentration of 300 nM A* and 0, 100, and 400 nM IgE in A through C respectively. Insert demonstrates a high sensitivity analysis of a sample containing 0 and 5 nM IgE with 300 nM A*. Insert is at 10-fold higher scale than the other electropherograms.

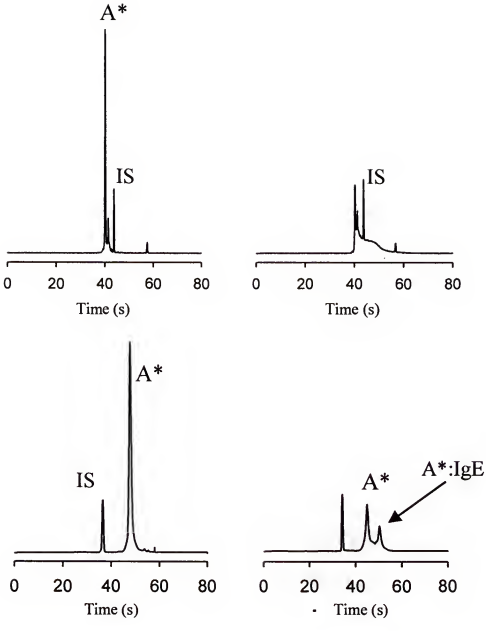

Figure 2-6. Determination of thrombin using FITC-labeled aptamer. (A) Electropherograms obtained for 2000 nM A* with 0 (left) and 3000 (right) nM of thrombin at pH 7.4 and no flow. 50 nM fluorescein was used as internal standard (IS). A large tail next to the free A* indicates presence of the quickly dissociating complex. (B) Electropherograms obtained for same concentrations (50 nM 4(5)-carboxyfluorescein as internal standard) at pH 8.2 and application of vacuum.

CHAPTER 3
RAPID SIMULTANEOUS DETERMINATION OF GLUCAGON AND INSULIN BY COMPETITIVE CAPILLARY ELECTROPHORESIS IMMUNOASSAYS

Introduction

Antibody (Ab) - antigen (Ag) interactions have long been used for highly sensitive and selective immunoassays. However, individual photometric or radioimmunoassays can take hours to complete and require lager sample volumes. While such assays can be performed in parallel formats for high throughput, the slow individual assays can limit utility in cases where rapid repetitive analyses are needed, e.g. chemical monitoring applications. Recently, significant progress has been made in development of rapid and sensitive immunoassays based on capillary electrophoresis (CE) with laser-induced fluorescence (LIF) detection (Ken97, Bao97, Sch97). Although CE is a serial technique, its ability to perform the analysis in < 10 s and ease of automation has potential to improve speed and throughput for a variety of applications. In addition, high speed, separation power, and ease of automation of CE assays suggests that high throughput can be achieved by performing assays either simultaneously or in parallel. Throughput achieved using such configurations would be much higher than other approaches (Che94a).

CE-LIF immunoassays can be performed in either a competitive or a non-competitive format. In a competitive assay, a fluorescently labeled antigen (Ag*)

competes with Ag for binding to a limited amount of Ab. CE-LIF separation of the mixture produces two distinct fluorescent peaks corresponding to Ag* and Ag*-Ab complex, the intensities of which can be related to the original concentration of Ag. In a non-competitive assay, excess of fluorescently labeled antibody (Ab*) is added to the solution containing Ag. A CE separation of Ab* and Ag-Ab* allows for determination of concentration of Ag based on the complex peak.

Although in this work competitive assays are examined, it is recognized that both approaches have strengths and weaknesses and their use is dictated by the application. Compared to competitive assays, the non-competitive assays have larger linear dynamic range (LDR), are less dependent on binding properties of antibodies, and can detect cross-reactivity (Shi94, Ger70). On the other hand, the competitive assay requires an easier separation since free Ag* must only be separated from Ag* bound to a large Ab. In addition, the difficult task of fluorescently labeling antibodies to produce a single homogeneous product is avoided in competitive immunoassays since only the antigen must be labeled. The advantages of competitive assays are especially apparent for the determination of small analytes such as peptides or small molecules.

An important advantage of CE-based immunoassays is that the separation step can be performed quickly, which not only allows for rapid analysis but also improves quantification. In immunoassays, non-covalent binding between Ab and Ag is governed by the equilibrium:

$$\mathrm{Ab} + \mathrm{Ag} \underset{k_{-1}}{\overset{k_1}{\leftrightarrows}} \mathrm{Ab{:}Ag} \tag{3.1}$$

where k_1 and k_{-1} are association and dissociation rate constants respectively; however, the equilibrium is disrupted as the constituents begin to separate. In a non-equilibrium environment, the half-life of the complex ($t_{1/2}$) is governed by:

$$t_{1/2} = \ln 2 / k_{-1}. \tag{3.2}$$

This effect indicates that with increasing dissociation constant, the speed of separation becomes increasingly important for quantitative detection of the complex and successful application of CE immunoassays. The importance of speed of the separation has been implicit in several examples of using CE-LIF to obtain immunoassays with detection limits <1 nM (Tao96, Che94a, Sch95); however, it should be noted that many assays have been developed using slow separation conditions. These assays typically rely on either tighter binding or detection of just the free Ag* for quantitation.

In this work, we describe the development of a CE-LIF competitive immunoassay for the pancreatic peptide glucagon. Development of the assay was simplified by universality of the conditions developed previously including use of low conductivity high concentration buffers at slightly basic (7 – 8.5) pH, narrow-bore capillaries, application of high electric field, as well as use of previously developed methodology for labeling, purification, and detection of fluorescein-derivatized analytes (Tao96). Further optimization of separation buffer type and pH that allows application of high electric field and prevents adsorption of analyte to the inner capillary walls has been performed. In addition, flow-gated injections were used to improve reproducibility. Finally, we explored the potential of using CE for simultaneous immunoassays by combining a previously developed assay for insulin (Tao97, Tao98) with the new assay for glucagon.

Experimental

Chemicals

Unless stated otherwise, all chemicals used in our experiments were purchased from Sigma Chemical Co. (St. Louis, MO, USA). FITC-labeled insulin (Ins*) was purified by HPLC using Vydac protein C4 column (Chrom Tech, Apple Valley, MN, USA). Kreb's Ringer buffer (KRB) contained (in mM): 118 NaCl, 5.4 KCl, 2.4 $CaCl_2$, 1.2 $MgSO_4$, 1.2 KH_2PO_4, 3 *d*-glucose, and 25 HEPES (N-hydroxyethyl]piperazine-N'-[2-ethanesulfonic acid]) (pH 7.4). Monoclonal anti-insulin C-terminal peptide (E86211M, K_d = 1 nM) used for the assays was purchased from Biodesign International (Kennebunk, ME, USA). The antibody was diluted to 100 nM in 20 mM phosphate buffered saline with 0.5% sodium azide and stored at 4°C prior to use. Monoclonal anti-glucagon from mouse ascites fluid (clone K79bB10, K_d = 1.6 nM) was diluted to 500 nM in separation buffer and stored at 4 °C prior to use. 5-(6)-carboxyfluorescein succinimidyl ester was purchased from Molecular Probes (Eugene, OR, USA).

Preparation of fluorescein-labeled glucagon (Glu*)

The labeling reaction was initiated by addition of 0.1 ml of 10 mg/ml 5-(6)-carboxyfluorescein succinimidyl ester dissolved in anhydrous dimethylforamide (DMF) to 1 mg of glucagon dissolved in 0.9 ml of 100 mM carbonate buffer (pH 8.3). The mixture was incubated for 1 hr at room temperature in the dark. Since glucagon has two possible labeling sites, three different products can be obtained from this reaction: two singly labeled and a doubly labeled glucagon. Singly-labeled glucagon was used in all experiments. Reaction products were purified by HPLC using Vydac protein C4 column (Chrom Tech, Apple Valley, MN, USA). The LC mobile phase composition was 69:31 mixture of 0.1% trifluoracetic acid and acetonitrile. Purified Glu* fractions were

collected and their concentrations were estimated using visible absorption of fluorescein at 496 nm ($\varepsilon = 75\ 000\ M^{-1}\ cm^{-1}$).

Capillary Electrophoresis

All fused silica capillaries used in our experiments had 360 μm outer diameter (o.d.) with various lengths and inner diameters (i.d.'s) (Polymicro Technologies, Phoenix, AZ, USA). The CE apparatus used in this work was similar to that reported previously . A low-pressure bomb machined from clear Plexiglas was used to flow-inject the sample onto the flow-gated interface (Hoo97) (Figure 3-1). The bomb was connected to the flow-gated interface using a 75 μm i.d. capillary. Analyte was pumped towards the flow-gated interface at a rate of 3 μl/min where it was washed with cross-flow of 0.1 ml/min supplied by the Dionex gradient pump (Smyrna, GA, USA). To make an injection, the cross-flow was stopped for 250 ms using an air actuated switching valve equipped with high speed switching accessory and digital interface (Valco Instruments, Houston, TX, USA). The separation capillaries used all were 12 μm i.d. Separation buffer for the majority of the experiments was 50 mM tricine (N-tris[hydroxymethyl] methylglycine) (pH 8.3); however, other buffers were also used as mentioned in the discussion section. High voltage power supply was CZE 1000R from Spellman High Voltage Electronics (Plainview, NY, USA). Detection was accomplished using a LIF detector described elsewhere (Ger98, Tao96).

Data Acquisition and Analysis

Data acquisition and analysis was accomplished by software written in-house using National Instruments Lab Windows (Austin, TX, USA). Data was acquired at 400 Hz and filtered with a 10 ms low pass filter. Peak width, migration time, theoretical

plates, and skew were calculated using statistical moments (Gid91). For the calibration curves, it was assumed that quantum yield of the complex is the same as that of the free Glu*.

Flow-Injection Immunoassay for Glucagon

The glucagon immunoassay was performed using a 7 cm long capillary. (4.3 cm injection to detection). Samples contained sample glucagon, 3 μl of 187 nM solution of Glu* and 5 μl of 500 nM solution of anti-glucagon. Additionally, 10 μl of 50 nM solution of fluorescein was added to the mixture as internal standard. Separation buffer was used to adjust final sample volume to 200 μl. Samples were incubated for 3 min before analysis and injected electrokinetically for 3 s at 1 kV. Ultrafast immunoassay was performed using a 5 cm long capillary (effective length 1.8 cm) with applied electric field of 2400 V/cm. In this case, 20 μl of 700 nM solution of Glu* was mixed with sample glucagon and 20 μl of 500 nM solution of anti-glucagon in glass microvial. Injections were made by application of flow-gating; the flow was stopped for 250 ms. Final concentrations of analytes are given in the Figures 3-3 and 3-4.

Simultaneous Immunoassay of Insulin and Glucagon

Simultaneous assays were performed using a capillary with 4.3 cm effective length (total length was 7 cm) and flow-gated injections. Samples contained 10.1 nM Ins*, 2.8 nM Glu*, 12.5 nM anti-glucagon, and 0.5 nM anti-insulin (final volume of 200 μl). In both cases, 10 μl of 50 nM solution of fluorescein was added to the sample as an internal standard. Standard concentrations were 0, 5, 10, 30, and 50 nM of each species.

Islet Content Analysis

Islets of Langerhans were isolated from CD-1 mice following ductal injection with collagenase XI and placed in RPMI culture medium (GIBCO, Gaithersburg, MD, USA) (Asp99). In less than one hour after isolation, islets were washed twice using each KRB and separation buffer. Islet contents were extracted using previously described procedure (Sch95). Briefly, islets were picked out of wash solution, placed into conical glass micro-vials containing 15 μl of CE separation buffer, and sonicated for 30 min. After sonication, 25 μl of 0.18 M solution of HCl in ethanol was added to each vial. Solutions were thoroughly mixed and incubated for 18 h. Vials containing disrupted islets were dried using gentle stream of helium to evaporate ethanol and HCl. Remaining residue was reconstituted using separation buffer. Necessary amounts of Ins* and Glu* were added to the solution followed by addition of antibodies to produce final concentration as developed for the simultaneous assay described in section 2.6. The final volume was brought to 200 μl using separation buffer. The solution was incubated for 3 min at room temperature and analyzed.

Results and Discussion

CE-LIF Based Immunoassay for Glucagon

Previous work on an immunoassay for insulin has demonstrated that rapid separation is important for successful separation of antibody-bound and free antigen. Similar experimental conditions were used for development of the glucagon immunoassay. An important step in any CE-based technique is selection of a separation buffer that allows application of high electric field and at the same time prevents analytes

from interacting with the inner wall of the capillary. Performance of the separation buffer is even more significant for rapid immunoassay since factors that affect dissociation rate of the complex, such as column temperature and interactions with the walls or buffer itself, can directly affect detection limit of the assay. Several different buffers were examined as summarized in Table 1. As shown in the table, only buffers with pH above 7.4 allowed reasonable efficiencies for the Glu* peak to be obtained, presumably due to prevention of adsorption of Glu* and the associated tailing of the Glu* zone (note the difference in skew as a function of pH). Increasing the pH above 8.3 tended to decrease resolution of bound and free Glu* zones. This effect was due to both poorer efficiency for Glu* and to increasing the rate of dissociation as evidenced by bridging between the bound and free Glu* zones. These results illustrate that increasing the pH is not necessarily advantageous for immunoassays, as it usually is with protein separations, since the change in pH can affect the binding reaction. The tricine buffer was clearly the best buffer of all those tested. Figure 3-2 depicts a representative separation obtained using tricine. The effect of tricine was not limited to just pH as it performed considerably better than TAPS-AMPD (TAPS - (N-tris[Hydroxymethyl]methyl-3-aminopropanesulfonec acid), AMPD - 2-amino-2-methyl-1,3-propanediol) at the same pH (see Table 1). The tricine appeared to be especially good at preventing adsorption of both Glu* and the complex peak. With TAPS-AMPD, the baseline continued to increase and ghost peaks were observed when the complex was repeatedly injected on to the column. Since this effect was not observed with just Glu*, it was concluded that the antibody was adsorbing in this buffer. These results highlight the important issues in selecting both pH and buffer type in optimizing an immunoassay.

Table 3-1. Summary of electrophoretic data for Glu* and Glu*-Ab complex with different electrophoresis buffers.[i]

pH	Buffer	Glu* Efficiency (plates/m)	Glu* skew	Resolution of Glu* / Ab-Glu*
7.4	10 mM Phosphate	6,000	0.23	N.D.[ii]
7.4	100 mM HEPES	16,000	0.42	N.D.[ii]
8.3	150 mM TAPS-AMPD	44,000	0.16	1.8
8.3	50 mM tricine	495,000	0.01	2.2
9.0	50 mM CHES[iii]	165,000	0.02	1.1
10.2	50 mM Borate	353,000	0.01	0.9

[i] All separations for buffer optimization utilized effective separation length of 3 to 4 cm and E = 2400 V/cm. Samples were injected electrokinetically at 1 kV for 3 s.
[ii] Not Determined because of poor peak shape for Glu*.
[ii] CHES - (2-[N-Cyclohexylamino]-ethanesulfonec acid)

While bound and free Glu* could be separated using tricine buffer with high efficiency and reproducible migration times (< 0.5% RSD), we found that peak areas were highly irreproducible with RSD's of 15-20% during repeated electrokinetic or hydrodynamic injections performed manually. This irreproducibility appeared to be primarily due to the difficulty of controlling injections on short columns for fast separations.

In order to improve injection reproducibility and investigate the potential for automation, we used flow-gated injections that allow sample to be electrokinetically injected onto the CE column from a continuous flowing stream (Hoo97). Figure 3-3 shows representative electropherograms obtained using a 4.3 cm long separation capillary with flow-gated injections with different concentrations of unlabeled glucagon. The flow-gated interface dramatically improved reproducibility with the free Glu* peak

having an RSD of 3.8% for all concentrations of glucagon tested (at least 20 electropherograms for each test); however, variability of the complex peak was still high at 10% RSD. Under these conditions, quantification of glucagon was best determined from the area of the free Glu* peak. The limit of detection (LOD) for the assay was estimated to be 4 nM by multiplying the standard deviation of the blank peak area for Glu* (no glucagon added) by 3 and dividing by the slope of the calibration curve. (Calibration curve constructed from standards of 5, 10, 50, 150 nM glucagon all analyzed 5 times). This concentration detection limit corresponds to a mass detection limit of 640 zmol given the 0.16 nl injection volume.

Several explanations could be proposed for continuing variability in the area of the complex peak. First, inspection of the electropherograms in Figures 2 and 3 reveals that two peaks migrate before free Glu* peak. These peaks appear only with addition of antibody to Glu* solutions and decrease with addition of unlabeled glucagon which indicates that both peaks are complexes of antibody and Glu*. Since a whole antibody was used in this experiment, these peaks may represent antibody with one or two Glu* bound. (Note that in calculation of resolution indicated in Table 1, only the first peak was used). It is suspected that some of the variability in the complex peak area is due to dynamic equilibrium between antibodies bound to one or two Glu* molecules. Broadening of the complex peak and formation of multiple complexes has been reported previously when whole antibodies were used in CE-immunoassays (Sch95). Second, commercial preparations of glucagon have been reported to contain multiple derivatives of glucagon mono- and di-desamidoglucagon and N-terminal degraded glucagon (Maz85). Previously reported MALDI analysis indicated presence of methionine

sulfoxide and doubly oxidized tryptophan side-chain (Kus97). Some of these derivatives were reported to be less effective in immunoassays (Bro72, Lin75), which could create various dynamic equilibria leading to irreproducibility of the complex peak. Finally, despite our efforts in buffer selection, adsorption of the complex to the inner capillary walls could contribute to irreproducibility of the complex peak area.

Ultrafast Determination of Glucagon

Utilization of the flow-gated interface allowed us to use capillaries as short as 1.8 cm and separations performed in 3.5 s as shown in Figure 3-4. Compared to the separations on the longer column, faster separations showed a larger second complex peak. We suspect that this complex peak is an Ab bound with two Glu* molecules. Possible reasons for the increase in size of this peak compared to longer runs are 1) faster separation results in less dissociated complex and 2) change in concentrations of Ab* and Glu* resulted in more of the complex being formed. The larger 2nd complex peak overlapped more with the free Glu* peak. Despite that, reproducibility of the overall area of both complex peaks during rapid separations was improved 5-fold to 2% RSD. This improvement allowed us to prepare a calibration curve based on bound to free ratio for the assay performed using 1.8 cm capillary (Figure 3-5). A detection limit for glucagon of 760 pM was calculated from this calibration. This detection limit is slightly higher than that reported for detection of insulin (Paa81) which could be explained by weaker dissociation constant of the antibody used ($K_{d\ Glucagon}$ = 1.6 nM, $K_{d\ Insulin}$ = 1.0 nM).

Simultaneous CE-LIF Immunoassay for Glucagon and Insulin

As mentioned earlier, a rapid competitive CE-immunoassay for insulin has been developed in our laboratory (Tao96). This assay was combined with the assay for

glucagon for simultaneous determinations. Initial attempt to resolve two complex peaks using 4.3 cm long (effective) capillary was not successful. In attempt to further improve separation, separation column length was increased to 7.3 cm while keeping the electric field the same, as illustrated on Figure 3-6. Electropherogram A shows a separation of Glu* and Ins*. Several small peaks around Ins* are impurities from the Ins* solution. In electropherogram B, antibodies against insulin and glucagon were added giving rise to complex peaks. Finally, electropherograms C and D demonstrate an effect of different concentrations of glucagon and insulin on the sizes of free and bound peaks of Glu* and Ins*. Several factors could contribute to poor separation between complexes. First, both antibodies used in the assay are IgGs and have similar electrophoretic properties that would make it difficult to separate them using short capillaries. Second, formation of multiple complexes between antibody and antigens, as mentioned earlier, may lead to broader peaks preventing complete separation. Third, bridging resulting from dissociating complex creates tailing in both complexes, which further complicates separation. Since the increase in the length of the capillary did not produce adequate separation of the complexes, the capillary length was cut back to 4.3 cm. The simultaneous calibration curves based on area measurements of free Glu* and Ins* peaks are shown on Figure 3-7. Detection limits of 4.3 nM for glucagon and 5.5 nM for insulin were obtained. Lower detection limits could most likely be obtained using a 1.8 cm long capillary; however, difficulties with resolution precluded us from using this condition. Error bars of 1 standard deviation (n=10) were placed on each of the points (Figure 3-7); however, they are too small to be observed. Given the high reproducibility of an assay, the deviation from the line for some standards most likely resulted from difficulties with

accurate pipetting of derivatized Ins* and Glu*. Stock solutions of some constituents of an assay contained 30% acetonitrile, which affected pipette accuracy.

Measurement of Glucagon Content of Islets

Measurement of glucagon content was performed using conditions developed for the simultaneous assay. Groups of 5 islets were prepared as described in the Materials and Methods sections and analyzed for glucagon content. Measured concentrations were in the range between 8 and 18 nM glucagon, which is well within linear region of the calibration curve. We have determined that each islet contained 1.9 ± 0.6 ng glucagon (errors are given as standard error of the mean). This value is in good agreement with published value of 1.5 ± 0.5 ng (Paa1). Additionally, all prepared samples, including calibration standards, were measured in less than 30 minutes, which demonstrates significant improvement in analysis time compared to RIA. Simultaneous measurement of glucagon and insulin content of the islets was complicated by the fact that the islets contain much more insulin than glucagon. The published value for insulin content of the mouse islets is ~ 48 ng (Asp99). Using experimental conditions described above, these values would require measurements of 1-3 nM glucagon and 40-60 nM insulin in the same assay. Although it is possible to adjust concentrations of Ins* and antibody to make the measurement possible, overlap of a large Ab-Ins* complex peak with free Glu* peak made it impossible to simultaneously measure insulin and glucagon content of the islet in a single separation. Insulin content of the islets was measured by itself in the separate experiment and was determined to be 58 ± 13 ng which compares well with the published value.

Conclusion

CE-LIF based immunoassay described in this work demonstrates that methodology, which includes application of the short separation distances, high electric fields, and low-conductivity buffers, for a CE-immunoassay could, with minor modifications, be transferred from one analyte to the other. Some of the important factors in development of rapid CE-immunoassay are proper choice of separation buffer and pH and reproducible injection techniques. As we have found, adsorption to the inner capillary walls of the capillary columns may be detrimental to the assay; thus, optimization of separation buffer to prevent this effect is required. Additionally, adsorption of reagents to pipette tips and to inner walls of sample vials during sample preparation significantly affects reproducibility and precision of the assay. Therefore, careful choice of materials and treatment for tips and vials may further increase reproducibility. Finally, in order to obtain best detection limits, it is important to choose an antibody with smallest dissociation constant possible.

Application of flow injection to rapid CE-immunoassays provides a simple means for future automation. Combination of fast separations demonstrated with ease of conjugation to a commercial autosampler can significantly increase throughput of analysis of biological samples. Using the described assay, we determined glucagon with results comparable to those obtained by RIA but in a fraction of the time required for RIA. Multi-analyte analysis in a single electropherogram was also demonstrated by CE immunoassay.

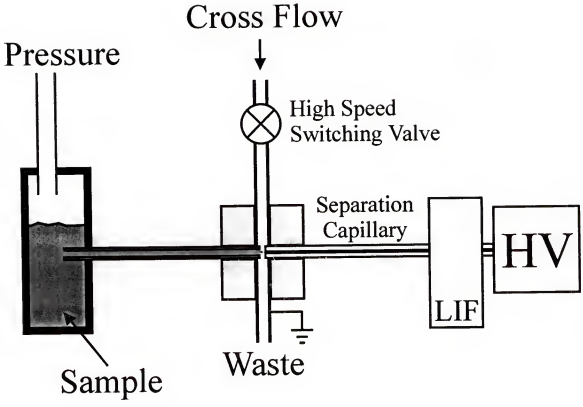

Figure 3-1. Diagram of an instrumental setup used to perform CE-LIF with flow-gated injections. 10 – 15 psi of helium pressure was used to flow the sample towards a flow-gated interface. A cross-flow of 0.1 ml/min supplied by the Dionex gradient pump (Smyrna, GA, USA) washes the sample to waste at the interface. To make an injection, the cross-flow is stopped for 250 ms using high speed switching valve. During the time when the cross-flow is off, a sample can reach the inlet of the separation capillary where it is electrokinetically injected.

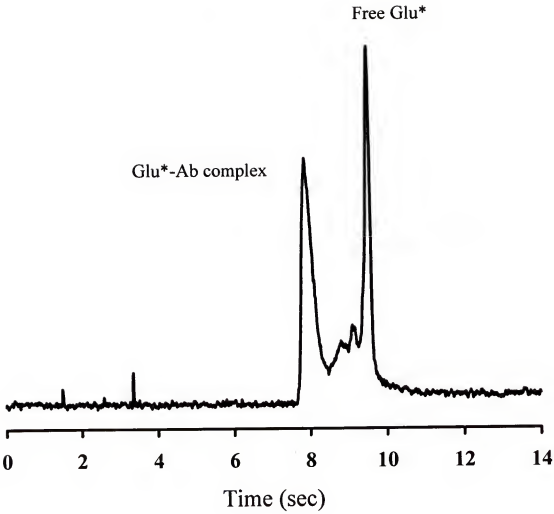

Figure 3-2. Separation of the free Glu* from Ab-Glu* complex. In this experiment, 7.5 nM Glu* and 22 nM antibody were used. A 6 cm long (effective, 9 cm total) capillary was used in this case with E=2000 V/cm, electrokinetic injections at 1kV for 3 s.

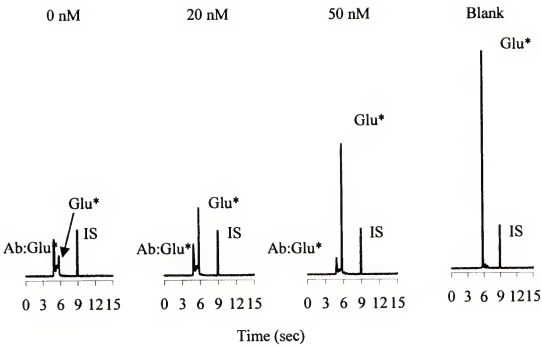

Figure 3-3. Rapid CE-LIF based competitive immunoassay for glucagon using 4.3 cm long capillary. Solutions contained 2.8 nM Glu*, 12.5 nM anti-glucagon (Ab), 2.5 nM fluorescein used as internal standard (IS), and 50, 20, or 0 nM glucagon as indicated in the figure. A blank electropherogram contained only Glu* and IS is shown for comparison. (E = 2400 V/cm, injections were 250 ms long)

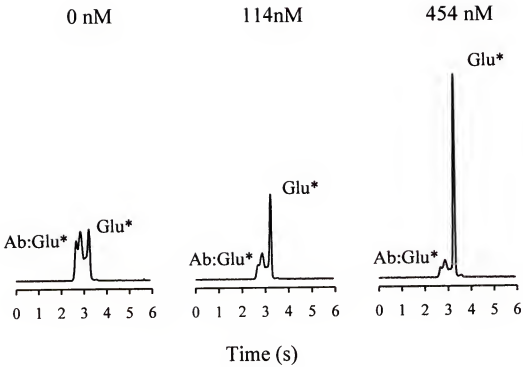

Figure 3-4. Rapid CE-LIF based competitive immunoassay for glucagon using 1.8 cm long capillary. Solutions contained 70 nM Glu*, 50 nM anti-glucagon, and 454, 114, or 0 nM glucagon. Internal standard is not needed since the ratio of the bound to free is used for quantitation. Presence of multiple complex peaks is probably due to formation of singly and doubly bound complexes with whole antibodies. (E = 3400 V/cm, injection time was 250 ms)

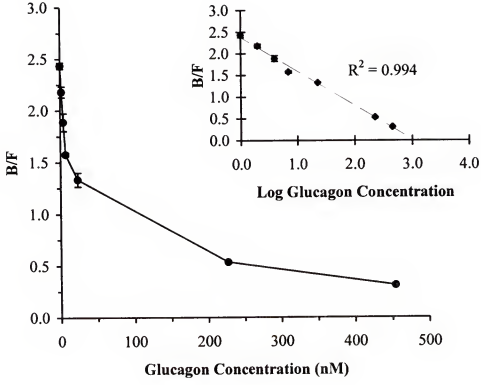

Figure 3-5. A calibration curve for the detection of glucagon obtained using conditions described in caption for Figure 3-2. Insert shows the sample calibration performed on a semi-log scale in the linear region of the calibration. A detection limit of 760 pM was determined for this calibration.

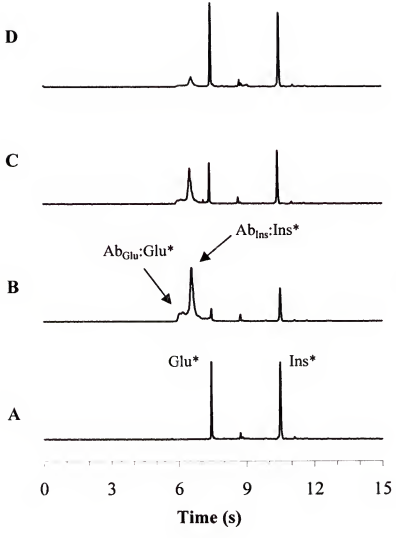

Figure 3-6. Simultaneous CE-LIF immunoassay for insulin and glucagon. Separation is performed in 7.3 cm long capillary, E = 2200 V/cm, injections were 250 ms. (A) Separation of 2.8 nM Glu* and 10.1 nM Ins*. (B) Separation of a mixture of same concentrations of Ins* and Glu* with 12.5 nM anti-glucagon and 0.5 nM anti insulin. Identification of the complex peaks was preformed in the separate experiment (not shown). (C) 25 nM glucagon and insulin added to the mixture described in B. (D) 100 nM glucagon and insulin added to the mixture described in B.

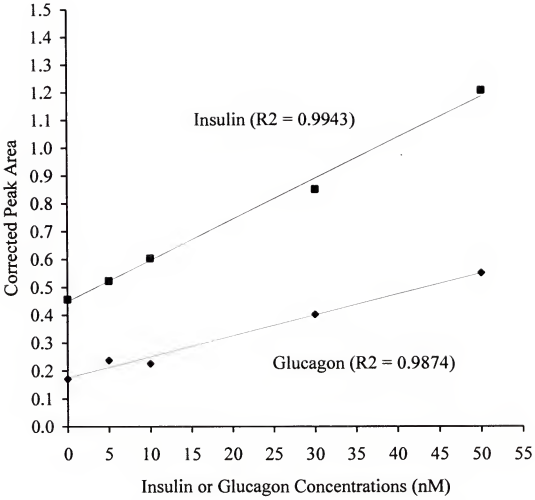

Figure 3-7. Simultaneous calibration curves for detection of insulin and glucagon prepared in the linear region of the calibration. Assay conditions are described in the legend of Figure 3-6.

CHAPTER 4
REVERSED-PHASE CAPILLARY LIQUID CHROMATOGRAPHY COUPLED ON-LINE TO CAPILLARY ELECTROPHORESIS IMMUNOASSAYS

Introduction

Many analytical problems involve detection and quantitative monitoring of analytes at picomolar concentrations in complex mixtures. Immunoassays, especially radioimmunoassay (RIA) and enzyme linked immunosorbent assay (ELISA), have traditionally been used for these applications; however, these methods generally involve long incubation and analysis times, large sample volume, and cumbersome automation. As a result, considerable effort has been made to develop instrumental formats for immunoassays. Capillary electrophoresis immunoassay (CEIA) is one approach that appears to offer a number of advantages over conventional immunoassays. These advantages include low sample volume requirements, easy automation, simultaneous detection of multiple compounds and high-speed (Tao96, Chi98, Che94c, Ger00b, Cas99). Such immunoassays have potential application in clinical and library screening applications among others.

Both competitive (Scz93) and non-competitive (Shi94) CE-based immunoassays have been developed. In a competitive assay, a fluorescently-labeled antigen (Ag*) competes with Ag for binding to a limiting amount of antibody (Ab). CE separation of the mixture produces two fluorescent peaks corresponding to Ag* and Ag*:Ab complex,

the intensities of which can be related to the original concentration of Ag. In non-competitive assays excess of fluorescently-labeled antibody (Ab*) is added to the solution containing Ag. A CE separation of Ab* and Ag:Ab* allows for determination of Ag concentration.

Non-competitive assays possess number of advantages over competitive assays including larger linear dynamic range, lower detection limits, and ability to distinguish among cross-reactive species (Shi94, Ger98). Despite these advantages, practical problems have limited the development of non-competitive assays. Fluorescent labeling of antibodies to produce a single homogenous product is challenging. Furthermore, Ab* may be difficult to separate from the Ab*-Ag complex, especially if the analyte is small and does not significantly affect the electrophoretic mobility of Ab*. Recent advances including use of non-antibody ligands as the affinity probe (Ger98, Fou98, Kel97, Tim00) and addition of mobility-shift ligands to aid in the separation (Tim00) ameliorate these difficulties; however, the ease of developing competitive CEIA suggests that this approach will remain popular. Developing a competitive CEIA only requires labeling the antigen in a way that does not interfere with binding and then identifying separation conditions that allow separation and detection of free and bound labeled antigen (Ken97, Bao97, Sch97). CEIA's have already been developed for drugs, toxins, environmental hazards, steroid hormones, peptide hormones, and proteins (see Ken97, Bao97 for review).

Given the utility of competitive CEIA, it is constructive to consider ways of minimizing the disadvantages of higher detection limit and sensitivity to cross-reactive species. Theoretical analysis shows that the detection limit of competitive assays is

determined by precision in detection of bound and free Ag* and the antibody's affinity for antigen (Jac86). Given typical CE reproducibility and antibody-antigen affinity constants, it is unlikely that competitive CEIA detection limits will improve much beyond the high pM to low nM level reported so far (Ken97, Bao97, Sch97, Hee99) unless preconcentration techniques are employed. CEIA does not distinguish among cross-reactive species because in the assay Ag is never directly detected, rather only Ag* and Ab:Ag* are detected. Any molecule, Ag′, that binds Ab will disturb the ratio of free-to-bound Ag* and give rise to a signal. Thus, the presence of unknown cross-reactive species can give false positives and quantification errors.

Coupling the competitive CEIA to reversed-phase capillary LC is one approach to eliminating both of these problems. LC has a well-known ability to preconcentrate samples by injecting large volumes of analyte dissolved in weak mobile phases. The use of capillary LC columns, as opposed to conventional HPLC columns, for preconcentration provides several advantages including: 1) minimization of eluting peak volume thus providing the greatest concentration enhancement, 2) minimization of the sample size required for preconcentration because of the small column volume, and 3) direct compatibility with on-line CEIA because of similar flow rate requirements (Tao96). In this work, we demonstrate an ~45-fold improvement in concentration detection limit by preconcentration on the LC column. In addition, the separation capability of the column allows separation of cross-reactive species prior to introduction to the immunoassay. This added separation component may allow other applications such as affinity screening of complex mixtures and "Western-blotting."

As a demonstration of this new method, we coupled a competitive CEIA for glucagon (Ger00b) with capillary LC in an on-line system. Glucagon is a 29 amino acid peptide hormone (MW 3482 g/mol) that is secreted from α-cells of the islets of Langerhans. This hormone functions as part of the glucose homeostasis system by increasing blood sugar levels and regulating insulin secretion. Detailed understanding of the role of glucagon requires measurements of secretion and cellular content. The system described here is used to quantify glucagon released from single rat islets of Langerhans. In addition, the system is used to measure multiple cross-reactive forms of glucagon with one assay.

Experimental

Chemicals

Unless stated otherwise, all chemicals were purchased from Sigma Chemical Co. (St. Louis, MO, USA). Ultra-pure water was obtained using Milli-Q Plus system (Millipore Corp., Bedford, MA). HPLC grade isopropanol was purchased from Fisher Scientific (Pittsburgh, PA). Monoclonal anti-glucagon in mouse ascites fluid (Sigma, clone K79bB10) was used for these experiments. According to the supplier, this antibody has K_d = 1.6 nM for glucagon. Prior to use, the antibody was diluted to 1 μM in separation buffer and stored at 4 °C. 5-(6)-carboxyfluorescein succinimidyl ester was purchased from Molecular Probes (Eugene, OR, USA). All solutions were filtered using 0.22 μm Teflon filters (Osmonics brand, Fisher Scientific, Pittsburgh, PA).

Preparation of fluorescein-labeled glucagon (Glu*)

Glu* was prepared as described previously (Ger00b). Briefly, the labeling reaction was initiated by addition of 0.1 mL of 10 mg/mL 5-(6)-carboxyfluorescein succinimidyl ester dissolved in anhydrous dimethylforamide (DMF) to 1 mg of glucagon dissolved in 0.9 mL of 100 mM carbonate buffer (pH 8.3). The mixture was incubated for 1 h at room temperature in the dark. The reaction mixture was purified and analyzed by HPLC using a Vydac C4 column (Chrom Tech, Apple Valley, MN, USA) with a mobile phase consisting of a 69:31 (v:v) mixture of 0.1% trifluoracetic acid and acetonitrile. As reported elsewhere (Ger00a), these reaction conditions produce three detectable products which is expected because glucagon contains two amines (a N-terminus and one lysine). Purified Glu* fractions corresponding to each of the peaks were collected and their concentrations estimated using absorption of fluorescein at 496 nm ($\varepsilon = 75\ 000\ M^{-1}\ cm^{-1}$). Each form of Glu* was tested for binding to the antibody by CE-LIF. All three fractions reacted with antibody; however, the least retained peak gave the strongest complex formation and was used for further all subsequent analyses. While the active component of this fraction was not identified, it presumably corresponds to a singly-labeled glucagon. Derivatized glucagon was stored in the HPLC mobile phase at –7 °C when not in use. These conditions prevented degradation of the Glu*.

Capillary Electrophoresis

All electrophoresis capillaries used were 7.2 cm long with 10 μm inner diameter (i.d.) and 360 μm outer diameter (o.d.) (Polymicro Technologies, Phoenix, AZ, USA). The CE apparatus used in this work was similar to that reported previously (Tao96, Ger00b). Injections were performed using a flow-gated interface (Hoo97). Cross-flow

was supplied by a HPLC pump (SSI 222C, Fisher Scientific, Pittsburgh, PA) which was connected to a flow-gated interface through a pulse dampener and in-line filter screen (Valco Instruments Co., Houston, TX). To make an injection, the cross-flow was stopped for 125 ms using an air-actuated switching valve (Valco Instruments, Houston, TX, USA). A high voltage power supply (CZE 1000R from Spellman High Voltage Electronics, Plainview, NY, USA) was used to apply an electric field of 3500 V/cm (25 kV total voltage applied) across the CE capillary. Detection was accomplished using a LIF detector (Yeu92, Tao96) using a 488 nM line of an Ar-ion laser for excitation. Fluorescence at 520 nm was collected with a 40x microscope objective and detected by a PMT. Separation buffer consisted of 50 mM tricine at pH 8.3 and was prepared daily.

Capillary RPLC

A diagram of the experimental arrangement for the capillary LC interfaced to the CE is shown in Figure 4-1. The RPLC column was 4.5 cm long by 50 μm i.d. packed with Proshere 300 Å, 5 μm, C4 particles (Alltech Associates, Inc. Deerfield, IL) as described elsewhere (Ken89). Packed columns were placed into the system and rinsed with 70% 10 mM phosphate buffer at pH 2.5 and 30% isopropanol for 30 min at 200 nL/min before use.

An Applied Biosystems 140B Solvent Delivery System (Perkin-Elmer, Wellesley, MA) was used to perform separations. The pump outlet was connected to an electrically actuated injection valve using a stainless steel tee (Valco Instruments Co., Houston, TX). HPLC mobile phase A (MP-A) was 10 mM phosphate buffer (pH 2.5) containing 5% isopropanol. HPLC mobile phase B (MP-B) was 10 mM phosphate buffer (pH 2.5) containing 30% isopropanol. Mobile phases were degassed by He sparging.

Samples were loaded into the injection valve using a sample reservoir pressurized with He to 25 psi and connected to the valve by a 25 cm long 75 μm i.d. capillary. This approach was used instead of a syringe port to avoid cross-contamination by a syringe and to reduce introduction of particulates. The injection system was similar to that reported earlier (She97). In this system, the sample loop (28 cm of 150 μm i.d. fused silica capillary) connects the injection valve to a tee that serves as the interface to the column. The tee allows a lower dead volume connection than the conventional arrangement. Mobile phase is split at the tee through a second capillary (80 cm long by 75 μm i.d.). The split can be closed with an on/off valve. After the pump is pressurized and equilibrated, the injection valve is set to fill position (depicted on the diagram) and the sample vial pressurized using a solenoid. Once the loop is filled, flow through the splitter is turned off by means of the on/off valve at the tee, the injection valve switched to 'inject/run' position, and HPLC pump flow rate is set to 5 μL/min allowing sample to be loaded onto the column for 2 min by constant flow. After sample injection, the on/off valve was opened and the pump flow rate increased to 85 μL/min which generated pressures of ~600 psi. The LC column was equilibrated at 100% MP-A for 2 min after which separation/desorption was initiated. Complete sequence of events required to perform sample injection and desorption is shown in Table 5-1.

Table 5-1. Steps required for performing sample injection and separation. Time 0 indicates beginning of data acquisition.

Time (min)	Pump Flow (μl/min)	Pump Pressure (psi)	%B	Event
-5.6	2000	----	5	Pump Pressurization
-5.4	900	3500	5	Pump Equilibration
-4.9	900	3500	5	Pump Ready. Injection loop is filled in this step by forcing the sample through the injection capillary by He pressure.
-4.2	900	3500	5	Loop fill is complete. Splitter is turned off by the On/Off valve.
-4.1	5	~3500	5	Sample is loaded onto column by switching injection valve to the Run/Load position which directs pump flow through the sample capillary into the separation column.
-2.2	5	~3500	5	End of sample loading step.
-2.1	85	~3500	5	Splitter is opened with the On/Off valve. Column equilibration is performed during this step.
-0.1	85	600	5	End of column equilibration.
0.0	85	600	90	Start of the desorption/separation step. Start of Data acquisition.
5.0	85	1300	90	End of the desorption/separation step. End data acquisition.

On-Line RPLC-CEIA

Immunoassay was performed by on-line mixing of 15 nM Glu*, 15 nM Ab, and effluent from the RPLC column (see Figure 4-1). A microliter syringe pump (Harvard Apparatus, South Natick, MA) was used to deliver Ab and Glu* to the mixing cross at 155 nL/min. Both Ab and Glu* were dissolved in 8 mM tricine (pH 8.3) containing 3 mM EDTA. As interaction with stainless steel rapidly degrades Glu*, 50 μm i.d. fused silica capillaries were used to connect each syringe to the mixing cross. Although glucagon can be easily oxidized under ambient conditions (Kus97), the Glu* solution does not come into contact with air once it is loaded into a syringe; therefore, this solution can be used for ~4 hours of experiments before oxidation products are observed.

A diagram of the mixing cross is shown in the insert of Figure 4-1. The cross was machined from clear Plexiglas with 0.0145 inch internal holes (drill index #79) which allows insertion of a 360 μm o.d. capillary. Square cut 18 cm long 50 μm i.d. reaction capillary is juxtaposed to the RPLC capillary such that capillaries touch in one of the straight areas of the cross (see insert of Figure 4-1). Other reagents are pumped through the space between the capillary and Plexiglas and between reaction and LC columns. Binding reaction was carried out while flowing through the reactor capillary (18 cm long by 50 μm i.d.). At the flow rates used, this allowed 45 s for mixing and reaction. The sample stream was analyzed by periodic flow-gated injections onto CE.

For experiments evaluating band broadening, the CE system was removed and samples detected directly in the reactor capillary or the chromatography column using a UV detector (Spectra Series UV100, Thermo Separations Products, Riviera Beach, FL). In experiments to characterize the immunoassay and on-line reaction, the LC column was removed and samples directly infused into the mixing cross.

Data Acquisition and Analysis

CE data was acquired at 300 Hz by a National Instruments AT-MIO-16F-5 data acquisition board (Austin, TX) installed in a 486-66 MHz personal computer. Automated system control and data analysis were performed using software written in-house using Lab Windows (National Instruments). Peak parameters for both CE and HPLC were calculated using statistical moments (Gru69).

Sample Analysis and Calibration

Stock glucagon solution was prepared by dissolving 1 mg of solid glucagon in 2.86 mL MP-B containing 1 μL of 6 M HCl and stored in the freezer. Working stock

solutions with concentrations of 50 and 100 nM were prepared daily by diluting main stock solution in MP-A containing 3 μM insulin and kept on ice. Samples were prepared by further diluting the working stock to the desired concentration using same solution. Analysis of samples was performed within 1 min of sample preparation to minimize sample loss and degradation.

Analysis of Islet Secretion

Islets of Langerhans were isolated from male Sprague-Dawley rats weighing 300-350 g following ductal injection with collagenase XI and placed in RPMI culture medium (Gibco, Gaithersburg, MD) (Asp99). Islets were incubated at 95% humidity, 37 °C for 4 days. On the 5th day, single islets approximately 150 μm in diameter were transferred in a 5 μL volume of media using a pipette to a glass micro-vial containing 95 μL of Kreb's Ringer Buffer (KRB). Kreb's Ringer buffer (KRB) contained (in mM): 118 NaCl, 5.4 KCl, 10 $CaCl_2$, 1.2 $MgSO_4$, 1.2 KH_2PO_4, 5 *d*-glucose, and 25 HEPES (pH 7.4). For islet stimulation, KRB was modified to contain 60 mM KCl and 63 mM NaCl. Vials were placed in the incubator for 10 min in case of stimulated secretion or 60 min in case of basal secretion. After incubation, 1 μL each of 1 M HCl and 300 μM insulin were added to the vial after which, three 30 μL samples were withdrawn and placed into sample vials containing 90 μL of MP-A with 3 μM insulin and stored on ice until analysis.

Results and Discussion

On-Line CE Immunoassay

The goal of this project was to improve the utility of the CEIA by coupling to capillary LC to take advantage of the preconcentration and separation capabilities of LC.

Such a coupling initially required optimization of the CE immunoassay. We had previously identified conditions for successful CE-based immunoassay of glucagon, the test analyte in this experiment (Ger00b); however, coupling to a chromatography column required investigation of on-line reagent mixing, high-speed immunoassay acquisition, on-line reaction time, and the effect of HPLC solvents on the immunoassay. To perform on-line reaction, we employed techniques that were previously developed in our laboratory for on-line immunoassay for insulin (Tao96). In this approach, sample stream is mixed with antibody solution and labeled antigen solution at a cross and continuously flowed through a reaction capillary to a flow-gated interface, which allows periodic injection onto a short CE column where bound and free zones are rapidly separated (Figure 4-1).

Figure 4-2a shows an electropherogram obtained using on-line mixing and incubation. As it is seen from the figure, complex formation was achieved with on-line mixing and incubation; however, a new peak was observed on electropherogram as indicated by an arrow. Increase in the size of the extra peak and decrease in the F/B ratios, as evident from Figure 4-2b, indicate that extra peak is a product of a degradation of Glu*. A possible source of degradation is reaction with metal ions originated from the syringe needle. To prevent reagents from interacting with needles we have inserted connecting capillaries through the needle such that the bulk of the reagent solution does not come in contact with the needle. Further decrease in the amount of metal ions in the solution was achieved by addition of 3 mM of EDTA to each syringe.

Figure 4-3 shows a series of electropherograms obtained using on-line mixing and incubation. Each electropherogram consists of three peaks migrating close together. The

third peak is free Glu* while the first two peaks have previously been identified as Ab:Glu* complexes based on the observation that they formed only by addition of Ab to Glu* solutions and they both decrease upon addition of glucagon to the sample. (Multiple complex peaks are formed because whole antibody has two binding sites allowing formation of Ab with one or two Glu* bound to it) (Ger00b). For the electropherograms shown, the RSD's of bound to free peak area ratio were 3.1% while for all data sets examined the RSD's varied from 2.5% to 5%. The figure also illustrates that electropherograms can be collected every 1.5 s. An individual electropherogram actually requires 3 s; however, in the continuous operation mode overlapping injections can be performed to increase the acquisition rate. Since the immunoassay will effectively be the detector for the capillary LC separation, the rate of immunoassay acquisition determines how well the chromatographic peaks can be characterized.

Reaction incubation time is an important parameter for the on-line CE-immunoassay since reagents must establish equilibrium to maximize sensitivity. In our previous report on the glucagon CEIA, reagents were manually mixed off-line and incubated for at least 3 min for complete reaction. In the on-line case, the sample must mix by diffusion while traveling through the reaction capillary. As will be discussed later, it is important for the reaction capillary to be as short as possible to prevent excessive zone broadening. Optimal reaction time was determined by varying the length of the reaction capillary (50 μm i.d.) while keeping the flow rate constant. Figure 4-4 shows a plot of resulting free to bound ratio for Glu* (F/B) as a function of incubation time. F/B ratios decrease with reaction time as the reaction of Ab with Glu* proceeds. After 15 s of reaction time the F/B is constant indicating equilibration of the reaction.

This time corresponds to a 9 cm long capillary at the flow rates used; however, all further experiments utilized an 18 cm long capillary to facilitate connections to the system.

Since it was our intention to use the immunoassay in conjunction with reversed-phase LC, we also investigated the effect of organic solvent on the F/B ratios. Increasing the concentration of acetonitrile, a commonly used organic modifier for reversed-phase HPLC, caused significant increase in F/B ratios as seen in Figure 4-5. From preliminary chromatographic experiments, it was found that ~60% acetonitrile was needed to completely desorb glucagon. Such large acetonitrile concentrations cause 600% increase in the F/B ratio indicating a significant loss of binding affinity. This loss of affinity may be due to partial denaturation of reacting species or disruption of non-covalent interactions. Such loss in binding is detrimental to the immunoassay as detection limits are determined by the affinity constant. To lower concentration of organic solvent required and provide a solvent more compatible for binding, we investigated the use of isopropanol (IPA) as organic modifier. As seen from Figure 4-5, F/B ratios do not change significantly up to 40% of IPA. As a stronger reversed-phase mobile phase than acetonitrile, only ~30% IPA is needed to desorb glucagon. Thus, IPA was chosen as a mobile phase for the RPLC preconcentrations and separations. A disadvantage of using IPA is that it is more viscous than acetonitrile thus creating larger back pressures and reduced efficiency. More extensive experiments may identify other solvents that are compatible with antibodies. In similar experiments we evaluated the effect of trifluoroacetic acid, a commonly used additive for peptide separations, and found that this compound had an adverse effect on the fluorescence signal and so it was omitted from the mobile phase.

RPLC Separation and Preconcentration

The highest level of preconcentration is obtained by maximizing injection volume and simultaneously minimizing the volume of eluted peak. The maximum injection volume depends upon both the capacity of the column and the time available for injection of large volumes. In the loading buffer used (10 mM phosphate at pH 2.5 with 5% IPA), the k' for glucagon was extremely high, thus volumes as large as 5 μL could be injected with no adverse effect on the retention time, zone width, or zone shape. The main limitation to using larger injection volumes is the time required for injection. At a flow rate of 150 nL/min, a 5 μL volume would require 33 min to inject. To prevent such long injection times, the system described in the Experimental section was employed in which the mobile phase split was closed during injection, allowing high flow rates through the column for injection, and reopened for the chromatographic separation to allow the optimal flow rate for desorption. With this system, the 5 μL samples could be loaded in 2 min.

Once the zone is compressed on the column, the goal for preconcentration and separation is to minimize the dilution that occurs by band broadening. To understand the relative contribution of the various system components to band broadening, the system was analyzed by considering the observed variance of a zone reaching the end of the reactor capillary to be given by the following (Sco84):

$$\sigma^2_{total} = \sigma^2_{col} + \sigma^2_{cross} + \sigma^2_{reactor} \tag{4.1}$$

where σ^2_{col} is variance caused by a peak moving through the capillary LC column, σ^2_{cross} is broadening cause by mixing in the cross, and $\sigma^2_{reactor}$ is variance due to parabolic flow

and diffusion in the reaction capillary. Variances can be calculated in time, length, and volume units. In this system, a substantial change in flow rate occurs after the column as the sample begins to be swept into the reaction capillary; therefore, the variance is calculated in volume units. Use of volume units is also appropriate as we are most concerned with the dilution of the zone with regards to preconcentration.

Column variance. For gradient elution, peak dilution is proportional to column flow rate and inversely proportional to the square root of the gradient time (Sny83). Thus, in order to minimize dilution it is important that the column flow rate is low and the gradient slope is maximized. For these experiments, we operated the column at 150 nL/min and step-gradients were used to desorb the analyte. Under these conditions, the peak variance measured by eluting glucagon from a column and detecting the zone on-column by UV detection was 8.8×10^{-12} mL^2.

Variance due to reactor capillary and cross. A further source of band broadening in our system is the cross and reactor capillary. To evaluate this variance, zones of glucagon were injected onto the column and eluted into the cross/reactor capillary. Buffer was flowed into the reactor capillary at the same flow rates used for on-line mixing. The zone was detected on the reactor capillary by UV absorbance. By varying the length of the reactor capillary, we obtained a linear plot of variance as a function of reactor capillary length. (Lengths used were 10, 20, 30 and 40 cm and the linear correlation coefficient was 0.99). The slope of the line is an estimate the variance of the reactor capillary. The slope was 8.0×10^{-12} mL^2/cm from which a variance of 14.4×10^{-11} mL^2 for the 18 cm length of capillary used in our experiments can be obtained. The y-axis intercept of the line is a measure of the variance at zero reactor capillary length, i.e.

the variance of the column and the cross. Subtracting the value for the column (measured above) from the y-intercept of 5.0×10^{-11} mL^2 gives the variance of the cross as 4.1×10^{-11} mL^2. Thus, for the total zone variance observed, 25% was due to the cross and 75% was due to the reactor capillary with an inconsequential amount caused by the column itself.

These results indicate that the majority of dilution and band broadening that occurs is due to flow through the cross and the reactor capillary. The extent of this broadening and dilution can be reduced by using a smaller radius or length of reaction capillary (capillary was twice as long as necessary for complete reaction), better interfacing of the column to the reactor capillary, and reducing the flow rate of reactants (concentrations would have to be increased proportionately in order to add enough reagent for the immunoreaction). One attractive possibility that may allow such improvements and therefore higher chromatographic performance is the use of microfluidics in coupling these systems. The use of microfluidics would also simplify the assembly of the system. Such improvements would ultimately put more pressure on the CE performance as faster CE would be required to adequately sample the narrower chromatographic peaks.

CE-Immunoassay with RPLC Preconcentration

Figure 4-6 shows a contour plot representing a series of electropherograms corresponding to a portion of a chromatography run in which 5 μL of 600 pM glucagon was injected onto the column. As shown by the figure, the free Glu* peak migrating at 0.95 s begins to increase and complex peaks migrating at 0.6 s and 0.8 s start to decrease at approximately 190 s in the chromatographic time axis indicating elution of the

unlabeled glucagon from the column that reacted with the antibody thus allowing detection by the rapid CE-immunoassay. It is possible to reconstruct a conventional chromatogram by calculating the F/B ratio from each of the electropherograms and plotting them as a function of time as illustrated at the top of Figure 4-6. Such plots are used for the presentation of other chromatograms.

The high sensitivity of the system is demonstrated by Figure 4-7, which shows the reconstructed chromatograms for a series of samples at different concentrations. From the chromatogram of 50 pM glucagon in Figure 4-7 we calculate a detection limit of 17 pM based on the concentration required to obtain a signal 3 times RMS noise in the chromatogram. Detection limits averaged 20 $\pm$ 15 pM (n = 5) with day-to-day variations in signal and baseline stability. In the off-line mode, the detection limit for this assay was 760 pM (Ger00b), thus the concentration detection limit was improved ~45-fold by the preconcentration step.

Analysis of glucagon with concentrations of less than 500 pM was complicated by progressive loss of signal for a given sample. This signal loss presumably occurred as a result of adsorption of glucagon to the inner walls of sample container or other types of sample degradation (Kus97). Attempts to prevent adsorption by addition of non-ionic detergents did not provide any improvement in the size or reproducibility of the peaks. Addition of insulin at 1 μM to the solutions to block adsorption sites greatly improved the detection limit and reproducibility as shown on Figure 4-8. Insulin was chosen as a site blocker because it has similar hydrophobicity to glucagon; however, as insulin was the only proteinaceous site blocker we tested, it is likely that other peptides or proteins could be added with equal effectiveness. Without addition of insulin, peak areas were

attenuated by as much as 5-fold. To further reduce adsorption, glass microvials used for the sample preparation were cleaned by soaking them in 50% nitric acid overnight followed by rinse in distilled water and drying at 100 °C for 2 hrs. Even with these precautions, sample degradation was significant after a few minutes and necessitated preparation of a fresh solution for each separation.

Considerable improvements in concentration detection limit are possible with this system. The noise shown in the chromatograms in Figure 4-7 is associated with irreproducibility of the F/B ratio detected in the electropherograms. Such noise can be caused by irreproducibilities in the injection and by fluctuations in the flow rate through the reaction capillary. Higher quality pumps and more sophisticated injection procedures may eliminate these errors. In addition, minimizing the band broadening may increase the signal and lower dilution as discussed above. Finally, larger injection volumes could easily be used to further improve the concentration detection limit if sufficient sample is available.

A representative calibration curve using concentrations from 50 to 1300 pM is illustrated in Figure 4-9. Based on the linear dynamic range of the competitive assay, we expected the standards to yield linear responses up to ~900 pM after preconcentration. As shown, this effect is observed with a small deviation from linearity occurring at the 1300 pM sample. Reproducibility of the method was moderate with an average RSD of 12% for all standards between 50 and 1000 pM (range was 3 to 23%). As discussed above, signals for a sample decline with time suggesting that sample degradation is an important source of variability at these low concentrations; however, further research is needed to determine the exact cause of signal variability.

Glucagon Secretion from Single Islets

To demonstrate application of the described system to the analysis of biological samples, we analyzed glucagon secretion from single rat islets. Rat islets contain ~2000 cells with only ~30% being glucagon secreting cells, thus secretion of glucagon from a single islet corresponds to secretion from ~600 cells. Basal secretion is expected to produce concentrations of ~300 pM (Kol90) in the volumes used here. Such low concentrations would be impossible to detect by CEIA without preconcentration. Figure 4-10 illustrates chromatograms obtained for media containing single islets under basal and stimulated conditions. The average concentrations measured were 120 ± 20 pM for basal and 580 ± 50 pM for the stimulated samples. Actual concentrations in the media were 4-fold higher as the samples were diluted to maintain their concentration in the dynamic range of the assay. Thus, the basal secretion corresponded to 470 pM which is in reasonable agreement with the literature value of 300 pM (Kol90).

RPLC Separation With CE-Immunoassay detection

A significant advantage of the coupled RPLC-CEIA system is the ability to differentiate multiple species that cross-react with the antibody. Such detection is impossible by the competitive CEIA alone since only antibody bound to the labeled complex is detected. Although antibodies can be highly selective, cross-reactivity can be a significant problem when multiple compounds are present that have the same epitope. For example, families of peptides with common amino acid sequences, isoforms of proteins, or small organic compounds with structurally similar metabolites are all analytes in which cross-reactivity can easily occur. The ability of our new system to

separate analytes by RPLC and detect them one at a time provides a solution to this problem.

To demonstrate the ability of our system to separate and detect cross-reactive species, we analyzed solutions that contained both oxidized and native forms of glucagon. A 100 nM solution of glucagon was prepared in 10 mM phosphate buffer at pH 7.4. These conditions were found to promote rapid oxidation of glucagon. After 10 min, an aliquot was removed, diluted in loading buffer, and analyzed as before. A typical chromatogram from this experiment is shown in Figure 4-11. Native glucagon is still present; however, two new peaks appear which are presumably oxidized products of glucagon.

Comparison to other techniques

The combination of capillary LC with CEIA may be considered analogous to HPLC coupled with RIA where samples are separated by HPLC and fractions collected to be analyzed by RIA. HPLC-RIA is often used when antibodies are not selective enough for the particular target such as analysis of peptide families; however, because this procedure uses manual fraction collection and RIA, it can be cumbersome, and because it uses HPLC it requires relatively large samples. With the miniaturization (microliter samples are compressed to nanoliter volumes) and automation of the capillary system described here, comparable information can be obtained faster, more simply, and with improved detection limit.

An automated method combining separation with affinity detection may open up a variety of other applications as well. For example, RPLC-CEIA may be used for Western-blot style analysis. In Western blotting, samples are separated by gel electrophoresis and resolved bands are detected by immunostaining. This technique is

widely used in biochemical analysis to identify immunoreactive species and to follow biochemical transformations. Although highly informative, such methods are not quantitative and consume significant time and labor. Our RPLC-CEIA system can be utilized to perform an RPLC-based Western blot and would allow automated quantitative analysis of samples in picomolar concentrations. Additionally, use of chromatographic methods provides separation mechanism previously unavailable for such analysis. The system may also provide a convenient tool for rapidly screening natural or synthetic compound libraries for specific affinity interactions. A complex mixture injected onto the LC column could be fractionated and then assayed by a competitive CE assay. The affinity reagents could include antibodies, enzymes, or receptors thus facilitating use of this approach for drug discovery.

Routine use of the method for these applications would be aided by improvements in resolution and peak capacity of the system. As mentioned above, this mainly would involve reduction of band broadening in the interface of the methods, perhaps by the use of microfluidics. Alternatively, if the sample size is not limiting, the use of a larger volume LC column and slower separation would minimize the contribution of the CEIA system to band broadening allowing a higher resolution LC separation to be obtained.

Conclusion

The RPLC-CEIA system presented here allows rapid and highly-selective quantitative determination of biological macromolecules present at low picomolar concentration in 5 μL samples. This system eliminates two of the most important disadvantages of the CE competitive immunoassay, namely a detection limit that depends

upon binding constant and inability to differentiate cross-reactive species. The method may have a variety of applications including assays of dilute biological samples, Western-blot style analysis, and library screening.

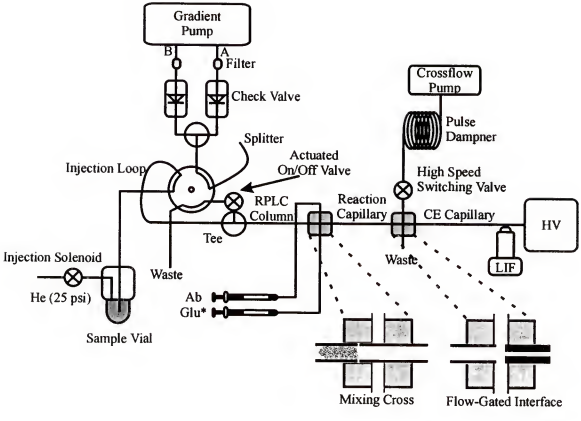

Figure 4-1. Schematic of HPLC-CEIA system used. Description of the system and operation are given in the text.

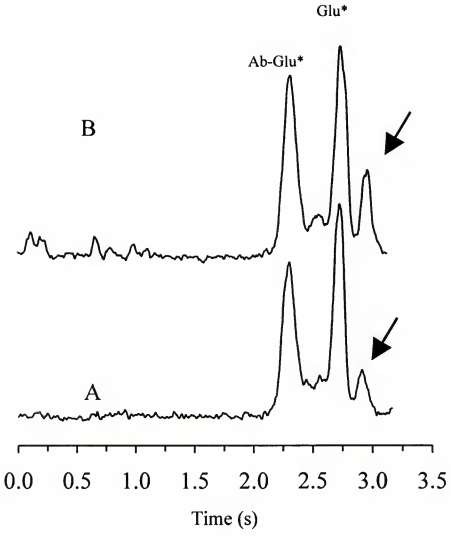

Figure 4-2. Representative electropherograms from the demonstrating on-line mixing and incubation. For this experiment only 15 nM Glu* and 15 nM Ab dissolved in 50 mM tricine buffer (pH 8.3) were used. Individual syringes containing reagents were attached to connecting capillaries using Teflon sleeves. (A) Sample electropherogram from the series with fresh reagents. (B) Sample electropherogram from the series with generated after 1 hr of continued pumping of reagents.

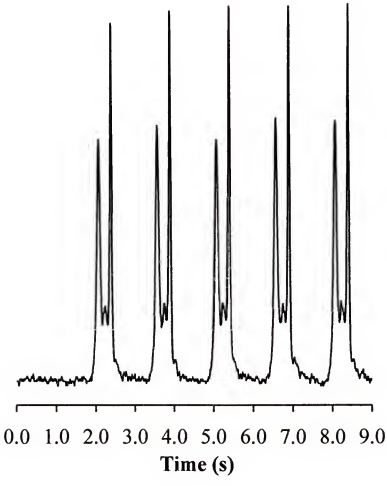

Figure 4-3. Series of five electropherograms illustrating the CEIA with on-line mixing and high-speed acquisition. Each set of three peaks represents the injection for one immunoassay. Injections lasting 125 ms were made every 1.5 s for this trace. Since each electropherogram required 3 s, this injection rate required overlapping electropherograms. The first two peaks in each set are complexes of Glu* and Ab while the third peak is free Glu*. (Peak identity established in (Ger00)). The apparatus shown in Figure 1 was used for this experiment except the RPLC column was replaced with a empty capillary and mobile phase A pumped (no Glu) by a syringe, thus the electropherograms are blanks for the CEIA. Flow rate through all channels was 150 nL/min. The Glu* channel contained 15 nM Glu* and the Ab channel contained 15 nM Ab both dissolved in 8 mM tricine buffer (pH 8.3) containing 3 mM EDTA. All other conditions are given in the Experimental section.

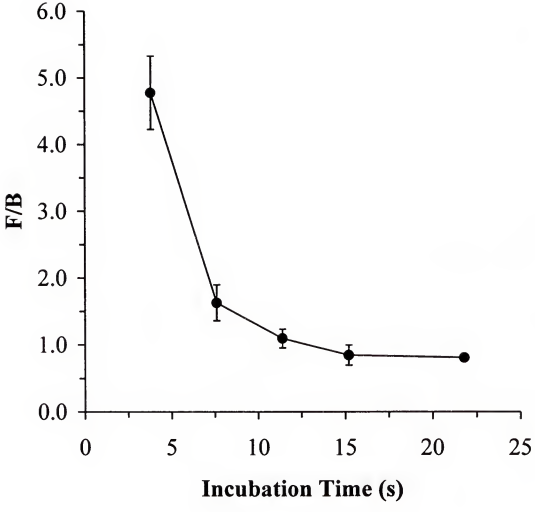

Figure 4-4. Effect of reaction time on F/B ratio for Glu*. CE-immunoassay conditions were as described in legend for Figure 2. Reaction times were varied by changing the length of 50 mm reaction capillary while keeping flow velocity at constant 0.76 cm/s. Each point represents the average of 10 electropherograms.

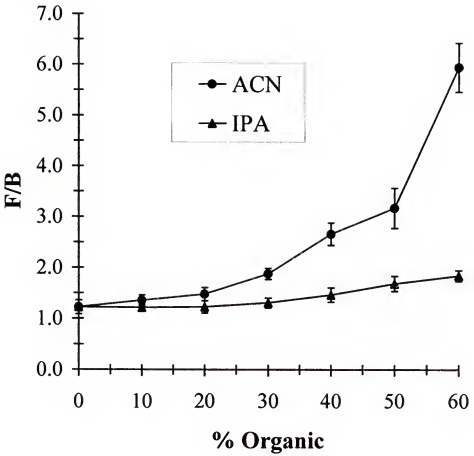

Figure 4-5. Effect of organic modifier on F/B ratio for Glu*. The experiment was performed as described in Figure 2 except that blank capillary contained a mixture of either acetonitrile or isopropanol in 10 mM phosphate buffer at pH 2.5. Percentage of the organic modifier mixture is shown on the x-axis of the plot. This arrangement is used to approximate expected chromatographic conditions.

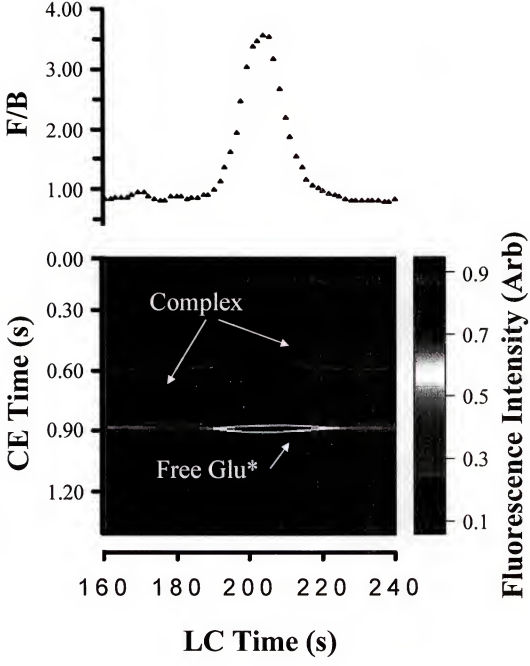

Figure 4-6. Contour plot of a RPLC chromatogram with CE-Immunoassay detection. Sample injected was 5 mL of 600 pM glucagon. Top portion of the figure represents a reconstructed chromatogram obtained by calculating a F/B ratio from each of the electropherograms.

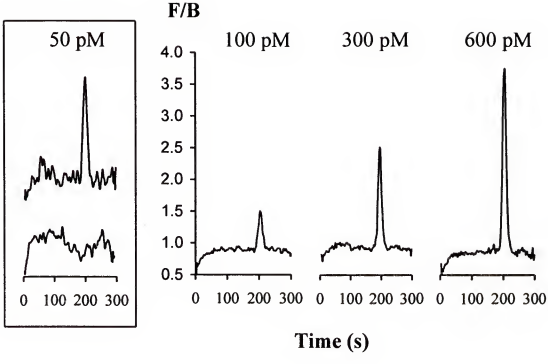

Figure 4-7. Series of chromatograms obtained using CE immunoassay detection. Each chromatogram represents a 5 mL injection of glucagon standard at the indicated concentration. Each standard contained 1 mM insulin to prevent adsorption of glucagon. Insert shows high sensitivity separation of 50 pM glucagon versus a chromatogram obtained by injection of sample matrix only.

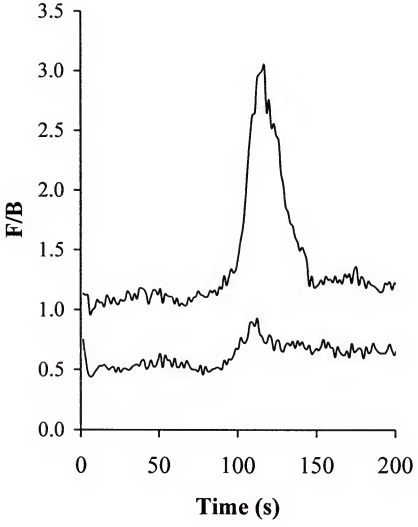

Figure 4-8. Effect of addition of 1 mM insulin to the glucagon sample. (A) Chromatogram of 500 pM glucagon without insulin present. (B) Same concentration of glucagon with addition of insulin. For this figure only, RPLC flow-rate of 300 nl/min, immunoassay reagent flow-rate of 300 nl/min each.

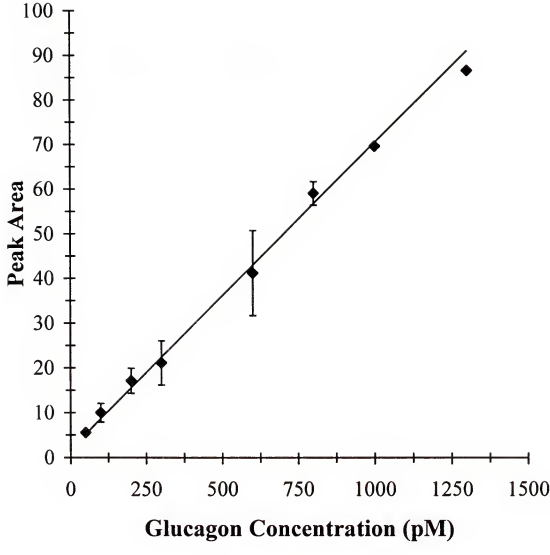

Figure 4-9. Calibration curve for the determination of glucagon. Each sample was prepared and analyzed in triplicate except 1 nM and 1.3 nM that were analyzed once. Error bars are ± 1 standard deviation.

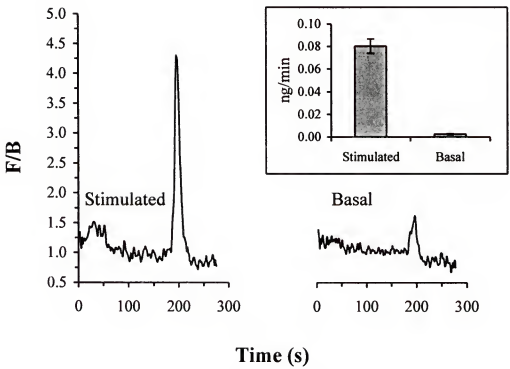

Figure 4-10. Analysis of glucagon secretion from single islets. Single islets were incubated in KRB buffer and media analyzed as described in the Experimental section. Measured concentrations were 120 ± 20 pM for basal and 580 ± 50 pM (n = 3) for stimulated samples. Insert compares secretion rates for the stimulated and basal secretions. Basal secretion rate was 2.7 pg/min for basal and 80 pg/min for the stimulated islet.

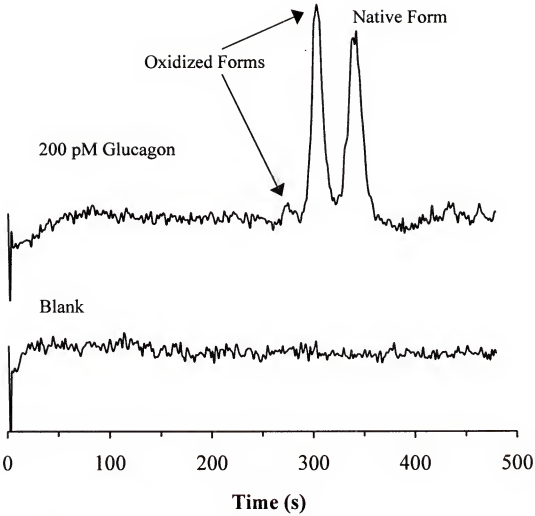

Figure 4-11. Capillary RPLC separation with CEIA detection. Chromatogram is obtained using same experimental parameters as in Figure 4-7 except gradient time was increased to 3 minutes. Stock glucagon solution was prepared in 10 mM phosphate buffer at pH 7.4 and allowed to stand for at least 30 min. (A) 200 pM sample. (B) Blank.

CHAPTER 5
HPLC PRECONCENTRATION AND SEPARATION OF PEPTIDES WITH ON-LINE CAPILLARY ELECTROPHORESIS IMMUNOASSAY DETECTION

Introduction

Many hormones and neurotransmitters are peptides found throughout mammalian body (Ems79). Due to high functional specialization, active peptides present in much lower concentrations than other molecules. Majority of neuropeptides and hormones are found in basal concentration range of 1 to 150 pM, which makes them difficult to detect and monitor (Rob91, Ger00a). Additionally, many large peptides are strongly hydrophobic and are easily oxidized, which makes detection further complicated.

Radio immunoassays (RIAs) are often used to measure low concentration of peptides since their detection limits are sufficiently low. Although a popular technique, RIAs possess a number of disadvantages that promote further development of the technology. RIAs main problem is large amount of time and effort required to perform. Frequently, RIAs are performed in a parallel format to decrease the analysis time. Although this makes time-per-assay reasonably short, samples collected early in the sequence must be stored for a prolonged period of time before the analysis. As a result, significant loss of recovery may occur for some of the samples. Another difficulty with RIAs arises from presence of cross-reactive to antibody molecules. Often, an HPLC separation is used to separate analytes prior to RIA analysis, which requires a large volume of sample and fraction collection.

Competitive capillary electrophoresis immunoassays (CEIA) have been developed in attempt to improve speed and ease of automation for the detection of the variety of biological molecules (Ken97, Bao97, Sch97). In a competitive assay, a fluorescently labeled antigen (Ag*) competes with antigen of interest (Ag) for binding to a limited amount of antibody (Ab). CE-LIF separation of the mixture produces two distinct fluorescent peaks corresponding to Ag* and Ag*-Ab complex, the intensities of which can be related to the original concentration of Ag.

Sensitivity and selectivity of competitive CEIAs can be significantly improved by coupling the assay on-line to the capillary reverse phase liquid chromatography (cRPLC). In this technique, a small volume of sample is loaded onto a short cRPLC column and preconcentrated. As mobile phase composition is changed during gradient elution, preconcentrated samples are separated and eluted from the column. Eluting peaks mix with necessary immunoassay reagents in the reaction cross, react while traveling through the reaction capillary, and are sampled on-line using rapid CEIA in a repetitive fashion. This allows separation of complex samples as well as significant enhancement in concentration limits of detection (Ger00a).

In many instances, separation step may be beneficial prior to detection of samples by immunoassay. By performing a separation, cross-reactive to the antibody analytes could be separated for better detection. Also, samples could be precleaned from potential interferences such as salt, large amounts of lipids, and other molecules.

Previously (Ger00a), we have indicated that mixing cross and reaction capillary contribute significantly to the overall peak broadening. In attempt to improve resolution of the system, we examined effects of wide-bore cRPLC columns on resolution in our

system. In situations were preconcentration is a primary purpose, utilization of a small-bore columns in conjunction with step gradient elution will provide lowest limits of detection. However, in cases were separation is of interest large bore capillaries with shallow gradients could be used.

Neuropeptide Y (NPY), a 36 amino acid peptide, is one of the most abundant neuropeptides present in brain (Chr89). Although implicated in many physiological functions, NPY has been recently identified to direct feeding in mammals (Kal91). Additionally, it was found that pancreatic islets of Lnagerhans, which are cell clusters that secrete many important hormones, secrete both NPY and glucagon (Nus00). In this work, we demonstrate development of a new method for determination of extra-cellular levels of NPY using competitive CEIA and capillary reversed phase cRPLC preconcentration. Initially, a new on-line competitive CEIA for NPY was developed and characterized. Subsequently, the assay was coupled on-line to the cRPLC using previously described technique (Ger00a). Once hyphenated HPLC-CEIA system for NPY was calibrated and detection limit determined, several push-pull samples form paraventrical hypothalamic nucleus (PVN) were analyzed to demonstrate the ability of the system to measure NPY in biological samples. Glucagon and NPY secretion from pancreatic islets was detected using the hyphenated system with gradient separation and simultaneous detection by CEIA.

Experimental

Chemicals

Unless stated otherwise, all chemicals used were from Sigma Chemical Co. (St. Louis, MO). HPLC grade isopropanol was purchased from Fisher Scientific (Pittsburgh, PA). Artificial cerebral-spinal fluid (aCSF) contained (in mM): 124 NaCl, 5 KCl, 0.1 $CaCl_2$, 3.2 Mg Cl_2, 3.2 *d*-glucose, and 26 $NaHCO_3$ (pH 7.4). Kreb's Ringer buffer (KRB) contained (in mM): 118 NaCl, 5.4 KCl, 2.4 $CaCl_2$, 1.2 $MgSO_4$, 1.2 KH_2PO_4, 3 *d*-glucose, and 25 HEPES (N-hydroxyethyl]piperazine-N'-[2-ethanesulfonic acid]) (pH 7.4). Mixing buffer (MB) contained (in mM): 25 Tricine, 3 EDTA, 1 NaN_3, 0.001 bovine serum albumin (BSA) pH 8.25. Capillary HPLC mobile phase A (MP-A) was 0.1% v/v trifluoroacetic acid (TFA) and 25 mM triethylamine (TEA), pH 2.5, containing 5% isopropanol. HPLC mobile phase B (MP-B) was 10 mM TFA, 25 mM TEA, pH 2.5, containing 40% isopropanol. Mobile phases were degassed by He sparging.

Anti-neuropeptide Y delipdized whole antiserum ($K_a = 5.0 \times 10^{10}\ M^{-1}$, Sigma) was diluted 1:20 in 10 mM phosphate buffer (pH 6.5) containing 100 mM NaCl and 10 mM NaN_3 to form a main stock and stored at 4 °C prior to use. Monoclonal anti-glucagon from mouse ascites fluid (clone K79bB10, $K_d = 1.6$ nM, Sigma) was diluted to 500 nM in mixing buffer and stored at 4 °C prior to use. Fluorescent labeling was performed using 5-(6)-carboxyfluorescein succinimidyl ester from Molecular Probes (Eugene, OR).

Preparation of fluorescein-labeled glucagon (Glu*) neuropeptide Y (NPY*)

Labeling of peptides was performed as previously described (Ger00b). Briefly, reaction was initiated by addition of 0.1 ml of 10 mg/ml 5-(6)-carboxyfluorescein succinimidyl ester dissolved in anhydrous dimethylforamide (DMF) to 0.1 mg of NPY

dissolved in 0.4 ml of 100 mM carbonate buffer (pH 8.3) or to 1 mg of glucagon dissolved in 0.9 ml of the same buffer. The mixture was incubated for 1 hr at room temperature in the dark. Since NPY and glucagon each possess two possible labeling sites, three different products, two singly labeled and a doubly labeled, can be obtained from this reaction for both peptides. Reaction products were purified by HPLC using Vydac protein C4 column (Chrom Tech, Apple Valley, MN). To perform separation, a 10 min gradient from 20 to 40% isopropanol in 0.1% trifluoracetic acid was used. Separation was monitored using a UV-Visible absorbance detector (Spectra Series UV100, Thermo Separations Products, Riviera Beach, FL) set to 220 nm. Each peak was collected, diluted 1:100, mixed with the respective antibody and binding verified by CE as described later. The peak that produced stronger affinity towards the antibody was chosen for all of the experiments. Purified labeled peptide fractions were collected and concentration estimated using visible absorption of fluorescein at 496 nm ($\varepsilon = 75\ 000\ M^{-1}\ cm^{-1}$). Derivatized glucagon and NPY were stored in the HPLC mobile phase at –7 °C when not in use. These conditions prevented degradation of both NPY* and Glu*.

Capillary Electrophoresis

All electrophoresis capillaries used were 7.2 cm long with 10 μm inner diameter (i.d.) and 360 μm outer diameter (o.d.) (Polymicro Technologies, Phoenix, AZ, USA). The CE apparatus used in this work was identical to previously reported one (Ger00a). Injections were performed using a flow-gated interface (Hoo97). Cross-flow was supplied by a HPLC pump (SSI 222C, Fisher Scientific, Pittsburgh, PA) which was connected to a flow-gated interface through a pulse dampener and in-line filter screen (Valco Instruments Co., Houston, TX). To make an injection, the cross-flow was stopped

for 125 ms using an air-actuated switching valve (Valco Instruments, Houston, TX, USA). A high voltage power supply (CZE 1000R from Spellman High Voltage Electronics, Plainview, NY, USA) was used to apply an electric field of 3500 V/cm (25 kV total voltage applied) across the CE capillary. Detection was accomplished using a LIF detector using a 488 nM line of an Ar-ion laser for excitation. Fluorescence at 520 nm was collected with a 40x microscope objective and detected by a PMT. Separation buffer consisted of 50 mM tricine at pH 8.3 and was prepared daily.

On-Line Competitive CEIA for NPY

To perform on-line immunoassay, equal flow rates of each 9 nM NPY* in MB, 1:33 fraction of anti-glucagon stock in MB, and sample in MB (this syringe could be replaced with a capillary HPLC column) were mixed using a PEEK cross (Valco, Instruments Co., Houston, TX). A microliter syringe pump (Harvard Apparatus, South Natick, MA) was used to deliver reagents to the mixing cross at 155 nL/min each. After mixing, analytes react while solution is flowing through 18 cm long 50 μm i.d. reaction capillary with total reaction time of ~45 s.

Composition of mixing buffer (MB) was chosen to prevent adsorption (addition of BSA), promote sample stability (azide and EDTA), and to have sample conductivity lower than separation buffer. As interaction with stainless steel rapidly degrades both labeled peptides, 75 μm i.d. fused silica capillaries were used to connect each syringe to the mixing cross. To prevent oxidation, Glu* and NPY* were prepared in a solution previously sparged with He and kept loaded in a gas-tight syringe to prevent air contact. With the above treatment, this solution can be used for ~4 hours of experiments before oxidation products are observed.

Capillary HPLC-CEIA

Two separate experimental arrangements were used in this work as shown in Figure 5-1. Applications that require high sensitivity utilized HPLC assembly and procedures described previously and shown on Figure 5-1A (Ger00a). Briefly, samples were filled into the sample capillary through the injection port and the opened splitter shut-off (depicted on the Figure 5-1A). To load the samples onto the column, splitter was closed by an actuated splitter shut-off valve and pumped directly at 3 μl/min into the column. Once the column was loaded, splitter was opened, system equilibrated at the separation pressure, and elution initiated. Samples were injected and column equilibrated at 5% MP-B, with subsequent step to the 85% MP-B to elute the preconcentrated zone.

The RPLC column was 4.5 cm long by 50 μm i.d. packed with Prosphere 300 Å, 5 μm, C4 particles (Alltech Associates, Inc. Deerfield, IL) using packing procedures described elsewhere (Ken89). Packed columns were placed into the system and rinsed with MP-B for 30 min at 200 nL/min before use; separation flow rates were ~ 150 nl/min. Five microliter sample capillary was used in all of the high sensitivity experiments. Capillary RPLC system was connected to the CEIA system with a previously described zero dead volume connector (Ger00a), which when properly aligned reduces broadening of the eluting zones. No experimental changes were needed to the immunoassay, which was used as described above.

Effect of the column diameter on the efficiency of the system was determined using a conventional injection arrangement with a 10 μl injection loop as seen on Figure 5-1B. Initially, UV-Visible absorbance detector (Spectra Series UV100, Thermo Separations Products, Riviera Beach, FL) was used in place of CEIA to simplify system

operation. In this case, distilled water was pumped by the syringes to prevent high absorbance caused by the buffer. Resolution between glucagon and NPY was compared using 50 and 150 μm i.d. columns both of 10 cm in length. Reaction capillary was 38 cm long. Samples were loaded with 5% MP-B for 10 min at 3000 psi, followed with a 2 min equilibration at 45% MP-B, and gradient elution using 45% to 70% change of MP-B over 10 min. Once separation conditions were determined, CEIA system was reattached. Typical HPLC flow rates in this case were between 0.5 and 1.0 μl/min obtained by applying ~200 psi at the head of the column. Pressure increased to ~800 psi at the end of the gradient due to change in mobile phase viscosity. To maintain proper concentrations and reaction time, immunoassay reagents flow rates were increased to 300 nL/min each and reaction capillary length was increased to 55 cm.

A MicroPro HPLC pump (Eldex, Napa CA) was used to perform all experiments. Both pump outlets were equipped with check valves and connected to an electrically actuated injection valve using a stainless steel tee (Valco Instruments Co., Houston, TX). Samples were loaded into the injection valve using a sample reservoir pressurized with He to 25 psi and connected to the valve by a 25 cm long 75 μm i.d. capillary. This approach was used instead of a syringe port to avoid cross-contamination by a syringe and to reduce introduction of particulates.

Measurements of the Anti-NPY—NPY* Affinity Constant

Measurements of affinity constants between anti-NPY and NPY* were performed to determine effect of HPLC mobile phase on binding using experimental setup shown on Figure 5-1B. In one experiment, 100 % CE separation buffer was pumped through the capillary HPLC column; in the other, 70% MP-B and 30% MP-A were delivered. To

determine antibody affinity constant (Mun80), plots of bound to free NPY* (B/F) peak area against concentration of free NPY* (F) were constructed by varying concentration of NPY* in the reagent syringe between 3 and 27 nM. Second reagent syringe contained a 1:13 dilution of the stock anti-NPY. Peak areas for the NPY* relative to internal standard (Glu*) were converted to concentrations means of a calibration curve. A 5 point calibration curve was linear up to 30 nM NPY* and had correlation coefficients of 0.998 or better. Once linearity of the calibration was established, a two point calibration curves were made on every day of analysis.

Data Acquisition and Analysis

CE data was acquired at 300 Hz by a National Instruments AT-MIO-16F-5 data acquisition board (Austin, TX) installed in a 486-66 MHz personal computer. Automated system control and data analysis were performed using software written in-house using Lab Windows (National Instruments). Peak parameters for both CE and HPLC were calculated using statistical moments (Gru69).

Sample Analysis and Calibration.

Stock peptide solutions were prepared by dissolving 0.1 mg of solid NPY or 1 mg of glucagon in MP-B (small quantities of 6 M HCl were added as needed to improve dissolution and acidify the sample) and stored in the freezer. Working stock solutions with concentrations of 50 and 100 nM were prepared daily by diluting main stock solutions in MP-A and kept on ice. Samples were prepared by further diluting the working stock to the desired concentration using MP-A. Analysis of samples was performed within 1 min of sample preparation to minimize sample loss and degradation.

Measurements of Biological Samples

Samples for measurements of the extracellular levels of NPY were obtained by push-pull perfusion of male Sprague-Dawley rats (250-400g, Charles River Breeding Laboratories) in the laboratory of S.P. Kalra of the University of Florida Brain Institute (Gainesville, FL), and analyzed using system depicted on Figure 5-1A. Push-pull canulae were implanted into the PVN and perused with aCSF at a rate of 20 μl/min. Collected 200 μl fractions were acidified and stored at –80°C prior to analysis (Kal91). Before the analysis, samples were allowed to thaw on ice, diluted 1:3 using MP-A, and 5 μl injected onto the high sensitivity system described earlier.

Secretion of NPY and glucagon from mouse islets was detected using arrangement shown on Figure 5-1B. Islets of Langerhans were isolated from CD-1 mice following ductal injection with collagenase XI and placed in RPMI culture medium (GIBCO, Gaithersburg, MD, USA) (Asp99). In 24 hours after isolation, groups of 10 islets were washed twice using KRB and placed either in KRB or in 30 mM KCl substituted KRB for basal and stimulated secretion experiments respectively. Islets were incubated in conical glass microvials with total solution volume of 50 μl for 30 min for stimulated secretion and 360 min for basal levels. After incubation, samples were diluted 50% with MP-A, and 10 μl of each sample were injected onto the system.

Results and Discussion

On-Line CE-LIF Immunoassay for NPY

Experimental conditions developed for analysis of glucagon (Ger00a, Ger00b) were used to perform CEIA for NPY. It was found that tricine buffer at pH 8.3 provided

good separation efficiency and minimal adsorption of zones onto the capillary walls. Figure 5-2 depicts two representative separations of the free and antibody-bound NPY* with and without addition of NPY. In both cases, a baseline separation of complex from the free NPY* peak was achieved in under 3 s. Since same conditions were also used in CEIA for insulin and glucagon (Ger00b), it is possible to hypothesize that many peptides could be analyzed by using these separation conditions.

Since it was planned to use CEIA system as a detector for capillary HPLC, several parameters including on-line reaction time, sampling frequency, as well as effect of mobile phase on binding were investigated. Optimal reaction time was determined by varying the length of the reaction capillary while keeping each syringes flow rate constant (overall flow velocity of 0.4 cm/s). It was found that at least 27 s (11 cm long reaction capillary) was required for complete reaction between antibody and NPY* (data not shown). However, to simplify instrumentation an 18 cm reaction capillary was used for the high sensitivity experiments.

Sampling frequency could be doubled by performing overlapping injections at every 1.5 s to fill unused separation space at the beginning of each electropherogram, as shown on Figure 5-3. Using CE separation buffer as a sample matrix, it was possible to triple sampling rate by performing overlapping injections every second. However, such frequent injections of HPLC eluent containing isopropanol resulted in severe irreproducibility of CE migration times possibly due to changes in viscosity of the CE separation media.

To determine the effect of mobile phase on binding, complex formation constants were determined in presence or absence of HPLC mobile phase. For these experiments,

mobile phase of the composition required to elute NPY (70% MP-B) or CE buffer was pumped through the column and mixed with immunoassay reagents. Results, shown on Figure 5-4, are presented in a form of bound to free (B/F) ratio vs. concentration of free (F) NPY*. The need for this format, compared to more conventional B/F vs. bound (B), is derived from possible presence of multiple binders and non-specific adsorption sites frequently found in solutions of polyclonal antibodies (Dia96, Mun80).

Both curves fitted well into the standard relationship for binding to a single class of binding sites with presence of non-specific adsorption as shown below (Equation 5-1) (Dia96).

$$B/F = \frac{NK_a}{1+K_aF} + n \tag{5.1}$$

In this relationship, B/F is the ratio between bound and free NPY*, F is concentration of free NPY*, K_a is affinity constant, N is total concentration of binders, and n represent non-specific adsorption (At large ligand concentration, $B/F \sim n$). In case of the top curve (CE buffer), obtained values were $K_a = 7.5 \pm 0.2 \times 10^9\ \mathrm{M}^{-1}$, $N = 3$ nM, and $n = 0.05$ (R^2=0.995); values for the bottom curve were $K_a = 2.0 \pm 0.3 \times 10^9\ \mathrm{M}^{-1}$, $N = 1$ nM, and $n = 0$ (R^2=0.988). Determined values indicate that a large pool of antibodies present, majority of binding sites possess similar affinity towards NPY*. Small amount of weak or non-specific binding was evident in the buffer case. Although non-specific binding may cause severe problems to the sensitivity of the assay, presence of organic molecules diminishes the effect. Previously, we reported that 0.1% TFA has caused reduction in the overall fluorescence signal (Ger00a). Such quenching may amend determined binding constants as well as contribute to differences in appearance of the curves. In both cases,

however, determined affinity constants were found lower compared to the value obtained by Sigma ($5x10^{10} M^{-1}$).

Although determined affinities were lower compared to the reported, the binding is sufficiently strong to warrant the assay. Figure 5-5 shows calibration curve for the NPY CEIA obtained with mixing buffer as a reaction media. To perform the experiment, NPY solutions with concentrations ranging from 0.5 nM to 200 nM were placed in one of the syringes, while the other two contained antibody and NPY*. Although calibration curve has the expected shape, it was not possible to fit theoretical binding model to the data points. This can be explained by two major factors: (1) Presence of significant non-specific binding evident by the fact that complex peak remains (*B/F* ratio does not change significantly) even at high excess of NPY; (2) Possible presence of binding sites capable of binding to NPY but not NPY*, which will severely decrease the slope of the linear region of the curve. Nevertheless, slope of the linear region of the curve as well as overall reproducibility of the system between 2 and 4 % RSD produced a concentration limit of detection of 850 ± 50 pM.

Detection of NPY with Capillary HPLC-CEIA

Figure 5-6 depicts a series of reconstructed chromatograms obtained by injection of 5 μl of 0, 100, 300, and 500 pM samples onto the HPLC-CEIA system. NPY peak migrates with retention time of ~ 140 s and increases in size with increasing concentration of injected sample. A sloping portion of the chromatogram between ~ 85 and 185 s represent change in the F/B ratio due to changes in HPLC eluent. Although gradient was stepped in 0.1 min by the pump, it is clear that the post HPLC reaction broadens gradient profile. The small peak at approximately 50 s migrates before the dead

time of ~ 85 s and represents a change in F/B ratio due to flow effects of the system. Although this peak presents no problems with respect to detection of NPY, allowing longer equilibration times after sample injection can eliminate it. Peak widths obtained ranged between 48 to 58 s, which is wider compared to 35-40 s reported for glucagon (Ger00a). Widening of the peaks is attributed to difficulties in aligning of the mixing cross and poor chromatography of NPY. Severe increases in widths are caused by slightest misalignment of two capillaries or presence of a gap between them. Improved performance could be achieved by utilization of a micromachined device, which will require no alignment or manual adjustment. Tailing of the peaks was most likely caused by the remaining ion exchange interactions. Utilization of alternative stationary phases and frits with minimized ion-exchange interaction would further improve overall peak widths and further lower limits of detection.

Insert on Figure 5-6 depicts a calibration curve obtained from the analysis of standards. Each sample was measured at least 3 times with average reproducibility of the system of 9% RSD. Detection limit of the assay was determined to be 40 pM based on the standard deviation of the low concentration sample and the slope of the calibration curve. Calibration curve was linear up to ~ 1 nM with expected curvature afterwards. This curvature is due to significant excess of preconcentrated NPY as it is analyzed by the immunoassay. Relatively large Y-intercept of the calibration curve is attributed to sloping background of the system.

Analysis of Brain Samples

The ability of the system to detect NPY obtained from push-pull samples of live rats is demonstrated by the chromatograms depicted on Figure 5-7. Five separate samples obtained from different rats were analyzed in triplicate with average relative

standard deviation for all replicate measurements of 12%, which is slightly higher compared to those of standards. This is most likely due to degradation of the replicate samples, which were kept on ice while earlier samples were analyzed. In many cases such samples gave slightly lower signals compared to those analyzed earlier.

Gradient Separations with CEIA Detection

Application of capillary HPLC preconcentration to enhance concentration limits of detection of CEIA is an extremely useful tool for analysis of dilute solutions. However, hyphenated capillary HPLC-CEIA system opens much larger possibilities for research applications. Examples of such applications include analysis of the cross-reactive to the antibody species (as was demonstrated for differentiation of crossreactive to the antibody forms of glucagon), HPLC-based western blotting, and screening of the complex libraries for tight binders. In all of these cases, a complex solution would have to be separated by the HPLC and affinity of the eluting peaks to the antibody or other molecule detected by the CEIA. For such applications, attention was directed towards improvement in efficiency of separation, with CEIA simply acting as a post column reactor and highly sensitive and specific detector or affinity analyzer.

As with any post-column derivatization, extra column band broadening can appreciably decrease overall efficiency of separation (5.2).

$$\sigma^2 = \sigma_c^{\ 2} + \sigma_A^{\ 2} \tag{5.2}$$

In this equation, the overall variance of the system, σ^2, is given as a sum of the variances due to column dispersion, $\sigma_c^{\ 2}$, and extra column dispersion $\sigma_A^{\ 2}$. A fraction of the extra column broadening, $f = \sigma_A^{\ 2}/\sigma_c^{\ 2}$, that can be tolerated by the system is an arbitrary value decided on the case-to-case basis. Assuming a well-packed column ($H=2d_p$), it can

be shown that for given f, magnitude of maximum tolerable extra column dispersion for the unretained peak (cm^4) can be estimated by:

$$\sigma_A^{\ 2} = f\frac{V_0^{\ 2}}{N} = f2\pi^2\varepsilon^2 d_p L r^2 \tag{5.3}$$

In this equation, ε is a column porosity factor, d_p is diameter of a particle, L is column length, and r is column radius. Therefore, any value of $\sigma_A^{\ 2}$ could be ameliorated by increasing the radius and length of the column at a cost of sensitivity.

One way to evaluate the effect of column diameter on the overall efficiency is to observe the change in resolution between two closely migrating compounds. NPY and glucagon were chosen as test molecules since both are highly hydrophobic. Results of the experiment are shown on Figure 5-7. Top chromatogram obtained using 50 μm i.d. 10 cm long column using 4.5 min linear gradient from 45% to 70% MP-B produced resolution of 1.1. To properly compare this result to the 150 μm i.d. column, gradient steepness must be the same for both columns(Dol98).

Gradient steepness is determined by a gradient steepness parameter b given by $b = \Delta\Phi \cdot S \cdot V_0 / t_G F$, where $\Delta\Phi$ is the change in organic modifier, V_0 is the void volume of the column, t_G is the gradient time, S is the solvent strength (4.2 for isopropanol), and F is column flow rate (Sny79). Using conditions reported for the top chromatogram (Figure 5-7), b was determined to be 0.25. The bottom chromatogram on the Figure 5-7 depicts separation of the same sample using 150 μm i.d. column. Since flow rate has changed from 133 nl/min to 500 nl/min, and due to change in the void volume of the column, gradient time t_G had to be increased to 10 min to maintain same gradient steepness. In this case, resolution between NPY and glucagon was 1.4 (See bottom

chromatogram on Figure 5-7). Since gradient steepness was maintained and assuming similar quality of packing, improvement in resolution could be attributed to decreasing importance of extra column band broadening. Utilization of even larger bore columns should further reduce effects of extra column broadening; however, increased column flow rate would have to be spilt for effective immunoassay reaction.

To demonstrate separation potential of capillary HPLC with CEIA detection, simultaneous CEIA for glucagon and NPY was arranged by simply mixing Glu* and NPY* in one reagent syringe and anti-glucagon and anti-NPY in the other (Figure 5-9). Due to higher cRPLC flow rates, adjustments of reagent concentrations and increase in length of the reaction capillary were needed. No changes in immunoassay separation conditions were necessary, which further underlines potential universality of conditions. Although complex peaks were not completely resolved due to similarity in their electrophoretic motilities, they could still be used for the analysis (see top of Figure 5-9).

Chromatograms shown on the bottom of the Figure 5-9 were obtained by selective monitoring of the F/B ratio for either NPY or glucagon. Although construction of a total immuno-chromatogram is possible, general differences in F/B ratios between individual assays makes it difficult. Each chromatographic peak was approximately 100 s wide, which was wider compared to peaks obtained under similar conditions using UV-Visible detector. In addition, resolution of 1.2 obtained with CEIA detection was lower compared to 1.4 obtained with UV-Visible detection. This can be explained by increase in reaction capillary length and poor CE resolution of complex peaks. Decreases in the size of one glucagon complex peak causes F/B ratio of the NPY to increase causing NPY peak to widen.

Top four electropherograms on Figure 5-9 are excerpts from a series of 660 electropherograms required to cover entire separation and show changes in immunoassays that occur as a result of elution of NPY and glucagon peaks. By observing a change in the sizes of peaks of free Glu* and NPY* as well as partially resolved complexes, identification of the chromatographic peaks is possible. Notably, measurements of NPY and glucagon could be performed without HPLC separation since no significant inter-assay interference was observed; however, in this case simultaneous assay was used to visualize the concept of HPLC separation with CEIA detection.

An application of this system to biological samples was demonstrated by detection of glucagon and NPY secretion from pancreatic islets of Langerhans. Islets are clusters of cells secreting such peptides as insulin, glucagon, somatostatin, and NPY (Nus00). Figure 5-10 shows results of detection of NPY and glucagon during basal and stimulated secretion. Although data shown on the figure was obtained simultaneously, for clarity NPY and glucagon immuno-chromatograms are shown separately. As it is seen from the NPY portion of the figure, sensitivity of the system is not adequate to detect basal secretion of the NPY; however, stimulated levels of NPY are easily detected. Interesting feature is observed on the immuno-chromatogram for stimulated glucagon. Since glucagon was secreted at large amounts for over 30 min in the physiological pH, fraction of glucagon was oxidized and could be observed at ~ 500 s. Although separation of oxidized forms of glucagon was previously reported (Ger00a), utilized separation conditions allowed baseline separation of two peaks.

Hyphenated HPLC-CEIA arrangement offers considerable advantages to both CEIA and HPLC. From the standpoint of immunoassay, coupling to HPLC eliminates

two major problems associated with the competitive immunoassay format by providing higher concentration sensitivity and linear calibration. On the HPLC side, CEIA detection offers sensitivity and selectivity rivaled mainly by mass spectroscopy, as well as ability to provide affinity information at the same time. Although described system still requires refinement, demonstrated concepts indicate significant potential for a variety of applications. As an example, a peptide library could be screened for binding to the protein of interest by being separated into individual components by HPLC and each of the peaks tested to compete with natural binder to the said protein. If any of the peaks possess affinity, competition would be successfully detected by the CEIA. Since flowrates required for the CEIA are small, it might be possible to split a fraction of HPLC eluent for simultaneous analysis by mass spectroscopy to obtain both binding and structural information simultaneously. Finally, utilization of microfluidics will alleviate majority of difficulties involved with routine use of this technique. By including both HPLC and CE columns on the chip, described system could be made disposable and completely automated.

Conclusion

This work further enhances our understanding of the parameters needed to perform rapid CEIA. Demonstrated utilization of polyclonal antisera in the assay indicates potential for use with wider range of antibodies and reduction of purification steps; however, disadvantages of antisera include non-specific bidning and non-uniformity of the binding sites. The HPLC-CEIA system presented in this work allows fast and selective measurement of peptide levels in physiological matrix. The system was successfully used to detect NPY extracted from the brain of a rat. In addition, directions

for possible improvements in separation efficiency were identified and demonstrated by separation of NPY and glucagon with CEIA detection.

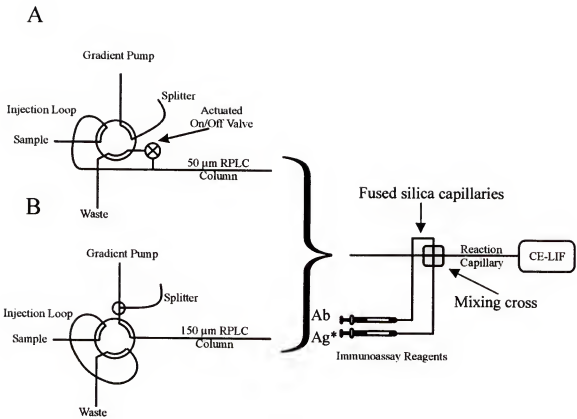

Figure 5-1. Diagram of the system configurations utilized in this work. Configuration (A) was used for high sensitivity measurements with 50 µm i.d. capillaries and step gradients. This system allows for high-speed large volume loading and maximum gradient steepness. Configuration (B) was used for improvements in separation efficiency with shallow gradients and for simultaneous measurement of glucagon and NPY.

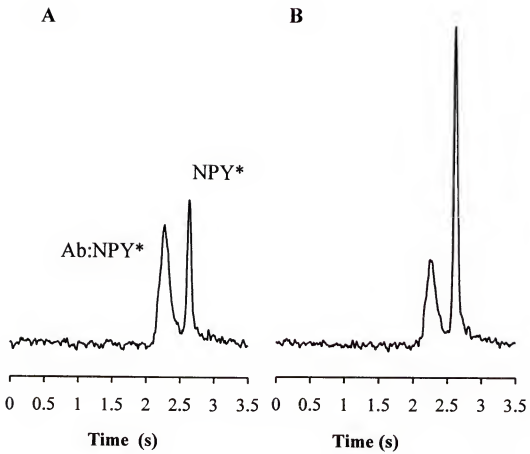

Figure 5-2. Separation of free and antibody bound NPY* with on-line mixing and flow-gated injections. Each electtopherogram was obtained bu mixing three 150 nl/min streams each containing (A) mixing buffer, 1:667th dilution of antibody stock, and 9 nM NPY*. To perform the assay, mixing buffer stream was substituted with the appropriate solution of glucagon. A representative assay containing 20 nM glucagon solution is shown in (B). To perform CEIA, 7 cm long (3.7 cm effective) 10 mm i.d. capillary was used under electric field of 3600 V/cm. Flow-gated sample injections were 125 ms long.

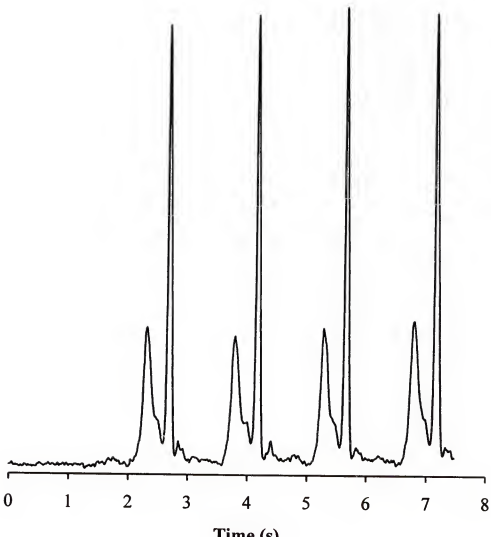

Figure 5-3. Series of representative electropherograms obtained by performing overlapping injections at every 1.5 s. Overlapping injections are possible since major peaks migrate between approximately 2 and 3 s leaving unused separation space. Other experimental conditions are as in Figure 5-2.

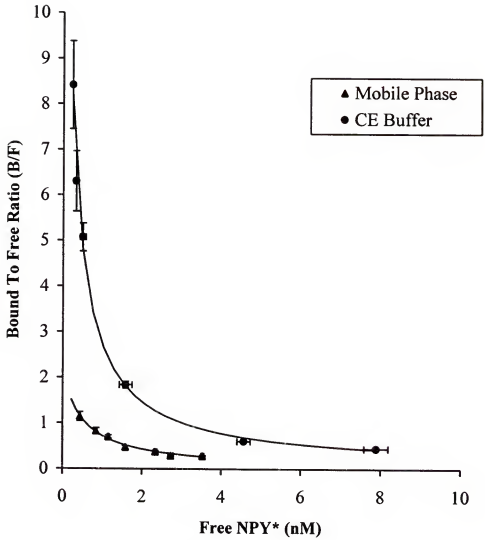

Figure 5-4. Determination of dissociation constant of antibody-NPY* complex under different experimental conditinons. To obtain the top curve, CE buffer was pumped through the HPLC column while different concentrations of NPY* was pumped by the surringe pump. In case of the bottom curve, HPLC mobile phase used for elution of NPY (70% MP-B) was pumped throught the HPLC column. Concentration of antibody was equal in all of the experiments. From the CE buffer, a 133 pM dissociation constant was determined with total concentration of binding cites of 3 nM. In the mobile phase experiment, dissociation constant of 500 pM was obtained with 1 nM of binding sites.

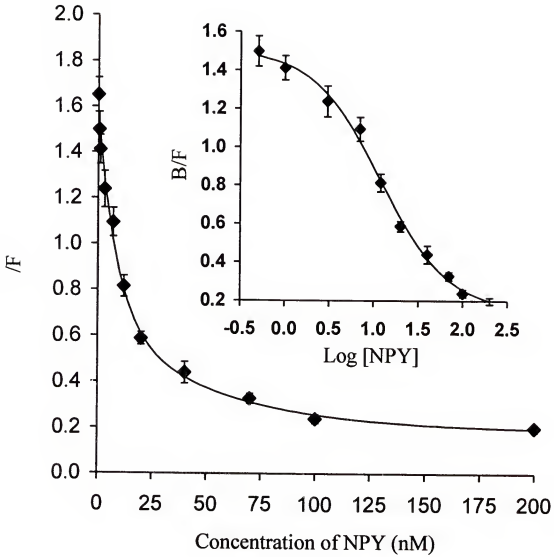

Figure 5-5. Calibration curve for the detection of NPY obtained using conditions described in Figure 5-2. Insert shows sample calibration performed on a semilog scale that demonstrates expected sigmoidal shape. A concentration detection limit obtained from this calibration was 850 pM.

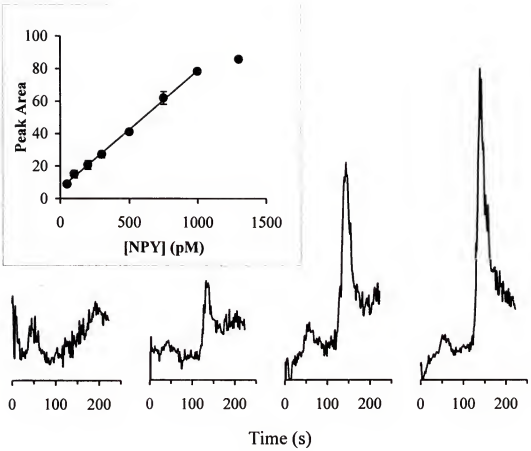

Figure 5-6. Detection of NPY by CEIA with cRPLC preconcentration. Five microliters of standards containing appropriate concentration of NPY were injected onto the system to obtain above chromatograms. Samples contained 0, 100, 300, and 500 pM NPY from left to right. Insert shows a calibraton curve obtained. Each sample was analyzed three times and error bars are 1 S.D. Concentration LOD for NPY was determined to be 40 pM.

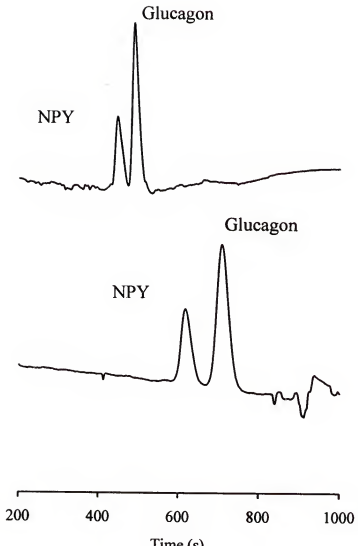

Figure 5-7. Effect of column diameter on chromatographic resolution of NPY and Glucagon with post-column reaction. Top chromatogram has resolution of 1.1 and was obtained using 10 cm long 50 μm i,d, column with the flow rate of 133 nl/min and gradient time of 4.5 min. Bottom chromatogram has resolution of 1.4 and was obtained using 10 cm long 150 μm i.d. column with flow rate of 500 nl/min and gradient time of 10 min. Both chromatograms have same gradient steepness of 0.25.

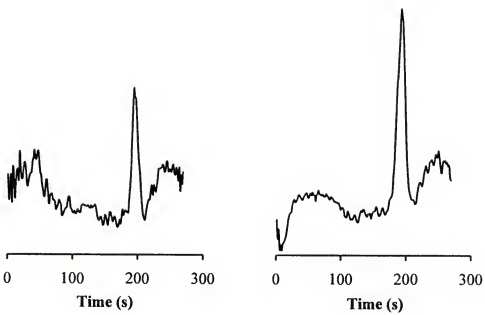

Figure 5-8. Analysis of push-pull samples obtained from PVN of the rat brain. Representative chromatogram form two samples form different animals. Each sample was treated as described in the materials and methods section and analyzed three times. Average reproducibility was 12% RSD.

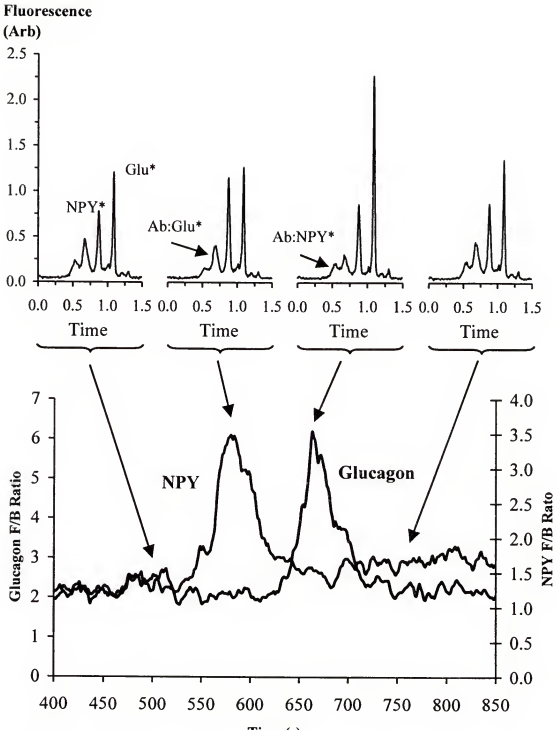

Figure 5-9. Capillary RP-HPLC separation of 500 pM each of NPY and Glucagon with simultaneous detecton by CEIA. Electropherograms at the top were taken from aporoximately indicated places on the chromatogram shown on the bottom part of the figure. LC separation was a 10 min gradient from 45 to 70 % MP-B.

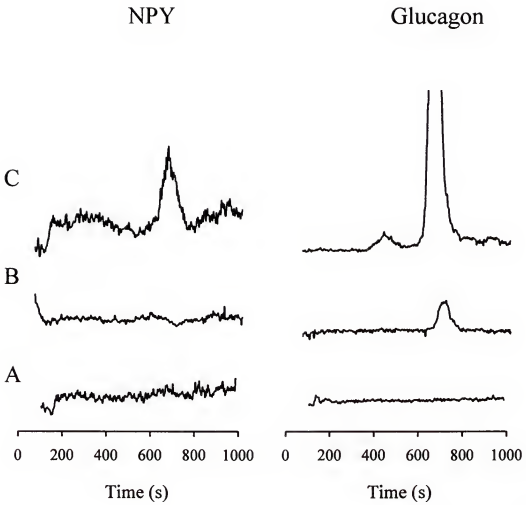

Figure 5-10. Detection of NPY and Glucagon secreted from pancreatic islets. Although data for both Glucagon and NPY was obtained simultaneously as in Figure 5-9, separate chromatograms are shown for clarity. Traces are: (A) blank, (B) basal secretion (C) stimulated secretion. To obtain samples, groups of 10 islets were incubated for the period of 6 hrs. in KRB for basal secretion and for 30 min in KRB substituted with

CHAPTER 6
SUMMARY AND FUTURE DIRECTIONS

Research efforts presented in this dissertation have been focused on improvement of existing capillary electrophoresis-affinity detection methods as well as development of novel approaches to measure proteins and peptides in biological samples. Chapter 2 presents work directed towards development of a non-competitive CE-affinity assay using combinatorially derived oligonucleotides (aptamers). Although demonstrated method was successful, significant improvement in separation conditions as well as development of new procedures would be required for wide utilization of this technique. New advances in biochemistry would undeniably improve affinity between aptamers and their targets, which would in turn provide new possibilities for aptamer-based assays.

Chapter 3 depicts work directed towards improvements to competitive immunoassays by capillary electrophoresis. Although competitive immunoassays considered inferior to non-competitive assays, their experimental simplicity would keep them utilized for a number of years ahead. Some efforts were directed towards development of universal conditions for competitive CE assays. Within the scope of this dissertation one set of optimized separation conditions could be used for all of the immunoassay, which indicates at least some extent of universality. However, additional testing and optimization would be required to demonstrate complete transferability of the experimental conditions.

Chapters 4 and 5 describe development of a novel conjugated system for performing ultrasensitive analysis of complex mixtures. The system was designed to combine high resolution and preconcentration powers of HPLC with high sensitivity and specificity of CE immunoassays. Deep understanding of separation conditions for the CE immunoassay and ability to perform assay at high speed allowed utilization of CEIA as a detector for the capillary HPLC. In this arrangement, CEIA rapidly samples the eluent of the HPLC to determine presence of the necessary analyte. By monitoring the ratio of free to bound peaks, it is possible to reconstruct original chromatograms. Using described methods, determination of glucagon content of the single islet of Langerhans, measurement of secretion of glucagon from the islet, measurement of extracellular concentration of NPY, and simultaneous detection of secretion of NPY and glucagon from islets were performed. This indicates that newly developed methods could be utilized for measurement of molecules from complex biological samples.

Future directions for this research should include development of a new affinity techniques as well as improvements to existing methods. Many simplifications and improvements are needed to the described systems to allow simple uninterrupted operation. Potential utilization of microfluidics may significantly simplify instrumentation setup and adjustment and would make described system more reproducible. Inclusion of a robotic sampling system would decrease amount of routine work involved and, therefore, decrease human error. For in-vivo operations, new sampling methods in conjunction with described detection schemes would without a doubt allow measurement of rare peptides with relatively good temporal resolution.

Improvements in immunoassay technology would play significant role in post genomic era of analytical chemistry. The ability to rapidly measure and classify phosphorylation patterns and glycoscillations as well as other signal transduction patterns could be addressed by affinity techniques described in this dissertation. Furthermore, future of proteomics goes beyond processing and identification of various proteins and peptides. Ability to provide rapid, specific, and quantitative measure of changes in levels of molecules could bring CE-immunoassays to the forefront of the proteomics.

Another area where described techniques could become significantly useful is drug discovery. Hyphenated HPLC-CEIA system has significant potential to perform rapid screening of a library of compounds and determination of the affinity of individual library components to the target of interest in real time. Rational drug design presently relies on screening of large libraries of compounds, which in many cases is a bottleneck in drug discovery process. Improvement in speed, reliability, and quality of information possible with described technology may shorten time to develop new and useful medicines.

APPENDIX A
FLUORESCENT LABELING AND PURIFICATION OF PEPTIDES

Two reactive groups that can be used to label peptides with fluorophores were examined during this work. Isothiocyanates (ITC's) and succinimidyl esters (SE's) are chemical groups that react with nucleophiles such as amines. SE's react with primary amines to form a very stable amide bond. When an ITC reacts with a primary amine, a thiourea linkage is formed. Although the thiourea product is reasonably stable, it has been reported that antibody conjugates prepared from fluorescent isothiocyanates deteriorate over time, prompting us to use fluorescent succinimidyl esters and sulfonyl halides almost exclusively for synthesizing our bioconjugates. Side-by-side comparisons in the literature have also found succinimidyl esters to be the preferred reactive functional group for conjugation to amines (Hua96).

Best results for labeling with fluorescein-SE were obtained when peptides were dissolved in 100 mM carbonate buffer at pH 8.3. There are two practical ways to initiate labeling reaction—one in which the dye is in excess and the other in which the peptide is in excess. In cases where peptide can form multiple products (multiple reactive groups) and only certain product is needed, it is beneficial to have peptide in excess. For instance, to label NPY, 0.33 mg/ml of NPY was mixed with 0.15 mg/ml of fluorescein-SE (final concentration).

Many peptides can be purchased in small sizes (1 mg or 0.1 mg) provided in dark glass vials. Such arrangement is the best since no handling of peptide is necessary;

moreover, brown glass provides protection from loss due to photobleaching. It is helpful to centrifuge vials with lyophilized peptides prior to dissolution to ensure that all of the peptide will be used. Reaction is initiated when appropriate amount of dye (dissolved in DMF or DMSO) is mixed with the solution of peptide and mixture kept in dark for 1 hour. Care should be taken to minimize amount of organic present in final solution so that RPLC purification could be performed. Solution must be gently swirled every 10 min preferably still in the dark. Use of Teflon coated stir-bars is not suggested.

After completion of the reaction, sample vessel must be placed on ice and purified immediately. Reaction termination step (addition of 1.5 M hydroxylamine, pH 8.5) has been suggested (ref); however, it was found that future purification is significantly complicated by this step. If sample cannot be purified immediately, it should be kept frozen until purification time.

Purification is performed using a standard 4.6 mm HPLC column, and detection is accomplished using UV-Visible absorption detector (usually set to 220 nm). Vydac protein-C4 column (Chrom Tech, Apple Valley, MN, USA) was used for all purifications performed. Generally, pH 2.5 is preferred for mobile phases, and nature of organic modifier has little effect on purification. For instance, glucagon purification was performed using 0.1% (v/v) trifluoroacetic acid and acetonitrile. On the other hand, NPY was purified using 10 mM phosphate buffer and 40% isopropanol. Initial step in purification is typically a linear gradient from 5 to 95% organic over 10 min (only 25 to 50 μl is needed for injection). During this step, all eluting peaks are collected and stored on ice. An aliquot from each fraction is diluted 100-fold and analyzed by CE (if fluorescent signal is too high, further dilution should be performed). Fluorescent

fractions are identified and tested for binding to the affinity probe. Although most fractions would not appear pure and may contain multiple CE and HPLC peaks, it should still be possible to identify potentially useful peaks.

In the next step, separation conditions are adjusted to completely resolve peaks of interest. Once that has been achieved a significantly higher volumes (250 μl was used for purification of NPY) may be injected to increase concentration of the purified fraction. CE experiments should confirm purity and functionality of obtained fractions, and concentration should be determined by measurement of visible absorption of fluorescein at 496 nm ($\varepsilon = 75\ 000\ M^{-1}\ cm^{-1}$).

APPENDIX B
BRIEF MANUAL FOR USE WITH SPF AUTOMATIC PEAK FINDER

Introduction

The main purpose of this program is to help an analytical chemist performing research in the area of chromatography or capillary electrophoresis with the analysis of the results. The Super Peak Finder (SPF) program will accept an individual data file or a sequence of data files and provide complete analysis of the peaks. Each file can contain up to 6000 data points (8000 for the uncompiled version). For each peak in each of the data files the retention time, height, FWHM (full width at half maximum), area, variance, and skew are calculated.

System requirements

Minimum system requirements are IBM® compatible computer with at least 486DX- 33MHz processor and VGA monitor. In order to load a file that has close to 6000 data points at least 620K of free memory should be present. Mouse is strongly recommended although it is possible to operate the program without a mouse. Files that must be present in the program directory are: 5.0DR, 7.0DR, 9.0DR, 11.0DR, 13.0DR, 25.0DR, SPF.EXE, PFL2.UIR.

Peak definition

Because SPF allows for a great flexibility of the operating parameters, some knowledge of the peak definition procedure used by the program is necessary. In order to find the peak and determine its parameters a general definition of the peak limits should be stated. In SPF, the peak is considered to begin or end when any one of the following two conditions is satisfied.

1. The difference between the current point's Y value and the previous point's Y value is less than Smallest Positive Difference (SPD) for a number of consecutive data points (Left and Right data entry box on the screen) This means that fluctuations are only allowed within the SPD interval.
2. The absolute value of the difference between the current point's Y value and the previous point's Y value is larger than Smallest Negative Difference (SND). This is used in case when two peaks are very close together. If difference between two points becomes negative (which may indicate the beginning of the new peak) and it is greater then SND, then it is the end of the peak.

The values for Smallest Positive Difference, Smallest Negative Difference, N1 and N2 are user definable parameters. Only peak's ends are defined, because the program first locates the approximate maximum of the peak, and then proceeds to the right or to the left of the maximum to find peak's ends. Once the beginning and the end of the peak are found, the program searches for the true peak maximum. It is clear that peak definition parameters must be adjusted for each individual data set. Once the optimal parameters are found, no further adjustment is needed.

Main Menu

- File: Used to load individual files, sequence files, and to save the output
- Find Peaks!: Used to initiate peak search
- Sequence!: Used to start the sequence file analysis process
- Size: Used to expand portions of data file and to revert back to original
- Smoothing: Used to perform smoothing using selected parameters. Allows undo.
- Peak Data!: Used for manual peak processing. The peak must be selected by cursors.
- Print!: Not implemented
- Exit!: Quits the program

Using the program to analyze individual data files

Before starting the program, make sure that mouse driver is loaded and that computer has enough memory. Next change to the program directory, type "spf" and press return key. Depending on the speed of your computer it may take several seconds for the program to load. Please note that all white boxes on the program screen allow the values to be changed; however, the values in green boxes are indicators and cannot be changed by user. Use your mouse and click on the File menu (or press Alt-F), Now press Open (move cursor down to highlight the command and press enter or use your mouse), The file selection box will appear. Select the file using your mouse, If you do not have the mouse you can use TAB and arrow keys to move around. Highlight the file name and press select. Please do not press Cancel button at any time, pressing it may cause global

error. This button is not used in this version of the program, it usually takes some time to load this file, will show the total number of data points in the file.

Once the file is loaded the box "Tot. Pts." will show total number of points in the file. Because this program is used primarily in chromatography, the data is acquired versus time at certain frequency. Scale of the graph is given in points. To determine the time at any point of the graph, move any cursor with your mouse to the point of interest. If you do not have the mouse, use the TAB key to highlight the cursor and use the arrow keys to move it (combination SHIFT-Arrow will allow for fine movement). The point location of the white cursor is located in the Cursor 1 box; the point location of the pink cursor is located in the Cursor 2 box. Use the point location of the point of interest and divide it by the frequency (see Frequency box). Using two cursors and the 'Diff.' box the time of certain interval can be determined.

To expand the chromatogram, locate two cursors around the area that you want to expand and use Expand command in the Size menu to expand any area of interest. Note that it is not possible to expand from already expanded area. Although you will get something on your screen, it will not make any sense. Also note that unless you know exactly the where you started, you cannot calculate time of the point while you are in expand mode. To return to full screen, use Full command from the Size menu.

For manual peak determination locate one of the cursors at approximately at the beginning of the peak and the other at the end (if necessary, zoom in before selecting peak). Press PeakData! in the main menu. All of the peak information is now displayed at the bottom of the screen. If you want to save this information you will have to write it

down. Note that this is the only place in program where white diamond at the summit of the peak is located at the true peak maximum.

Smoothing could be performed using the appropriate command in the main menu. In the Smoothing bar SG stands for Savitzky-Golay filter. This program only uses cubic filters with 5, 7, 9, , 13, and 25 points. As an example, locate the Smoothing bar to the SG 9 location and press 'Do it!' in the smoothing menu. To perform boxcar averaging, select it from the Smoothing bar, enter the number of points for the boxcar into the Box Car Size box and press Do It!. Please note that in this program, the boxcar averaging is used as a data reduction technique and will use the average as a replacement for the points used.

Automatic Peak determination

Load one of the files in the sequence and press Full in the Size menu. Adjust peak definitions parameters and press Find Peaks! in the main menu. If you get a "Too many peaks! select data reduction. This error is due to the fact that the program found more than 200 peaks, Press OK. In addition, area reject feature could be used to decrease the number of found peaks. Every time you use the automatic peak finder, the program rejects peaks that have the area smaller than some user defined value entered in the respectively called box on the screen. Please note that Due to unknown bug peak #1 marking are may be missing. This error can be simply ignored because the missing peak is not real peak but a creation of the program. The peaks are numbered from left to right. To see the data, either enter peak number into the white box in the bottom left corner of the screen (press return) or use left and right arrow buttons to advance through peaks in

the peak list. White diamonds at the top of the peaks are approximate location of the peak and do not represent exact peak locations.

Note that all calculations on the peaks are preformed using original data. The screen reflects only treated data. The information determined can now be saved using 'Save output' command in the File menu, Press the Save output command and enter the file name under which you want to save the data (remember not to press cancel in the file selection dialog). The only allowed extension for this part of the program is *.out.

Processing the sequence of files automatically

Load any of the files in the sequence. Let the program find all of the peaks of interest by manipulating with the peak definition boxes and filtering (Box car averaging is highly recommended since it usually provides best results). Press Sequence button on the main menu. The program will ask you to enter the start file number. Enter extension number of the fist file in the sequence. The program will now ask you to enter the end file number. Now the program will display the number of files in the sequence and ask if the user wants to start the sequence. Note that this is the last place to exit the sequence subroutine without causing the error. Press Yes. The program will now ask you for the output file name. Note that the program will generate 2 output files: one with the extension specified will contain all of the information determined by the program. The other with the extension *.pk will only contain peak heights (or areas).

Press Select and the program will now load every file in the sequence, expand it, box-car averaged it, processed it and store the information. It is very useful to observe the program in action and to determine if all of the peaks are found correctly. If some of the files were not correctly processed, adjustment of peak definition parameters may be

required. Note, the filename displayed during the sequence is the name of the file being loaded and not the name of the file on the screen.

APPENDIX C
FREQUENTLY USED RELATIONSHIPS IN CHROMATOGRAPHY

Chromatographic Resolution

In a well-behaved chromatography where the bands are symmetrical, or more specifically Gaussian, the separation of the peak maxima increases in proportion to the distance migrated, z, while the peak width increases as the square root of the distance migrated.

The complete equation for resolution is given by:

$$R_s = \tfrac{1}{4} \times \underbrace{\left\{\frac{1-a}{1+a}\right\}}_{\text{Relative Partition Factor}} \times \underbrace{\left\{\frac{\bar{k}'}{1+\bar{k}'}\right\}}_{\text{Degree of Retention factor}} \times \underbrace{\sqrt{N}}_{\text{Column Efficiency factor}},$$

where $a = k_2'/k_1'$, $\bar{k}' = \tfrac{1}{2}(k_1' + k_2')$, and k_1', k_2' are the column capacity factors of the two components whose resolution is R_s. N is the number of theoretical plates.

$$k' = \frac{\text{Equilibrium quantity of solute in the SP}}{\text{Equilibrium quantity of solute in the MP}} = \frac{\text{Time spent in SP}}{\text{Time spent in MP}}$$

Three factors in above equation emphasize:

1. Solutes must have different partition rations between the mobile and stationary phases or zones: $k_2'/k_1' \neq 1$.
2. Solutes must be retained: $\bar{k}' \neq 0$.
3. The column must be equivalent to the certain number of plates N.

Good values for the above parameters are: $N = 20000$, $k' = 2\text{-}10$, and $a = 1.15$. The first two factors in the equation are thermodynamic in nature, while N is kinetic.

Column Parameters

Plate Number: $N = 16(\frac{t_R}{w_t})^2 = 5.54(\frac{t_R}{w_{1/2}})^2$, where t_R is retention time of the retained solute, w_t is the base width, and $w_{1/2}$ is half height width.

Reduced Plate Height: $h = H / d_p = (L / 16\ d_p)(w_t / t_R)^2$, where L is the column length, d_p is particle size, and H is column plate height. Best value for $h = 2.25$, and more conservative is $h = 4$.

Reduced Velocity: $\upsilon = u d_p/D_m = (L/t_0)(d_p/D_m)$, where u is column linear velocity, t_0 is migration time of the unretained solute, and D_m is solute's diffusion coefficient. This means that values for υ depend on the size of the molecule. For a small molecule $3 < \upsilon < 15$, and for macromolecules $\upsilon > 50$. Optimal value for $\upsilon = 2.25$. If volumetric flow rate F

is given (ml/min), it can be converted to linear velocity (cm/s) using: $u = 0.0212\ F / d_c^2$, where d_c is column diameter in cm.

Reduced Length: $l = L / d_p$

Column Flow Resistance: $\phi = \Delta P\ d_p^2\ t_0 / L^2 \eta$, where ΔP is the pressure drop across the column and η is the eluent viscosity.

Peak Volume: $V_{Peak} = (\pi d_c^2/4)\ \varepsilon\ (L/t_0)$, where d_c is column inside diameter and ε is the column porosity. Good porosity values are 0.4 for the pellicular columns and 0.75 for the porous silica columns.

Reduced Knox Equation: $h = A\upsilon^{0.33} + B/\upsilon + C\upsilon$, where A is the flow dispersion term which is 1 for well packed columns. B is the longitudinal diffusion term—2 for well packed columns. C is the resistance to mass transfer term frequently 0.05 for porous columns and 0.003 for non-porous. From the discussion on the reduced velocity (above) it can be approximated that for small molecules $h = A\upsilon^{0.33}$ and for macromolecules $h = C\upsilon$.

Peak Variance: There are three different ways to describe peak variance: length units, time units, and volume units.

- $\sigma^2_l = HL$ (length)
- $\sigma^2_v = \sigma^2_l \pi^2 r^4$ (volume), where r is column radius
- $\sigma^2_t = \sigma^2_l / u^2$ (time), where u is linear velocity (t_0 / L)
- $\sigma^2_v = \sigma^2_t F^2$ (F is column flow rate)

Overall system variances are additive in the same units:

$\sigma^2_{total} = \sigma^2_{injection} + \sigma^2_{column} + \sigma^2_{detector}$

LSS Gradient Elution

In linear solvent strength (LSS) gradients, the mobile phase strength is linearly increased during the separation time causing the capacity factor, k', to change since it is directly affected by mobile phase composition. Therefore, $\bar{k}'$ is the average capacity factor for the separation. Such average capacity factor is related to the gradient profile by the gradient steepness parameter b. This comes from the relationship, which gives the values of capacity factor k_1 at the separation time t: $\log k_1 = \log k_0 - b(t / t_0)$

The value for $\bar{k}'$ can be approximated by $\bar{k}' = 1/1.3b$. To optimize the resolution in LSS gradient, $\bar{k}'$ should fall somewhere between 2 and 10. The way to relate b to the experimental parameters is given by $b = \frac{\Delta\Phi S V_0}{t_G F}$, where $\Delta\Phi$ is the change in organic modifier during the gradient (e.g. if the gradient is from 5% B to 90% B then $\Delta\Phi = 0.85$), S is the solvent strength of the organic modifier (see table below), V_0 is the void volume

of the column, and t_G is the time over which the gradient is varied linearly. For majority of applications the values of b should be in the range between 0.5 and 0.1.

Retention Time: $$V_g = (V_m/b) \log (2.3\, k_0\, b + 1) + V_m,$$

where V_m is the total volume of MP contained within the column and k_0 is the k' value at the beginning of the gradient. Actual retention time can be obtained by $t_g = V_g / F$. The value b is the gradient steepness parameter (see later).

Band Width: The band width in the gradient elution separation is the result of three independent processes:

1. Normal broadening of sample bands as they move through the column.
2. A band compression that arises from the faster migration of the tail of bands in gradient elution compared to the equal migration of all parts of the band in isocratic elution. This compression reduces the value of σ_x (standard deviation of the Gaussian peak) that would have been obtained in isocratic separation by the factor G. For intermediate values of b ($0.2 < b < 0.5$), G is roughly constant and equal to 0.8.
3. Instantaneous k' value of the band as it leaves the column (k_f').

The final width of the gradient elution band in time units, σ_t, is given by:

$$\sigma_t = (2.3b + 1)\, G t_0 / 2.3b\, N^{1/2}$$

Resolution: Resolution in gradient elution is defined by the same equation as in isocratic elution (see above) but using the value for the average capacity factor $\bar{k}$.

Solvent strengths of various organic modifiers.

Methanol	Acetonitrile	Ethanol	Acetone	Dioxane	2-propanol	THF
3.0	3.1	3.6	3.4	3.5	4.2	4.4

REFERENCES

Asp99 Aspinwall C.A., Lakey J.R., Kennedy R.T., *J Biol Chem.* **1999**, *247,* 6360-6365

Bao97 Bao, J.J., *J. Chromatogr. B.*, **1997**, *699*, 463-480.

Bar97 Bardelmeijer, H.; Waterval, J.; Lingeman, H.; van't Hof, R.; Bult, A.; Underbug, W. *Electrophoresis* **1997**, *18*, 2214

Boc92 Bock, L.C., Griffin, L.C., Latham, J.A., Vermaas, E.H., Tool, J.J., *Nature*, **1992**, *355*, 564-566

Bro72 Bromer, W.W.; Boucher, M.E.; Patterson, J.M.; Pekar, A.H.; Frank, B.H.; *J. Biol. Chem.*, **1972,** *247,* 2581-2582

Bru95 Bruin, G.J.M.; Paulus, A.; *Anal. Methods. Instrum.*, **1995**, *2*, 3-26

But84 Butt, W.R., Ed. *Practical Immunoassay.* **1984**, Marcel Dekker: New York

Can98 Cann, J.R.; *Electrophoresis*, **1998**, *19*, 127-141

Cas99 Caslavska, J.; Allemann, D.; Thormann, W. *J. Chrom. A.* **1999**, 197-211

Che94a Chen, D.Y.; Dovichi, N. *J Chromatogr. A* **1994**, *657*, 265

Che94b Chen, F. A.; *J. Chromatogr. A*, **1994**, *680*, 419-423

Che94c Chen, F.A.; Evangelista, R.A.; *Clin. Chem.* **1994**, *40*, 1819-1822

Che90 Chervet, J.P.; van Soest, R.E.; Urmsem, M. *LC packings* **1990** tech comm

Chi98 Chiem, H.H.; Harrison, D.J.; *Clin. Chem.* **1998,** *44*, 591-598

Chi97 Chiem, N., Harrison, D.J.; *Anal. Chem.*, **1997**, *69*, 373-378

Chr92 Chriswell, D.J.; McCafferty, J.; *Tibtech*, **1992**, 10: 80-84

Chr89 Chronwall, B.M.; *Anatomical Distribution of NPY and NPY messenger RNA in rat brain.* Neuropeptide Y. Mutt, V.; Ed. **1989**, Raven Press, New York

Chu92 Chu, Y.H.; Avila, L.Z.; Biebuyck, H.A.; Whitesides, G.M. *J. Med. Chem.* **1992**, *35*, 2915

Cul98 Culbertson, C.; Jorgenson, J. *Anal. Chem.* **1998**, *70*, 2629

Dav96 Davis, K.A., Abrams, B., Lin, Y., Jayasena. S.D., *Nuclec Acids Res.*, **1996**, *24*, 702-706

Dia96 Diamandis, E.P., Christopoulos, T.K., *Immunoassay*, **1996**, Academic Press, New York, Chapter 3

Dol98 Dolan, J.W., Snyder, L.R., *J. Chrom. A*, **1998**, *799*, 21-34

Dro96 Drolet, D.W., Moon-McDermott, L., Romig, T.S., *Nature Biotechnology*, **1996**, *14*, 1021-1025

Ell92 Ellington, A.D., Szostak J.W., *Nature*, **1992**, *355*, 850-852

Ell90 Ellington, A.D.; Szostak, J.; *Nature*, **1990**, *346*, 818-822

Ems79 Emson, P.C.; *Prog. Neurobiol.* **1979**, *13*, 61-116

Eva94 Evangelista, R.A.; Chen, F.A.; J. Chromatogr. A, **1994**, *680*, 587-591

Ewi94 Ewing , A.; Mesaros, J.; Gavin, P. *Anal. Chem.* **1994**, *66*, 527a

Fam94 Famulok, M. *J. Am. Chem. Soc.*, **1994**, *116*, 1698-1706

Fam92 Famulok, M., Szostak J.W., *J. Am. Chem. Soc.*, **1992**, *114*, 3990-3991

Fis98 Fister, J.; Jacobson, S.; Davis, L.; Ramsey, J. *Anal. Chem.* **1998**, *70*, 431

Fou98 Foulds, G.J.; Etzkorn, F.A.; *Nuc. Acids Res.*, **1998**, *26*, 4304-4305

Ger98 German, I.; Buchanan, D.D.; Kennedy, R.T. *Anal. Chem.* **1998**, *70*, 4540-4545

Ger00a German, I.; Kennedy, R.T.; *Anal. Chem.*, **2000**, *72*, 5365-5372

Ger00b German, I; Kennedy, R.T.; *J. Chrom. B*, **2000**, *742*, 353-362

Gid91 Giddings J.C., *Unified Separation Science;* **1991**, John Wiley & Sons, N.Y.

Gru69 Grushka, E.; Myers, M.N.; Schettler, P.D.; Giddings, J.C.; *Anal. Chem.* **1969**, *41*, 889

Hau96 Haugland, R.P., ed.; *Handbook of Fluorescent Probes and Research Chemicals*, **1996**, Molecular Probes Inc.

Hee99 Heegaard, N.H.H.; Kennedy, R.T. *Electrophoresis* **1999**, *20*, 3122-3133

Hie98 Hieftje, G.M., Ellington, A.D., Conrad, R.C., Potyrailo, R.A., *Anal. Chem.*,**1998,** *70*; 3419-3425

Hoo97 Hooker, T.; Jorgenson, J. *Anal. Chem.* **1997**, *69*, 4134-4142

Hua87 Huang, X.; Pang, T.; Gordon, M; Zare, R. *Anal. Chem.* **1987**, *59*, 2747

Hua91 Huang, X.; Zare, R. *Anal. Chem.* **1991**, *63*, 2193

Hus89 Huse, W.D.; Sastry, L.; Iverson, S.A.; *Nature*, **1989**, *246*, 1275-1281

Hut00 Hutterer, K.M; Birrell, H.; Camilleri, P.; Jorgenson, J.W.; *J. Chromatogr. B*, **2000,** *745*, 365-72

Jac86 Jackson, T.M.; Ekins, R.P. *J. Immunol Methods* **1986**, *87*, 13-20

Jay99 Jayasena, S.D.; *Clin. Chem.* **1999**, *45*, 1628-1650

Jen94 Jenison, T.D., Gill, S.C., Pardi, A., Polisky, B., *Science*, **1994**, *263*, 1425-1429

Joc89 Joce, G.F., *Gene*, **1989**, *82*, 83-87

Joh67 Johansson, S.G.O., Bennich. H., *Immunology*, **1967**, *13*, 381-394

Kal91 Kalra, S.P.; Dube, M.G.; Sahu, A.; Phelps, C.P.; Kalra, P.S.; *Proc. Natl. Acad. Sci. USA*, **1991**, *88*, 10931-10935

Kel97 Kelly, J.A.; Lee, C.S. *J. Chrom. A.* **1997**, *790*, 207-214

Ken89 Kennedy, R.T.; Jorgenson, J.W., *Anal. Chem.*, **1989**, *61*, 1128-11235

Ken97 Kennedy, R.T.; Tao, L. Schultz, N.M.; Rose, D.R., "*Immunoassays and Enzyme Assays Using CE" in CRC Handbook of Capillary Electrophoresis*, (ed. Landers, J.) , **1997**, CRC Press, Boca Raton, Chapter 22, pp. 523-545

Kle98 Kleinjung, F., Klussmann, S., Erdmann, V.A., Scheller, F.W., Furste, J.P., Bier, F.F. *Anal. Chem.*, **1998**, *70*, 328-331

Klu94 Klug, S.J., Famulok, M., *Mol. Biol. Rep.*, **1994**, *20*, 97-107

Koh75 Kohler, G.; Milstein, C.; *Nature*, **1975**, *256*, 496-497

Kol90 Kolehmainen, E.; Knip, M.; Leppaluoto, J. *Acta Physiol. Scand.* **1990**, *139*, 493-501

Kou96 Kounty, L.B.; Schmalzing, D.; Taylor, T.A.; Fuchs, M.; *Anal. Chem.*, **1996**, *68*, 18-22

Kus97 Kussmann M.; Nordhoff E.; Rahbek-Nielsen H.; Haebel S.; Rossel-Larsen M.; Jakobsen L.; Gobom J.; Mirgorodskaya E.; Kroll-Kristensen A.; Palm L.; Roepstorff P.; *J. Mass. Spec.* **1997**, *32*, 593-601

Lad96 Lada, M.W.; Vickroy, T.; Kennedy, R.T. *Anal. Chem.* **1996**, *68*, 2790

Lad97 Lada, M.W.; Vickroy, T.; Kennedy, R.T. *Anal. Chem.* **1997**, *69*, 4560

Lad98 Lada, M.W.; Vickroy, T.; Kennedy, R.T. *J. Neurochem.* **1998**, *70*, 617

Lam97 Lam, K.S.; Lebl, M.; Krchnak, V.; *Chem. Rev.*, **1997**, *97*, 411-448

Lau95 Lausch, R.; Reif, O.; Riechel, P.; Scheper, T.; *Electrophoresis*, **1995**, *16*, 636-641

Lem93 Lemmo, A.; Jorgenson, J. *Anal. Chem.* **1993**, *65*, 1576

Lin75 Lin, M.C.; Wright, D.E.; Hurby, V.J.; Rodbell, M.; *Biochemistry*, **1975**, *14*, 1559-1563

Maz85 Mazzola G.; Longhi R.; Carrea G.; *Anal Biochem.;* **1985**, *151*, 350-357

Moo93 Moore, A.W. Jr; Jorgenson, J.W.; *Anal Chem*, **1993**, *65*, 3550-3560

Mun80 Munson, P.J.; Rodbard, D.; *Anal. Biochem.* **1980**, *107*, 220-239

Nie95 Nieuwlandt, D., Wecker, M., Gold, L., *Biochemistry*, **1995**, *34*, 5651-5659

Nus00 Nussdorfer, G.G.; Bahcelioglu, M.; Neri, G.; Malendowicz, L.K.; *Peptides*, **2000**, *21*, 309-324

Oft88 Oftebro, H.; Falch, J.A.; Holmberg, I,; Haug, E. *Clin. Chim. Acta*, **1988**, *176*, 157-168

Osb97 Osborne, S.E.; Ellington, A.D.; *Chem. Rev.*, **1997**, *97*, 349-370

Paa81 Paabo, S.; Lundqvist, G.; Petersson, B.; Andersson A.; *Experentia*, **1981**, *37*, 1213-1214

Par96 Parma, D.; *J. Clin. Invest.*, **1996**, *98*, 2688-2692

Pic90 Piccirilli, J.A., Krauch, T., Moroney, S.E., Benner, S.A., *Nature*, **1990**, *343*, 33-37

Rei94 Reif, O.; Lausch, R.; Scheper, T.; Freitag, R.; *Anal. Chem.*, **1994**, *66*, 4027-4033

Rob91 Robinson, T.E.; Justice, J.B. Jr.; Ed.; *Microdialysis and the Neurosciences* (Techniques in the Behavioral and Neural Sciences, Vol. 7), **1991**, Elsevier, Amsterdam

Sas93 Sassanfar, M., Szostak, J. *Nature*, **1993**, *364*, 550-553

Sch97 Schmalzing, D.; Nashabeh, W.; *Electrophoresis.* **1997**, *18*, 2184-2193

Sch95a Schmalzing, D.; Nashabeh, W.; Fuchs, M.; *Clin. Chem.*, **1995**, *41*, 1403-1406

Sch95b Schmalzing, D.; Nashabeh, W.; Yao, X.; Mhatre, R.; Regnier, F.E.; Afeyan N.B.; Fuchs, M.; *Anal. Chem.*, **1995**, *67*, 606-612

Scz95 Schultz, N.M.; Huang, L.; Kennedy, R.T.; Anal. Chem., **1995**, *67*, 924-929

Scz93 Schulz, N.M., Kennedy, R.T., *Anal. Chem.* **1993**, *65*, 3161-3165

Sco84 Scott, R.P.W, Ed. *Small Bore Liquid Chromatography Columns: Their Properties and Uses*, **1984,** Wiley, New York, Chapter 2

She97 Shen, H.; Lada, M.W.; Kennedy, R.T. J. *Chromatogr. B*, **1997**, 689, 43-52

Shi94 Shimura, K.; Karger, B.; *Anal. Chem.*, **1994**, *66*, 9-15

Smi97 Smith, G.P.; Petrenko, V.A.; *Chem. Rev.*, **1997**, *97*, 391-410

Sny79 Snyder, L.R., Dolan, J.W., Grant, J.R. *J. Chromatogr.*, **1979**, *165*, 3-30

Sny83 Snyder L.R.; Stadalius, M.A.; Quarry, M.A. *Anal. Chem.* **1983**, *55*, 1412A-1430A

Sri97 Srinivasan, K., Pohl, C., Avdalovic, N., *Anal. Chem.*, **1997**, *69*, 2789-2805

Ste96 Stebbins, M.A., Hoyt, A.M., Sepaniak, M.J., Hurlburt, B.K.; *J Chromatogr B*, **1996**, *683*, 77-84

Ste95 Steinmann, L., Casalvaska, J., Thormann, W., *Electrophoresis*, **1995**, *16*, 1912

Ste83 Stevens, T.S.; Cortes, H.J. *Anal. Chem.* **1983**, *55*, 1365 – 1370

Tao97 Tao, L., Kennedy, R.T., *Electrophoresis*, **1997**, *18*, 112-117

Tao98 Tao, L.; Aspinwall, C.A.; Kennedy, R.T.; *Electrophoresis*, **1998**, *19*, 403-408

Tao96 Tao, L.; Kennedy, R.T. *Anal. Chem.* **1996**, *68*, 3899

Tha96 Thaler, D.S., Liu, S., Tobline, G., *Proc. Natl. Acad. Sci. USA*, **1996**, *93*, 1352-1356

Tim00 Tim, R.C.; Kautz, R.C.; Karger, B.L. *Electrophoresis*, **2000**, *21*, 220-226

Tsu90 Tsuda, T.; Zare, R.; Sweedler, J. *Anal. Chem.* **1990**, *62*, 2149

Tue90 Tuerk, C., Gold, L., *Science*, **1990**, *249*, 505-510

Tue92 Tuerk, C., MacDougal, S., Gold, L., *Proc. Natl. Acad. Sci. USA*, **1992**, *89*, 6988-6992

Van92 Van Regenmortel, M.H.V. *Structure of Antigens*, **1992**, Vol 1: 1-27. CRC Press, Boca Raton

Wal88 Wallingford, R.; Ewing, A. *Anal. Chem.* **1988**, *60*, 1762

Wan91 Wang, T.; Aiken, J.; Huie, C.; Hartwick, R. *Anal. Chem.* **1991**, *63*, 1372

Wie96 Wiegand, T.W., Williams, P.B., Dreskin, S.C., Jouvin, M., Kinet, J., Tasset, D., *J. Immunol.*, **1996**, *157*, 221-230

Wil97 Williams, K.P., Liu, X., Schumacher, T.N.M., Lin, H.Y., Ausiello, D.A., Kim, P.S., Bartel, D.P. *Proc. Natl. Acad. Sci. USA*, **1997**, *94*, 11285-11290

Woo98 Woolley, A.T.; Lao, K.; Glazer, A. N.; Mathies, R. *Anal. Chem.* **1998**, *70*, 684

Xue97 Xue, B., Gabrielsen, O.S., Myrset, A.H.; *J Capillary Electrophor.* **1997**, *4*, 225-231

Xue94 Xue, Y.; Yeung, E. *Anal. Chem.* **1994**, *66*, 3575

Ye98 Ye, L.; Le, C.; Xing, J.Z.; Ma, M.; Yatscoff, R.; *J. Chromatogr. B*, **1998**, *714*, 59-67

Yeu92 Yeung, E.S.; Wang, L.; Li, W.; Giese, R.W.; *J. Chromatogr.* **1992**, *608*, 73-80

BIOGRAPHICAL SKETCH

Igor German was born on May 14, 1973, in Odessa, Ukraine, former USSR. In September of 1991, his family immigrated to the United States, where he immediately began to study English and computer science at the North Technical Education Center in West Palm Beach, Florida. Upon completion of the computer applications program at the Center, he enrolled at the Palm Beach Community College and received an Associate of Arts Degree in August of 1994. In the fall of 1994, he began to attend the University of Florida and graduated with a B.S. in chemistry with high honors in August of 1996. Immediately following graduation, he began his graduate work under supervision of professor Robert T. Kennedy.

I certify that I have read this study and that in my opinion it conforms to acceptable standards of scholarly presentation and is fully adequate, in scope and quality, as a dissertation for the degree of Doctor of Philosophy.

Robert Travis Kennedy, Chairman
Professor of Chemistry

I certify that I have read this study and that in my opinion it conforms to acceptable standards of scholarly presentation and is fully adequate, in scope and quality, as a dissertation for the degree of Doctor of Philosophy.

James D. Winefordner
Graduate Research Professor of Chemistry

I certify that I have read this study and that in my opinion it conforms to acceptable standards of scholarly presentation and is fully adequate, in scope and quality, as a dissertation for the degree of Doctor of Philosophy.

Weihong Tan
Assistant Professor of Chemistry

I certify that I have read this study and that in my opinion it conforms to acceptable standards of scholarly presentation and is fully adequate, in scope and quality, as a dissertation for the degree of Doctor of Philosophy.

Jon Dale Stewart
Associate Professor of Chemistry

I certify that I have read this study and that in my opinion it conforms to acceptable standards of scholarly presentation and is fully adequate, in scope and quality, as a dissertation for the degree of Doctor of Philosophy.

Mark A. Atkinson
Professor Pathology, Immunology and
Laboratory Medicine

This dissertation was submitted to the Graduate Faculty of the Department of Chemistry in the College of Liberal Arts and Sciences and to the Graduate School and was accepted as partial fulfillment of the requirements for the degree of Doctor of Philosophy.

May, 2001

_____

Dean, Graduate School